Towards understanding TSWV particle assembly:

analysis of the intracellular behavior of the

viral structural proteins

Daniela Ribeiro

Promotor:
Prof. Dr. R. W. Goldbach
Hoogleraar in de Virologie
Wageningen Universiteit

Co-promotor:
Dr. Ir. R. J. M. Kormelink
Universitair Docent bij de leerstoelgroep Virologie
Wageningen Universiteit

Promotiecommissie:
Prof. Dr. P. J. M. Rottier (Universiteit Utrecht)
Prof. Dr. A. J. W. G. Visser (Wageningen Universiteit)
Dr. Ir. M. Kikkert (Universiteit Leiden)
Dr. Ir. J. Wellink (Wageningen Universiteit)

Towards understanding TSWV particle assembly:

analysis of the intracellular behavior of the

viral structural proteins

Daniela Ribeiro

To my parents

CONTENTS:

CHAPTER 1

GENERAL INTRODUCTION

Tomato spotted wilt virus (TSWV), type species of the genus *Tospovirus*, is one of the few plant-infecting members of the *Bunyaviridae* family. TSWV has a very broad host range (Peters, 1998) and is propagatively transmitted by various species of thrips (order *Thripidae*) (Wijkamp *et al.*, 1993).

The TSWV virus particle (Fig. 1) is spherical and enveloped, presenting at its surface the two viral glycoproteins Gc and Gn. In its core, the three RNA segments are encapsidated by the nucleocapsid protein (N) and the RNA polymerase (L) (Fig. 1B) (Mohamed *et al.*, 1973; Mohamed, 1981; Tas *et al.*, 1977; van den Hurk *et al.*, 1977; van Poelwijk *et al.*, 1993)
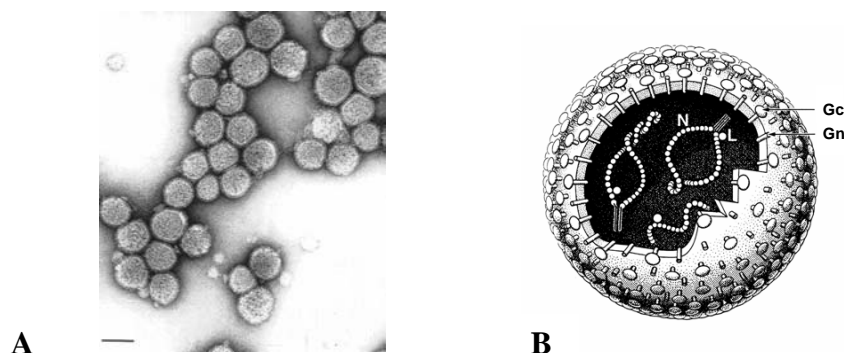
Figure 1: Tomato spotted wilt virus particle. A, electronmicrograph of purified TSWV particles (size bar represents 100nm). B, schematic representation of a virus particle.

THE *BUNYAVIRIDAE*

Most members of the *Bunyaviridae* family are arthropod-born (with the exception of the *Hantavirus* genus) animal-infecting viruses (Elliott, 1996). This family is composed of five genera: *Orthobunyavirus*, *Hantavirus*, *Nairovirus*, *Phlebovirus* and *Tospovirus* (Table 1).

Table 1: The *Bunyaviridae* family

	Genus	Type species	Arthropod vector	Host
Bunyaviridae family	*Orthobunyavirus*	Bunyamwera virus	Mosquitoes	Vertebrates
	Hantavirus	Hantaan virus	None	Verterbrates
	Nairovirus	Crimean Congo haemorrhagic fever virus	Mosquitoes	Vertebrates
	Phlebovirus	Rift Valey fever virus	Mosquitos, ticks, phlebotomines	Vertebrates
	Tospovirus	Tomato spotted wilt virus	Thrips	Plants

All bunyaviruses, including TSWV, share a number of characteristics concerning their virion structure and genome. The envelope particle is spherical or pleomorphic in shape, ranging from 80 to 120 nm in diameter (Fig. 1A). Their 11-19 kilobases (kb) genome is composed of three single stranded RNA segments of negative or ambisense polarity denoted as S (small, ranging from 0.8 to 2.9 kb), M (medium, ranging from 3.6 to 4.8 kb) and L (large, ranging between 6.4 and 12 kb), that encode four to six different structural and non-structural proteins (Elliott, 1996). Genome replication of all members occurs in the cytoplasm of the host (and arthropod vector) cells.

TSWV GENOME ORGANIZATION AND PROTEIN FUNCTION

In analogy to the animal-infecting bunyaviruses, TSWV's genome consists of three single stranded RNA segments (S, M and L) of negative or ambisense polarity (Fig. 2) (de Haan *et al.*, 1989; van den Hurk *et al.*, 1977; Verkleij *et al.*, 1982)
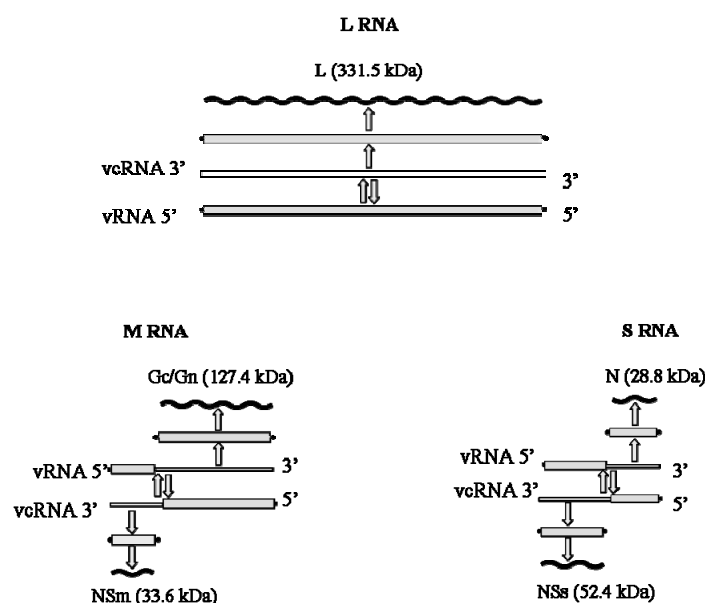
Figure 2: Organization and expression strategy of the TSWV genome

The L RNA segment is entirely of negative polarity and contains one open reading frame (ORF) in its viral complementary strand (vc) that codes for the L protein. This large protein is the putative viral RNA-dependent RNA polymerase (de Haan *et al.*, 1991) and has been suggested to be involved in several enzymatic activities such as transcriptase, nuclease and replicase (Adkins *et al.*, 1995; Chapman *et al.*, 2003; van Knippenberg *et al.*, 2002)

The M RNA segment is of ambisense polarity, coding for the cell-to-cell movement protein (NSm) in the viral (v) strand and for the glycoprotein precursor (GP) in the vc strand. The NSm protein forms tubular structures that extend from plasmodesmata into newly infected cells and assist the in cell-to-cell movement of viral ribonucleocapsids (Kormelink *et al.*, 1994; Soellick *et al.*, 2000; Storms *et al.*, 1995). The glycoprotein precursor GP (Fig. 3) is co-translationally cleaved into the viral glycoproteins Gc and Gn, where c and n refer to the carboxy- and amino-terminal position within the precursor (Kormelink *et al.*, 1992a). Both glycoproteins are type I membrane spanning proteins and are present at the surface of the virus particles where they act as major determinants for insect transmission and specificity (Wijkamp, 1995) through the interaction with cell-surface receptors on the insect midgut epithelium (Bandla *et al.*, 1998; Nagata *et al.*, 2002; Tsuda *et al.*, 1996; Ullman *et al.*, 1992; Whitfield *et al.*, 2004; Wijkamp *et al.*, 1993). Furthermore, the glycoproteins play a major role in (dictating the site of) particle assembly (Kikkert *et al.*, 1999; Kikkert *et al.*, 2001), likely triggered by the interaction of ribonucleoproteins (RNPs) with their cytoplasmic tails (Snippe *et al.*, 2007b).
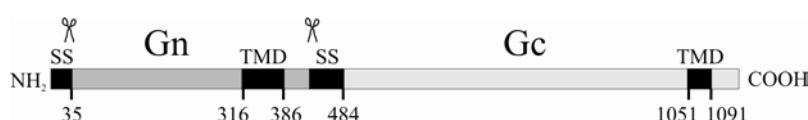

Figure 3: Schematic representation of the topology of the glycoprotein precursor. Predicted cleavage sites (scissor symbols), hydrophobic areas (black boxes) and aminoacid positions are indicated. Other symbols: SS, signal sequence; TMD, transmembrane domain.

The v strand of the ambisense S RNA segment codes for the non-structural NSs protein and its vc strand for the nucleocapsid (N) protein (de Haan *et al.*, 1990). The NSs protein has been shown to act as a suppressor of RNA silencing (Bucher *et al.*, 2003; Takeda *et al.*, 2002). The N protein is the major component of RNPs, and is assumed to be required for transcription/replication of the viral genome. For particle assembly, the interaction of this protein with (one of the) glycoproteins is thought to be essential (Snippe *et al.*, 2005a; Snippe *et al.*, 2007b). The N protein is the least conserved among all tospoviral proteins and is used for taxonomic classification (Snippe *et al.*, 2005a).

TSWV INFECTION CYCLE

After introduction of TSWV into a plant cell by its thrips vector, the viral envelope is removed and the RNPs are released into the cytoplasm (Fig. 4). Primary transcription results in the production of the glycoprotein precursor, the N and the L proteins (Kormelink *et al.*, 1992b),

followed by replication of the viral RNA genome that results in the production of new full length genome copies. The major production of NSs and NSm proteins, by means of secondary transcription, completes the set of viral proteins being synthesized.

The N protein and small amounts of the L protein encapsidate newly synthesized RNA segments, forming RNPs that, associated with NSm, spread the viral infection through plasmodesmata into neighboring cells. The processing of the glycoprotein precursor renders Gc and Gn which are post-translationally glycosylated and eventually accumulate in the Golgi complex (Kikkert *et al.*, 2001). The RNPs are enwrapped by glycoprotein-containing Golgi membranes, giving rise to the formation of new virus particles which accumulate in large cytoplasmic vesicles from where they await uptake by the thrips vector. Thrips-mediated infection of new plant cells restarts the infection cycle.
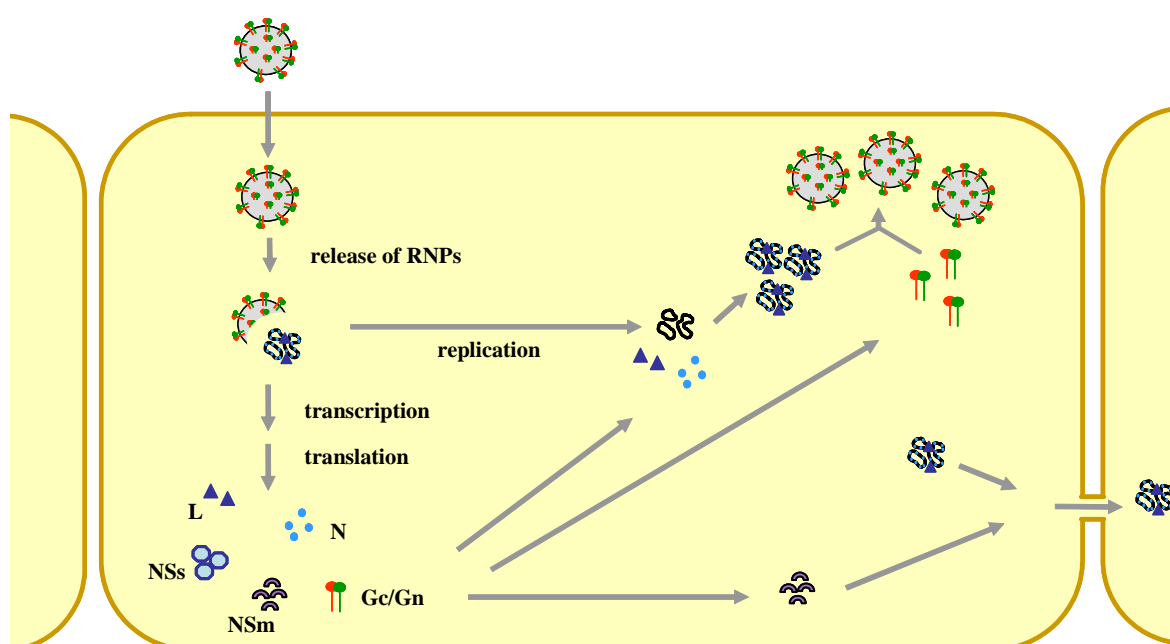
Figure 4: TSWV infection cycle in a plant cell. The figure and sequential steps are explained in the text.

TSWV PARTICLE ASSEMBLY

Studies performed in a plant protoplast system (Kikkert *et al.*, 1997; Kikkert *et al.*, 1999) have resulted in important insights concerning the virus particle assembly mechanism of TSWV in plant cells. These studies have shown that the viral glycoproteins Gc and Gn ultimately concentrate in specific regions of the Golgi membranes (Kikkert *et al.*, 1999). The RNPs, that localize in close proximity to these loci, are enwrapped by these glycoprotein-containing membranes, forming doubly-enveloped virus particles (DEVs, Fig. 5 A-C) (Kikkert *et al.*, 1999;

Kitajima *et al.*, 1992a; Milne, 1970). In a later stage of maturation, the DEVs fuse with each other and ultimately with ER-derived membranes, leading to the formation of large vesicles containing singly enveloped virus particles (SEVs, Fig 5 A and D) (Kikkert *et al.*, 1999; Kitajima *et al.*, 1992a; Milne, 1970). Mature virions accumulate in these subcellular compartments until uptake by the insect vector.
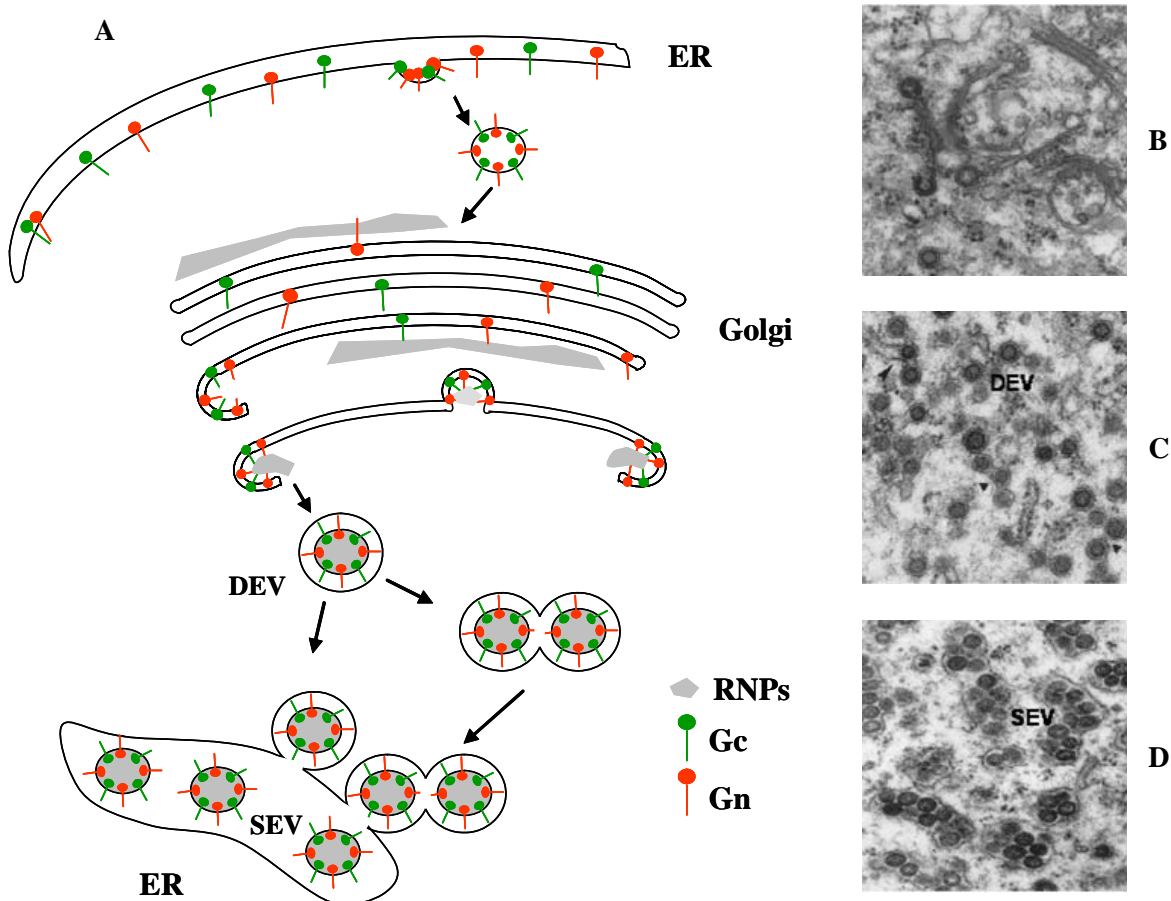
Figure 5: TSWV particle assembly in plant cells. A, schematic representation of the assembly mechanism. The figure and the sequential steps are explained in the text. B, C and D, electronmicrographs representing different stages of the particle assembly process. DEV, doubly enveloped virus particles; SEV, singly enveloped virus particles

TSWV is also able to replicate and assemble in its insect vector cells (Ullman *et al.*, 1992; Ullman *et al.*, 1993; Wijkamp *et al.*, 1993). However, not much is known about the virus life cycle in these cells and very little information is available on the stages involving virus assembly. Almost no enveloped particles can be discerned, and these are only found in the lumen of the salivary ducts (Wijkamp *et al.*, 1993). A remarkable difference observed between plant and insect

cells involves the fate of the mature virions after processing. As previously explained, in plant cells, SEVs accumulate in larger clusters and retain intracellularly. In contrast, mature virus particles are secreted from the thrips salivary glands. Since this secretion is also observed upon particle formation of the animal-infecting bunyaviruses, it was hypothesized that TSWV particle maturation in insect cells would occur through a similar mechanism. Bunyaviruses particle formation in animal cells (Anderson and Smith, 1987; Booth *et al.*, 1991; Gahmberg *et al.*, 1986; Jantti *et al.*, 1997; Kuismanen *et al.*, 1982; Kuismanen *et al.*, 1984; Lyons and Heyduk, 1973; Ravkov *et al.*, 1997; Rwambo *et al.*, 1996; Salanueva *et al.*, 2003; Smith and Pifat, 1982) involves the budding of the RNPs into vacuolized glycoprotein-rich Golgi membranes (Fig. 6), in contrast to the enwrapment phenomenon observed in plant cells (Fig.5). This budding leads to the formation of SEVs inside the Golgi complex which are ultimately secreted.

These differences seem to indicate that TSWV is able to adapt to cells of two different types of organisms, using alternative mechanisms for its virus particle assembly. These observations may to reflect what has earlier been hypothesized: that TSWV has an animal-infecting ancestor from which it evolved upon adaptation to plant cells, retaining the capability to replicate and form virus particles in thrips (animal) cells (Goldbach and Peters, 1996).
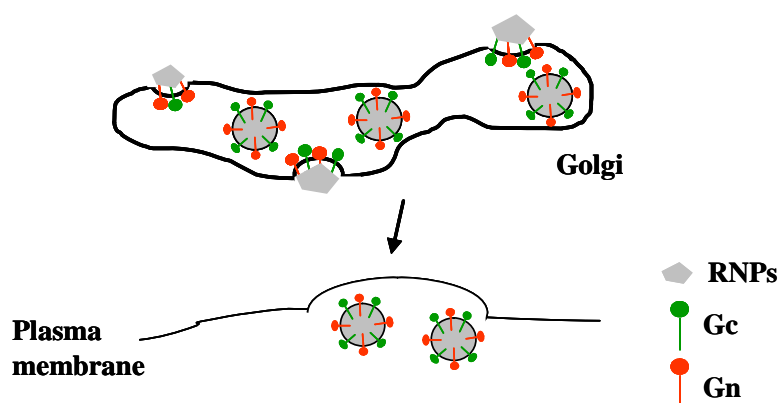
Figure 6: Animal-infecting bunyavirus particle assembly: budding and secretion. The figure and the sequential steps are explained in the text.

Transient expression studies of the TSWV glycoproteins in mammalian BHK21 cells (Kikkert *et al.*, 2001) have shown that Gn is able to translocate from the ER to the Golgi. Gc was found to retain in the ER, unless upon co-expression with Gn, when both glycoproteins are able to co-migrate to the Golgi complex. These results suggested a heterodimerisation of Gc and Gn, as well as the presence of a Golgi retention signal in Gn.

OUTLINE OF THE THESIS

From the information presented in this chapter it is clear that the assembly of TSWV particles is a far from fully understood process and detailed insight herein would require the unraveling of the intracellular targeting, interactions and behavior of the viral proteins involved. Such studies have been previously performed in mammalian cell systems (Kikkert, 1999; Snippe, 2006) but studies in plant cells have been hampered, due to the relative difficulty of plant-based cell systems. This thesis encompasses directed studies on the intracellular localization and behavior of individual or combined TSWV proteins upon transient expression in plant cells. Crucial for establishing a suitable plant-based system, was the application of an optimized electroporation protocol involving the introduction of high amounts of DNA constructs into high quality leaf protoplasts. By fusing different fluorophores to the structural viral proteins (N, Gn and Gc) their *in vivo* behavior could be easily monitored with the use of fluorescence confocal microscopy.

Our main goal was to analyze the cellular mechanisms involved in TSWV proteins translocation and the dynamics of intracellular membranes induced by viral infection, in order to further unravel the process of viral particle formation in plant cells.

As a first step, a detailed analysis was performed on the viral Gn and Gc glycoproteins upon their single or co-expression, and their location was identified using specific organelle marker molecules (Chapter 2).

To analyze whether the behavior of the viral glycoproteins would be affected by the additional presence of N (more closely resembling the natural infection), co-expression studies were performed and potential interactions between these proteins were analyzed by Förster Resonance Energy Transfer (FRET) and Fluorescence Lifetime Imaging microscopy (FLIM) (Chapter 3).

The trafficking of N from its cytoplasmic location to the vicinity of the ER and/or Golgi was investigated in Chapter 4. The possible involvement of the cytoskeleton in N's trafficking was investigated using drugs that specifically inhibit the polymerization of the microtubule or actin networks.

The localization of Gc in the presence of N was identified using specific organelle markers, and the effect of N on the localization of a foreign, non-viral, protein provided with the cytoplasmic tail of Gc was also investigated (Chapter 5).

In Chapter 6 more attention has been paid to the mechanisms and conditions involving ER-exit of the viral glycoproteins and their subsequent migration to the Golgi.

Chapter 7 finally discusses the major results obtained and compares them with earlier data and with the information available for animal bunyaviruses. Moreover, a model is presented, accommodating most of the described findings, with special reference to intracellular viral protein behavior and intracellular dynamics during virus particle assembly in plant cells.

CHAPTER 2
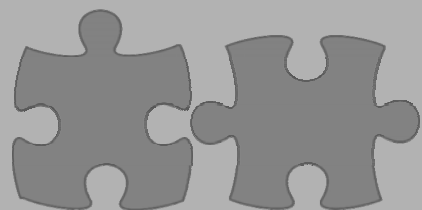
BEHAVIOR OF TRANSIENTLY EXPRESSED TOMATO SPOTTED WILT VIRUS GLYCOPROTEINS: INTRACELLULAR LOCALIZATION AND MEMBRANE INDUCTION IN PLANT CELLS

ABSTRACT

Tomato spotted wilt virus (TSWV) particles are spherical and enveloped, an uncommon feature among plant-infecting viruses. Previous studies have shown that virus particle formation involves enwrapment of ribonucleoproteins at viral glycoprotein-containing Golgi stacks. In this study, the localization and behavior of the viral glycoproteins Gn and Gc were analyzed, upon transient expression in plant protoplasts. When separately expressed, Gc was solely observed in the ER whereas Gn was found both within the ER and Golgi membranes. Upon co-expression, both glycoproteins were found at ER export sites and ultimately at the Golgi complex, confirming Gn's ability to rescue Gc from the ER, possibly due to heterodimerisation. Interestingly, both Gc and Gn were shown to induce the formation of (respectively) ER- and Golgi-derived circular/pleomorphic membrane structures. This membrane deformation was also observed upon co-expression of the two glycoproteins. The behavior of both glycoproteins and the formation of these peculiar membrane structures are discussed in light of the natural viral infection process.

INTRODUCTION

Tomato spotted wilt virus (TSWV) is the type species of the *Tospovirus* genus within the family of arthropod-borne *Bunyaviridae*. Unlike most members of this family, tospoviruses are able to infect plants, rather than animals, and are transmitted in a propagative manner by thrips species (Thysanoptera; order *Thripidae*) (Elliott, 1990; Goldbach and Peters, 1996). TSWV particles have a lipid envelope containing the virally encoded glycoproteins Gn and Gc (n and c refer to the amino and carboxy-terminal topology within the precursor protein), a rather unique feature among plant viruses, reflecting the requirement for uptake and replication of the virus in its insect vector (Wijkamp *et al.*, 1993). Virus particles harbour a tripartite negative/ambisense RNA genome that, in association with the nucleocapsid protein (N) and the viral RNA-dependent RNA polymerase (L), forms infectious ribonucleoproteins (RNPs) (Goldbach and Peters, 1996; Mohamed *et al.*, 1973).

For the animal-infecting bunyaviruses, particle assembly involves budding of RNPs into the vacuolized lumen of the glycoprotein-containing Golgi, leading to the formation of singly enveloped virus particles (SEVs) which are then secreted from the cells (Elliott, 1996; Griffiths and Rottier, 1992; Petterson and Melin, 1996). In contrast, during TSWV infection of plant cells, mature virus particles arise as a result of the wrapping of entire Golgi cisternae around RNPs (Kikkert *et al.*, 1997; Kikkert *et al.*, 1999; Kikkert *et al.*, 2001; Kitajima *et al.*, 1992a; Petterson and Melin, 1996). As result, doubly enveloped virus particles (DEVs) are formed that fuse with each other and with ER-derived membranes leading to the formation of mature SEVs clustered inside large vesicles within the cytoplasm. There, the virus is retained prior to uptake by the insect vector upon feeding (Kikkert *et al.*, 1999). However, upon infection of thrips (salivary gland) cells, mature TSWV particles do not accumulate inside the cells. Instead, they are secreted in resemblance to what is observed during the maturation pathway of animal-infecting bunyaviruses (Whitfield *et al.*, 2005).

The final fate of mature TSWV particles in plant and insect cells is clearly distinct and likely reflects adaptations of this virus to either cell type. It has earlier been hypothesized that, based on sequence homologies, TSWV and members of the *Orthobunyavirus* genus share a common ancestor from which TSWV evolved upon adaptation to plant cells, still retaining the capacity to replicate and form virus particles in thrips (animal) cells (Goldbach and Peters, 1996).

As the viral glycoproteins localize, guide and potentiate the process of enveloped virus assembly, studies have been undertaken to express and analyze the TSWV glycoproteins in mammalian and plant cells to identify domains within the glycoproteins responsible for the critical differences between the intracellular targeting in either cell system. Initial studies in mammalian cells revealed that, upon individual expression, Gc entirely localizes in the ER whereas Gn is able to additionally target to and retain at the Golgi complex. Upon co-expression of both proteins from separate constructs, Gn is able to redirect Gc from the ER to Golgi, likely due to heterodimerisation (Kikkert *et al.*, 2001), demonstrating that, in mammalian cells, the TSWV glycoproteins exhibit a similar trafficking behavior to those from the animal-infecting bunyaviruses (Andersson *et al.*, 1997a; Elliott, 1996; Matzuoka *et al.*, 1996; Rönnholm, 1992).

In order to further unravel and understand the entire virus particle maturation process in its natural host, i.e. plant cells, a detailed study of the localization and behavior of the viral glycoproteins (upon transient expression in protoplasts) is presented in this study.

MATERIALS AND METHODS

PLASMID CONSTRUCTION AND ORGANELLE MARKERS

The pMON999 vector (containing a 35S-driven promotor) was used for cloning and expression of the fluorophore-fused and non-fused TSWV proteins. The previously established pSFV plasmid containing the glycoprotein precursor (GP) (Kikkert *et al.*, 2001), as well as the Gc-YFP and Gn-YFP (Snippe *et al.*, 2007b), were subjected to a restriction enzyme digestion with BamHI, which resulted in the isolation of a cloning cassette containing the respective fused and non-fused glycoproteins. The BamHI site of the multiple cloning site was used to insert these cassettes into the (previously digested and dephosphorylated) pMON999 vector.

For the fusion of the YFP to the C-terminus of the glycoprotein precursor, pMONGP was digested with NheI (single restriction site within Gc) and BamHI, allowing the isolation of a cassette containing a part of the glycoprotein precursor cleaved at 500 nucleotides from the 5' end. The digestion with NheI and BamHI was also performed on the pSFVGcYFP, allowing the isolation of a cassette containing a part of the Gc-YFP, cleaved at 1765 nucleotides from its 3' end. A three-point ligation was performed between the two previously mentioned cassettes and the BamHI digested pMON999 resulting in the construction of pMONGP-YFP.

A plant expression vector containing CFP fused to the C-terminus of Gc (p2GW7.0Gc-CFP) was obtained using the GATEWAY^{TM} system (Invitrogen), following the manufacturer's instructions. The primers GcFwdGW (GGGGACAAGTTTGTACAAAAAAGCA GGCTGGATGAGTGTACTAAAGTCTGCATTTC) and CFPRvsGW (GGGGACCACTTTGT ACAAGAAAGCTGGGTGTTACTTGTACAGCTCGTCC) were used to PCR amplify Gc-CFP from the pSFVGc-CFP construct (Snippe *et al.*, 2007b). The PCR fragment was introduced into pDonr207 by BP recombination and subsequently into the p2GW7.0 (Karimi *et al.*, 2002) destination vector by LR recombination.

The fluorescent proteins used in this study for fusion to the viral glycoproteins were a pH-insensitive form of YFP, CFP and mGFP5 (Haseloff *et al.*, 1997). The spectral properties of mGFP5 allow efficient spectral separation from YFP (Brandizzi *et al.*, 2002b).

In these experiments we made use of the GFP-HDEL ER-marker (Carette *et al.*, 2000), the ST-GFP Golgi-marker (Boevink *et al.*, 1998), the YFP-Sec24 ER export sites-marker (Stefano *et al.*, 2006) and the prevacuolar compartment marker GFP-BP80 (da Silva *et al.*, 2005).

PLANT MATERIAL AND TRANSIENT EXPRESSION

Tobacco plants (*Nicotiana tabacum* cv Petit Havana) (Maliga *et al.*, 1973) were grown in Murashige and Skoog medium (Murashige and Skoog, 1962) and 2% sucrose in controlled sterile conditions at 25°C with a 16 hours period of light per day. Tobacco leaf protoplasts preparation and transfection were performed as described by Denecke and Vitale (1995), with some minor modifications. In short, leaves of fully-grown plants were pierced and digested overnight in TEX [B5 salts, 500 mg/l MES, 750 mg/l CaCl$_2$·2H$_2$O, 250 mg/l NH$_4$NO$_3$, 0.4 M sucrose, pH 5.7] containing 0.2% Macerozyme and 0.4% Cellulase. Protoplasts were recovered by filtration and washed by multiple centrifugations with Electroporation Buffer (EB) [0.4 M sucrose, 2.4 g/l

HEPES, 6 g/l KCl, 600 mg/l $CaCl_2 \cdot 2H_2O$, pH 7.2]. Healthy living protoplasts were recovered and resuspended in the proper EB volume. 100 µl of the plasmids in EB (applied plasmid concentrations depended upon experiment: 30 µg of each construct for multiple transfections and 60 µg of the construct when singly transfected) was added to 500 µL of the protoplast suspension and this mixture was subjected to electroporation (160V, 925µF, $\infty\Omega$) in 4 mm cuvettes using a BIO-RAD X-cell electroporator. After 10 min recovery, the protoplasts were incubated in 2 mL TEX in the dark (the incubation times differed per experiment, ranging between 24 and 48 hours, as mentioned in the figure legends).

Nicotiana tabacum plants stably expressing the Golgi-marker ST-GFP (kindly provided by Prof. Chris Hawes) were grown under the previously described conditions and the analyses were conducted in protoplasts isolated and transfected according to the previously described methodology.

SAMPLING AND IMAGING

Twenty four to forty eight hours post-transfection, the living protoplasts were isolated by centrifugation and confocal sections images were obtained using an inverted Zeiss 510 Laser Scanning Microscope and a 40x oil or 63x oil and water immersion objective.

For the imaging of the single expression of YFP-fused viral proteins, excitation lines of an argon ion laser of 488 nm were used with a 505/530 nm bandpass filter in the single-track facility of the microscope. For the imaging of the co-expressing YFP-fused and the GFP-fused proteins (as well as for the imaging of the co-expressing CFP- and YFP-fused proteins), excitation lines of an argon ion laser of 458 nm for GFP and 514 nm for YFP were alternately used with line switching using the multi-track facility of the microscope. Fluorescence was detected using a 458/514 nm dichroic beam splitter and a 470/500 nm bandpass filter for GFP and a 535/590 nm bandpass filter for YFP. Appropriate controls were performed to exclude possible crosstalk and energy transfer between fluorochromes. For the simultaneous imaging of YFP and TRITC, excitation lines of an argon ion laser of 488 nm for YFP and 543 nm for TRITC were alternately used with line switching using the multi-track facility of the microscope and fluorescence was detected using a 488/543 nm dichroic beam splitter and the filters BP 505/530 nm LP 560 nm for YFP and TRITC, respectively.

INDIRECT FLUORESCENCE ANALYSIS

Living protoplasts were selected as previously described and carefully placed on a microscope slide previously coated with 0.05% poly-L lysine. Approximately 5 min after, the slides were submerged in 96% ethanol where the fixation occurred for about 20 min. After a 20 min wash in PBS (0.137 M NaCl, 1.5 mM KH_2PO_4, 8.1 mM Na_2HPO_4, 2.7 mM KCl, 3.1 mM NaN_3), the protoplasts were blocked with 5% BSA in PBS for 45 min. The cells were subsequently incubated for one hour in a 1:1000 dilution of the polyclonal antibody against Gc (raised in rabbit) (Kikkert *et al.*, 1997) in 1% BSA in PBS. Three washing steps of 20 min in PBS preceded one hour incubation in the dark, in a 1:100 dilution of the secondary antibody (swine

anti-rabbit conjugated with Tetramethyl Rhodamine Iso-Thiocyanate, TRITC) in 1% BSA in PBS. The cells were again washed with PBS in three steps of 20 min, always in the dark. Two drops of citifluor were added to the slides, prior to their examination under an inverted Zeiss 510 Laser Scanning Microscope.

RESULTS

TSWV GN AND GC GLYCOPROTEINS SHOW DIFFERENT LOCALIZATION PATTERNS AND ARE ABLE TO INDUCE THE FORMATION OF PLEOMORPHIC MEMBRANE STRUCTURES IN PROTOPLASTS

To study the properties and behavior of the TSWV glycoproteins in plant cells, both proteins, Gn and Gc, were transiently expressed in protoplasts, either individually or from their common precursor. Separate constructs were made (Fig.1) and cloned in pMON999 for 35S-driven transient expression in plant cells. Both Gn and Gc were fused to YFP at their C-terminus (Fig.1) to allow immediate monitoring. YFP was also fused to the C-terminus of the glycoprotein precursor gene (GP) (Fig.1), for easy monitoring of Gc's behavior in the presence of Gn, as the *in situ* processing of such precursor fusion-protein leads to mature Gc-YFP and Gn.
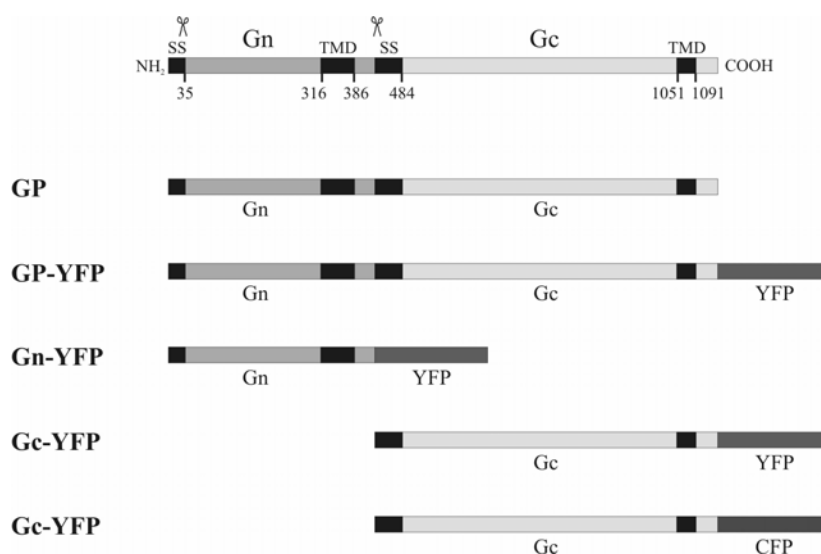
Figure 1: Topology of the TSWV glycoprotein precursor. Constructs used for expression studies aligned below the precursor. Predicted cleavage sites (scissor symbols), hydrophobic areas (black boxes) and amino acid positions are indicated (SS, signal sequence; TMD, transmembrane domain). In all constructs, the YFP or CFP fluorophores were fused in frame at the position of the stop codon.

N. tabacum protoplasts were transfected with the individual constructs and analyzed by confocal microscopy. These analyses revealed the presence of Gn-YFP in a reticular pattern, indicative of ER-localization, at earlier time points (until 24 hours) post-transfection (p.t.) (Fig. 2a). At 48 hours p.t. (and later), the reticular signal was rarely observed and Gn-YFP was mainly localized in different globular structures (Fig. 2b). Surprisingly, in about 25% of the cells

Gn was also found in non-dense pleomorphic structures (Fig. 2c and Fig. 3), mostly circular (Fig. 2c and 3 e-h), although in some cases different shapes were observed (Fig. 3 a-d). These structures varied in size, ranging from 0.5 to 4 µm, and in some cases appeared "open" at one side (Fig. 3g, arrow).
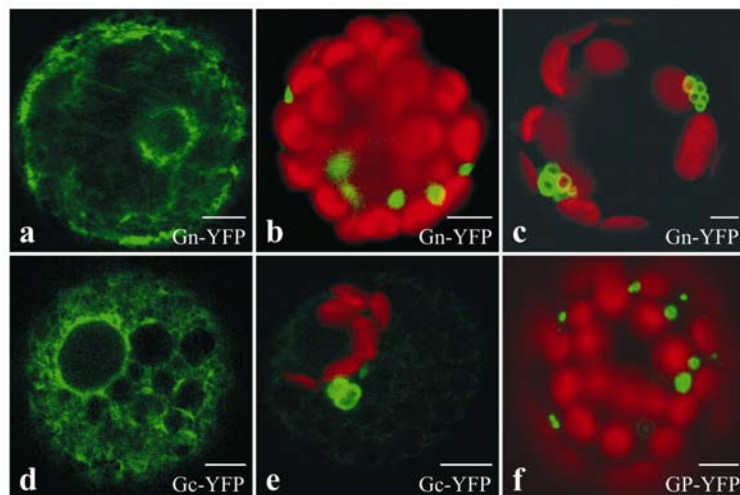
Figure 2: Fluorescence images of *N. tabacum* protoplasts transfected with constructs coding for the TSWV glycoproteins. Panels a-c: protoplasts transfected with Gn-YFP observed 24h (a) and 48h (b and c) p.t.; Panels d and e: protoplasts transfected with Gc-YFP observed at 48h p.t.. Panel f: protoplast transfected with GP-YFP observed at 24h p.t.. Size bars represent 5 µm.
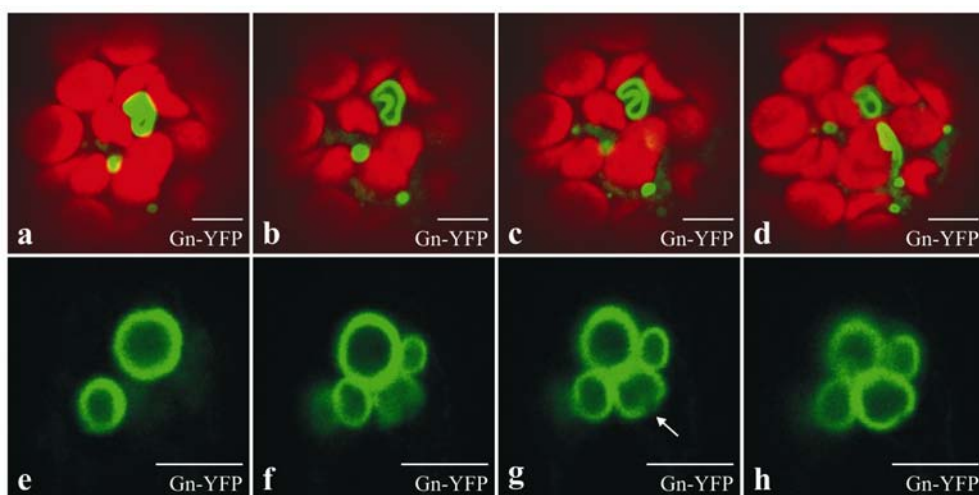
Figure 3: Z-stack fluorescence images of *N. tabacum* protoplasts transfected with Gn-YFP; a-d and e-h represent 4 sequential sections of two different protoplasts. An opening at one end of a pseudo-circular membrane structure is indicated by an arrow. Size bars represent 5 µm.

Single expression of Gc-YFP showed a clear reticular localization pattern (Fig. 2d), even after longer periods of expression. Surprisingly, in about 10% of the cells, Gc also localized in pleomorphic membrane structures (Fig. 2e) somewhat similar in appearance to those observed upon expression of Gn-YFP. During several independent experiments more of these structures were discerned, some of these being exceptionally large in size, with a "diameter" up to 4 µm.

When both glycoproteins were co-expressed from their common precursor gene fused at the carboxy-terminus with YFP (GP-YFP, Fig.1), monitoring of Gc (i.e. Gc-YFP processed from the precursor) showed that this protein accumulated in small globular structures localized all over the cell (Fig. 2f), a quite distinct pattern from the one earlier observed for Gc-YFP upon single expression (Fig. 2d and e). To analyze whether Gn co-localized with Gc-YFP in these structures, protoplasts were transfected with GP-YFP and prepared for immunolocalization analysis using antibodies directed against Gn. As expected, both glycoproteins co-localized in these structures (results not shown). Furthermore, the presence of Gn greatly boosted the expression level of Gc (based on the percentage of cells in which the glycoprotein could be detected) to about 5-fold.

Fusion of YFP at the C-terminal side of the glycoproteins has recently been shown not to influence their intracellular localization pattern in mammalian cells (Snippe *et al.*, 2007b). To verify that, similarly, this fusion did not affect their behavior in plant cells, protoplasts were transfected with non-fused glycoprotein constructs and analyzed by indirect immunolocalization. The non-fused glycoproteins localized similarly to those containing a YFP fusion (data not shown), indicating that the fluorophore fusions did not alter the glycoproteins' behavior *in planta*.

GN LOCALIZES TO ER, GOLGI AND GOLGI-DERIVED PLEOMORPHIC MEMBRANE STRUCTURES

To determine the localization of Gn as well as the origin of the globular/pleomorphic structures, co-expression analyses were performed using ER- and Golgi-specific markers. When protoplasts were co-transfected with Gn-YFP and GFP-HDEL (ER-marker) the reticular Gn pattern observed at early times p.t. completely co-localized with this organelle marker (Fig. 4 a-c). Analyses of protoplasts from plants stably transformed with ST-GFP transfected with Gn-YFP revealed that, at later times post-transfection, Gn co-localized with the Golgi marker. This co-localization was not only observed when the Gn localized at the small globular structures (Fig. 4 d-f) but also when it localized in the pleomorphic non-dense structures (Fig. 4 g-i). These results suggested that Gn, once localized at the Golgi membranes, is able to induce their deformation into (pseudo-) circular and pleomorphic structures.

GC IS RETAINED IN ER AND ER-DERIVED PLEOMORPHIC MEMBRANE STRUCTURES

To confirm its putative ER localization, Gc-YFP was co-expressed with the ER-marker GFP-HDEL. Confocal fluorescence analysis of protoplasts transfected with both constructs revealed a clear co-localization (Fig. 5 a-c), which was not restricted to the Gc localizing in a reticular pattern, but also when localizing in pleomorphic membrane structures (Fig. 5 a-c, arrows).

When protoplasts from tobacco plants stably transformed with ST-GFP were transfected with Gc-YFP, no co-localization between Gc and this Golgi marker (Fig 5. d-f) was observed, even at longer p.t. times (results not shown).

These analyses altogether suggested that Gc is arrested in the ER where it is, similarly to Gn in the Golgi complex, able to modify the morphology of the membranes into pseudo-circular/pleomorphic structures.

Figure 4: Fluorescence images of *N. tabacum* protoplasts co-transfected with a construct coding for the Gn glycoprotein and organelle specific (ER or Golgi) marker. Panels a-c: protoplast transfected with Gn-YFP and GFP-HDEL 24h p.t.: (a) Gn-YFP, (b) GFP-HDEL, (c) merge image of a and b. Panels d-f: protoplast isolated from plants stably transformed with ST-GFP and transfected with Gn-YFP 48h p.t.: (d) Gn-YFP, (e) ST-GFP, (f) merge image of d and e. Panels g-i: protoplast isolated from plants stably transformed with ST-GFP and transfected with Gn-YFP 48h p.t.: (g) Gn-YFP, (h) ST-GFP, (i) merge image of g and h. Size bars represent 5 µm.

Figure 5: Fluorescence images of *N. tabacum* protoplasts co-transfected with a construct coding for the Gc glycoprotein and organelle-specific (ER or Golgi) marker. Panels a-c: protoplast transfected with Gc-YFP and GFP-HDEL: (a) Gc-YFP, (b) GFP-HDEL, (c) merge image of a and b; arrows indicate pleomorphic structures. Panels d-f: protoplast isolated from plants stably transformed with ST-GFP and transfected with Gc-YFP: (d) Gc-YFP, (e) ST-GFP, (f) merge image of d and e. Size bars represent 5 µm.

GN IS ABLE TO REDIRECT GC FROM THE ER TO ER EXPORT SITES AND SUBSEQUENTLY TO THE GOLGI COMPLEX

To identify the localization and trafficking of the glycoproteins when expressed from their common precursor gene, GP-YFP was co-expressed with the GFP-HDEL ER-marker. The earlier described globular structures containing both glycoproteins (Fig. 2f) did not co-localize with this ER marker (Fig. 6 a-c).

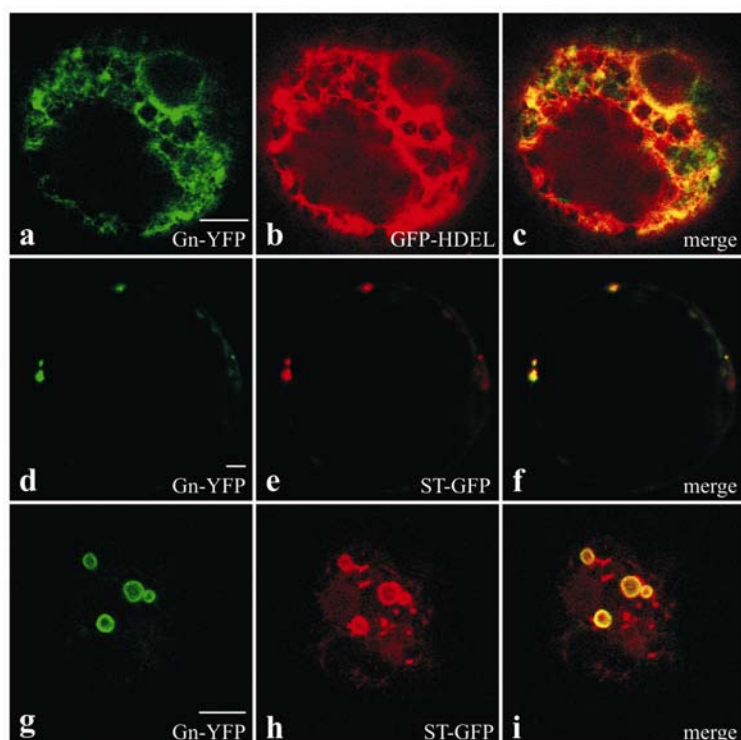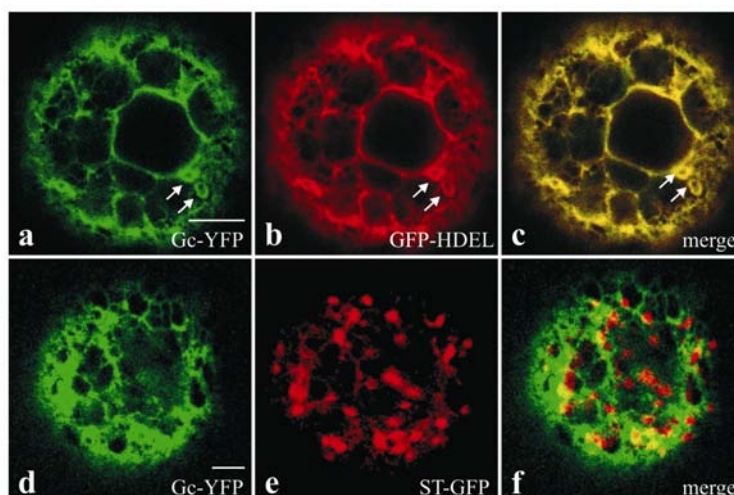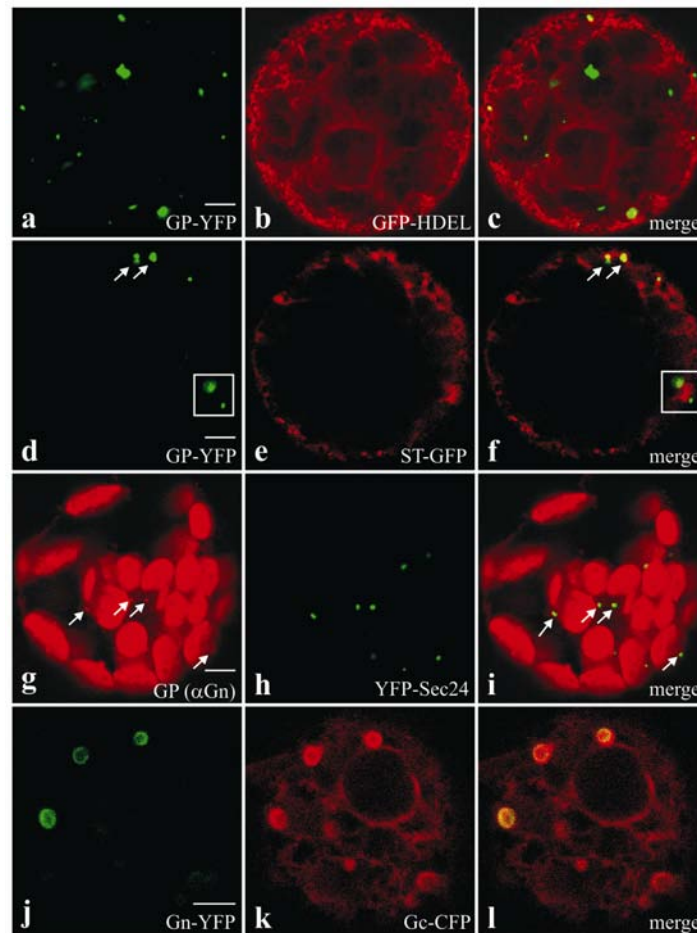**Figure 6**: Fluorescence images of *N. tabacum* protoplasts transfected with constructs coding for the glycoproteins Gn and Gc (from the common glycoprotein precursor, or independent constructs) and organelle-specific (ER, Golgi) or ERES markers. Panels a-c: protoplast transfected with GP-YFP and GFP-HDEL 24h p.t.: (a) GP-YFP (Gc-YFP), (b) GFP-HDEL, (c) merge image of a and b. Panels d-f: protoplast isolated from plants stably transformed with ST-GFP and transfected with GP-YFP 24h p.t.: (d) GP-YFP (Gc-YFP), (e) ST-GFP, (f) merge image of d and e, arrows and square indicate globular structures containing GP-YFP that, respectively, co-localize and do not co-localize with ST-GFP. Panels g-i: protoplast transfected with GP and YFP-Sec24 and immunolocalized with antibodies raised against Gc 24h p.t.: (g) Gc (GP) indicated by arrows, (h) YFP-Sec24, (i) merge image of g and h with co-localizations indicated by arrows. Panels j-l: protoplast transfected with Gn-YFP and Gc-CFP 24h p.t.: (j) Gn-YFP, (k) Gc-CFP, (l) merge image of j and k. Size bars represent 5 µm.

Since individually expressed Gn was found to localize in Golgi membranes, and previous

studies identified the Golgi complex as the viral assembly locus (Kikkert *et al.*, 1999), Golgi localization of Gc and Gn expressed from their precursor gene was analyzed. To this end, protoplasts from plants stably transformed with the ST-GFP Golgi-marker were transfected with GP-YFP. Some of the Gc-YFP processed from the precursor and localizing in globular structures co-localized with the Golgi marker (Fig. 6 d-f, arrows), but, surprisingly, some clearly did not (Fig. 6 d-f, square) (about 80% of the expressing cells contained, on average, 40% of non-colocalizing structures). To analyze whether a part of the glycoproteins would still be retained in specific domains of the ER, non fluorophore-fused GP was co-expressed with the ER export sites (ERES)-marker YFP-Sec24. After 24-48h protoplasts were harvested and subjected to immunolocalization with a primary antibody specific for Gc and a secondary antibody fused to TRITC. The results showed (Fig. 6 g-i) that part of the glycoproteins indeed co-localized with the ERES marker (whose localization pattern was in all similar to the one described by Steffano *et al.* (2006), which altogether allowed us to conclude that Gn is able to induce Gc's concentration at ER-export sites from where they co-migrate, most likely as a heterodimer, to the Golgi complex. To exclude that some of the (non-Golgi) glycoproteins would be present at the prevacuolar compartment (PVC), co-expression studies were performed with the PVC marker GFP-BP80 and, as expected, no co-localization was observed (results not shown).

When co-expressed from the common precursor gene, the glycoproteins did not seem to induce the formation of pleomorphic/circular membrane structures. However, one can not exclude the possibility that the observed (small, dense-like) globular structures (up to 1µm) may have hollow characteristics that could not be discerned as such due to the microscope resolution. Furthermore, the migration to the Golgi complex of both glycoproteins when expressed from the common precursor gene generally proceeds very quickly, when compared to the single expressions or to the co-expression from separate constructs (results not shown). To test whether the formation of these pleomorphic/circular membrane structures could be visualized upon the (kinetically slower) co-expression of the glycoproteins from separate constructs, CFP was fused to the C-terminus of Gc (Gc-CFP, Fig. 1). Confocal microscopy analysis of protoplasts transfected with Gn-YFP and Gc-CFP revealed (in about 60% of the expressing cells) the co-localization of the glycoproteins at globular structures, similar to those previously observed upon GP-YFP expression, as well as at the ER (results not shown). Furthermore (in the remaining 40% of the expressing cells), the glycoproteins were indeed also found to co-localize at pleomorphic/circular structures (Fig. 6 j-l). These results altogether demonstrate that the (pseudo-) circular and pleomorphic membrane structures can be induced by any of the glycoproteins, either when singly or co-expressed.

DISCUSSION

In this study we have, for the first time, successfully expressed the TSWV glycoproteins in plant cells without the complicating background of a full infection, and, using fluorescence microscopy techniques, described their intracellular localization and behavior *in vivo*. The data obtained demonstrated that both Gc and Gn glycoproteins, either when co-expressed from separate constructs or from their common precursor gene, are able to reach and retain at the Golgi complex. During this process Gn is able to rescue Gc from the ER, directing it to the Golgi, most

likely involving heterodimerization. Upon individual expression, Gn and Gc behave differently, i.e. Gc remains arrested in the ER whereas Gn is able to leave this organelle and target to the Golgi complex, although less efficiently than upon co-expression with Gc. These results confirm the earlier observed properties of the viral glycoproteins upon expression in mammalian cells (Kikkert *et al.*, 2001) and support the idea that, similar to what has been reported for several animal-infecting bunyaviruses (Andersson *et al.*, 1997a; Elliott, 1996; Matzuoka *et al.*, 1996; Rönnholm, 1992), the combined glycoproteins contain all information required for their transport and retention in the Golgi complex. Also for TSWV, the glycoproteins seem to guide the process of virus particle assembly.

Surprisingly, our analyses have additionally shown that both glycoproteins, either singly or co-expressed, are capable of causing membrane deformation, inducing the formation of pleomorphic, mostly circular, membrane structures. In case of individual Gc expression these structures were shown to derive from ER, whereas the ones induced by Gn derived from the Golgi. These hollow structures are apparently absent upon glycoproteins' co-expression from their common precursor. However, upon co-expression from separate constructs, these Gn- and Gc-containing membrane structures were again observed, maybe due to the slower kinetics of glycoprotein processing in this situation. Hence, it can not be excluded that the small (dense-like) globular structures containing both glycoproteins expressed from the precursor gene, may represent smaller similar structures, whose hollow characteristics could not be discerned due to the microscope's limited resolution. The same may also apply for the small Golgi-derived globular structures where Gn localizes upon single expression.

Confocal Z-stack analysis showed that, in some cases, these circular membrane structures did not seem to be completely closed. Whether this observation points towards the presence of a heterogeneous pool of membrane structures remains an interesting question to be tackled with 3D-tomography.

Modification of endomembranes has been earlier reported ((Kikkert *et al.*, 1999); Fig. 7) upon a natural TSWV infection of plants cells. In those studies, electron microscopy analysis revealed that these modifications (referred to as Paired Parallel Membranes – PPM) were always restricted to Golgi membranes and ranged in size between 100 and 300 nm. The (pseudo-)circular and pleomorphic membrane structures observed in the present study ranged in size from 1 to 4 µm whereas the small globular structures (in which no surrounding membrane could be discerned) ranged from 200 to 500 nm. Although speculative, it is tempting to hypothesize that the large membrane structures may arise as a result of membrane fusion of smaller membrane structures. Supporting data comes from studies on TSWV infected plant cells where, at a certain stage of the infection cycle, newly formed doubly enveloped virus particles (Kikkert *et al.*, 1999; Kitajima *et al.*, 1992a) fuse with each other and with ER-derived membranes, giving rise to large membrane vesicles containing accumulating amounts of mature, singly enveloped virus particles. This process suggests the viral glycoproteins' capability to induce membrane fusion, and hence could explain the formation of large, (pseudo-)circular/pleomorphic membrane structures. Another justification for the large size of these observed membrane structures may lie in induced membrane proliferation. This may be due to the accumulation of high amounts of glycoproteins at these membranes (as result of their transient expression) or reflect (on a larger scale) a naturally occurring phenomenon essential for virus assembly, as has been demonstrated for other plant and animal-infecting viruses (Barco and Carrasco, 1995; Carette *et al.*, 2002). This glycoprotein-induced membrane deformation/circularization might also reflect the formation of a spherical enveloped virus particle, as likewise proposed earlier for several other membrane

enveloped (animal-infecting) viruses (Kolesnikova *et al.*, 2004; Latham and Galarza, 2001; Shaw *et al.*, 2003). Transient expression of their glycoproteins gave rise to the formation of virus-like particles (VLPs). Some of the latter were shown to be pleomorphic in shape, not at all resembling mature virus particles, whereas in other cases VLPs were quite similar to authentic virus particles. Whether the pleomorphic membrane structures observed in this study indeed do represent TSWV VLPs, remains to be further analyzed.
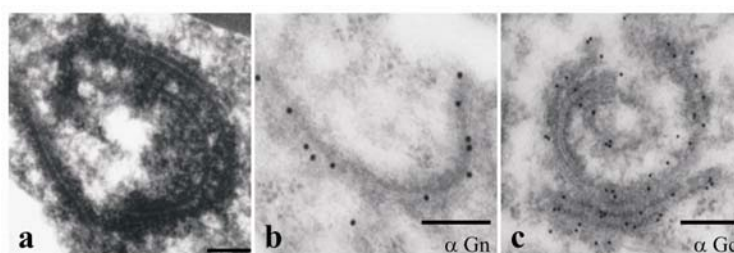

Figure 7: Electronmicrograph showing dilated Golgi stacks and paired parallel membranes in TSWV-infected *Nicotiana rustica* plant cells [with permission from Kikkert *et al.* (1999)]. (a) Curved Golgi cisternae surrounding ribonucleocapsids; immuno-gold labeling analysis with antiserum against Gn (b) and Gc (c). Size bars represent 200 nm.

The ER-arrest of Gc in the absence of Gn may be due to an improper folding and subsequent entrapment in the ER by interaction with one of the ER-resident chaperone proteins, as previously observed for Uukuniemi phlebovirus' newly synthesized Gn and Gc glycoproteins (Veijola and Pettersson, 1999).

Our studies, furthermore, demonstrate that Gn suppresses ER-arrest of Gc, most likely by heterodimerization, leading to a change of Gc's spatial distribution within the ER to ERES. Since these loci are the regions within the ER where the COPII-coated membranes and/or vesicles responsible for the ER to Golgi transport are concentrated (Hanton *et al.*, 2006), our results suggest a COPII-dependency of the glycoproteins' transport between these two organelles, that remains to be further investigated.

TSWV is special in its property to multiply and form virus particles in both plant and animal (insect vector) cells. Hence its virus assembly process bridges (and should be compatible with) these two distinct cell types. From this point of view TSWV may prove to be an interesting tool to study and compare glycoprotein behavior and cell sorting signals in relation to the endomembrane system between plant and animal cell systems.

ACKNOWLEDGEMENTS

CHAPTER 3
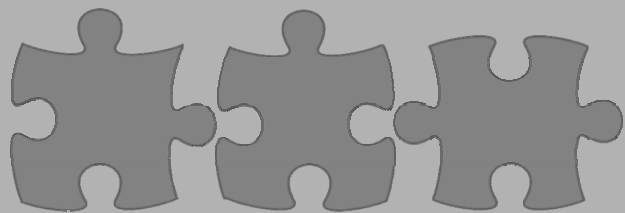
TOMATO SPOTTED WILT VIRUS NUCLEOCAPSID PROTEIN INTERACTS WITH BOTH VIRAL GLYCOPROTEINS GN AND GC

ABSTRACT

The intracellular trafficking and behavior of the Tomato spotted wilt virus (TSWV) glycoproteins Gn and Gc in the presence of the nucleocapsid protein N were studied using fluorophore-tagged constructs, and the possible interactions between these three major viral structural proteins were analyzed *in vivo* using FRET/FLIM. It was shown that the N protein co-localizes and interacts with both Gn and Gc separately, with a possible preference for Gn. Additionally it is shown that the presence of the N protein causes a dramatic change in the distribution of the glycoprotein Gc within the ER. These observations are discussed in relation to virus particle formation during the infection process.

Tomato spotted wilt virus (TSWV) is the type species of the genus *Tospovirus*, the only genus containing plant-infecting viruses among the *Bunyaviridae* (Elliott, 1990, 1996; Goldbach and Peters, 1996). Like all members of this family, TSWV's viral particles are spherical and enveloped, harboring a tri-partite RNA genome of negative or ambisense polarity. The infectious ribonucleoproteins (RNPs) are formed upon tight association of genomic RNA with the nucleocapsid protein (N) and small amounts of the viral RNA-dependent RNA polymerase (L) (Goldbach and Peters, 1996). The virally encoded glycoproteins Gn and Gc (n and c refer to the amino and carboxy-terminal topology within the precursor protein) are embedded within the particle's lipid envelope, and are required for the virus' uptake and replication in its thrips vector (Wijkamp *et al.*, 1993).

During particle assembly in plant cells, RNPs concentrate at glycoprotein-containing Golgi membranes prior to enwrapment with a (part of a) Golgi stack (Kikkert *et al.*, 1997; Kikkert *et al.*, 1999; Kikkert *et al.*, 2001; Kitajima *et al.*, 1992a; Petterson and Melin, 1996), leading to the formation of doubly enveloped virus particles (DEV). These fuse together and with ER-derived membranes, giving rise to an accumulation of mature singly enveloped virus (SEV) particles in large membrane-bound vesicles (Kikkert *et al.*, 1999).

To further unravel the complex virus assembly process, recent studies have reported the individual expression of the two envelope glycoproteins Gn and Gc, in the absence of the background of a full infection process and associated cytopathological effects (Chapter 2). These studies revealed that, in plant cells, Gn accumulates within both the ER- and Golgi-membranes whereas Gc is retained in the ER. Upon co-expression though, either from their common precursor gene or from co-transfected separate constructs, both glycoproteins are found at the Golgi complex. Furthermore, both Gn and Gc can induce the formation of (pseudo-)circular and pleomorphic membrane structures which have been postulated to reflect stages of Golgi membrane enwrapment of RNPs as observed during a natural infection of plant cells (Chapter 2, (Kikkert *et al.*, 1999; Kitajima *et al.*, 1992a)).

Recent studies in mammalian cells have shown that the localization of Gc (in the absence of Gn) within the ER altered in the presence of N, concentrating at a distinct non-Golgi perinuclear region (Snippe *et al.*, 2007b). The interaction between both proteins (as well as between N proteins (Snippe *et al.*, 2005b) was confirmed by Förster Resonance Energy Transfer (FRET) and Fluorescence Lifetime Imaging Microscopy (FLIM). In contrast, no interaction was observed between Gn and N, which altogether suggested that membrane envelopment of RNPs is triggered by an interaction between Gc and N.

In this chapter, the *in planta* localization of N and its influence on the behavior of the viral glycoproteins have been analyzed, as well as the possible interactions between these proteins using FRET/FLIM microscopy (Borst *et al.*, 2003; Gadella, 1999; Gadella *et al.*, 1999). The results obtained are discussed in relation to the genuine virus particle assembly process.

MATERIALS AND METHODS

PLASMID CONSTRUCTION AND ORGANELLE MARKERS

The previously constructed pSFV plasmids containing Gn-CFP (Snippe *et al.*, 2007b) and N, N-YFP and N-CFP (Snippe *et al.*, 2005b) were subjected to BamHI digestion, resulting in the cloning cassettes containing the respective fused and non-fused glycoproteins. The BamHI site of the multiple cloning site was used to insert these cassettes into the (previously digested and dephosphorylated) pMON999 vector (containing a 35S-driven promotor).

The pMONGP-YFP, pMONGc-YFP, pMONGn-YFP and p2GW7.0Gc-CFP plasmids used have been previously described in Chapter 2.

A plant expression vector containing the Gn-408 (p2GW7.0Gn-408) was obtained using the GATEWAY^{TM} system (Invitrogen), following the manufacturer's instructions. The primers GnFwdGW (GGGGACAAGTTTGTACAAAAAAGCAGGCTGGATGAGAATTCTAAAACTACTAGAACTAGTGG) and 408RvsGW (GACACTCTGAAGAATGGGGGACCACTTTGTACAAGAAAGCTGGGTGTCATCAGG) were used to PCR amplify Gn-408 from the pSFVGc-CFP construct (Snippe *et al.*, 2007a). The PCR fragment was introduced into pDonr207 by BP recombination and subsequently into the p2GW7.0 (Karimi *et al.*, 2002) destination vector by LR recombination.

The fluorescent proteins used in this study for fusion to the viral glycoproteins were the pH-insensitive forms of EYFP, ECFP and mGFP5 (Haseloff *et al.*, 1997). The spectral properties of mGFP5 allow efficient spectral separation from YFP (Brandizzi *et al.*, 2002b).

In these experiments we made use of the GFP-HDEL ER-marker (Carette *et al.*, 2000) and the ST-GFP Golgi-marker (Boevink *et al.*, 1998).

PLANT MATERIAL AND TRANSIENT EXPRESSION

Tobacco plants (*Nicotiana tabacum* cv Petit Havana) (Maliga *et al.*, 1973) were grown in Murashige and Skoog medium (Murashige and Skoog, 1962) and 2% sucrose in controlled sterile conditions at 25°C with a 16 hours period of light per day. Preparation and transfection of tobacco leaf protoplasts were performed as described by Denecke and Vitale (1995), with some minor modifications. In short, leaves of fully-grown plants were pierced and digested overnight in TEX [B5 salts, 500 mg/l MES, 750 mg/l CaCl$_2$·2H$_2$O, 250 mg/l NH$_4$NO$_3$, 0.4 M sucrose, pH 5.7] containing 0.2% Macerozyme and 0.4% Cellulase. The cells were recovered by filtration and washed by multiple centrifugations with Electroporation Buffer (EB) [0.4 M sucrose, 2.4 g/l HEPES, 6 g/l KCl, 600 mg/l CaCl$_2$·2H$_2$O, pH 7.2]. Healthy living protoplasts were recovered and ressuspended in the proper EB volume. 100 µl of the plasmids in EB (plasmid concentrations used depended upon experiment: 30 µg of each construct for multiple transfections and 60 µg of a singly transfected construct) was added to 500 µL of the protoplast suspension and this mixture was subjected to electroporation (160V, 925µF, ∞Ω) in 4 mm cuvettes using a BIO-RAD X-cell electroporator. After 10 min recovery, the cells were incubated in 2 mL TEX in the dark (the

incubation times differed per experiment, ranging between 12 and 48 hours, as mentioned in the figure legends).

Nicotiana tabacum plants stably expressing the Golgi-marker ST-GFP (kindly provided by Prof. Chris Hawes) were grown under the previously described conditions and the analyses were conducted in protoplasts isolated and transfected according to the previously described methodology.

SAMPLING AND IMAGING

Twenty four to forty eight hours post-transfection, the living protoplasts were isolated by centrifugation and confocal sections images were obtained using an inverted Zeiss 510 Laser Scanning Microscope and a 40x oil or 63x oil and water immersion objective.

For the imaging of the single expression of YFP-fused viral proteins, excitation lines of an argon ion laser of 488 nm were used with a 505/530 nm bandpass filter in the single-track facility of the microscope. For the imaging of the co-expressing YFP-fused and GFP-fused proteins (as well as for the imaging of the co-expressing CFP- and YFP-fused proteins), excitation lines of an argon ion laser of 458 nm for GFP (and CFP) and 514 nm for YFP were alternately used with line switching using the multi-track facility of the microscope. Fluorescence was detected using a 458/514 nm dichroic beam splitter and a 470/500 nm bandpass filter for GFP (and CFP) and a 535/590 nm bandpass filter for YFP. Appropriate controls were performed to exclude possible crosstalk and energy transfer between fluorochromes. For the simultaneous imaging of YFP and TRITC, excitation lines of an argon ion laser of 488 nm for YFP and 543 nm for TRITC were alternately used with line switching using the multi-track facility of the microscope and fluorescence was detected using a 488/543 nm dichroic beam splitter and the filters BP 505/530 nm LP 560 nm for YFP and TRITC, respectively. For the imaging of FITC, excitation lines of an argon ion laser of 488 nm were used with a 505/530 nm bandpass filter in the single-track facility of the microscope.

INDIRECT FLUORESCENCE ANALYSIS

Living protoplasts were selected as previously described and carefully placed on a microscope slide previously coated with 0.05% poly-L lysine. Approximately 5 min later, the slides were submerged in 96% ethanol where the fixation occurred for about 20 min. After a 20 min wash in PBS (0.137 M NaCl, 1.5 mM KH_2PO_4, 8.1 mM Na_2HPO_4, 2.7 mM KCl, 3.1 mM NaN_3), the protoplasts are blocked with 5% BSA in PBS for 45 min. The cells were subsequently incubated for one hour in a 1:1000 dilution of the polyclonal antibodies against N and Gn (raised in rabbit) (Kikkert *et al.*, 1997) in 1% BSA in PBS. Three washing steps of 20 min in PBS preceded one hour incubation in the dark, in a 1:100 dilution of the secondary antibody (swine anti-rabbit conjugated with Tetramethyl Rhodamine Iso-Thiocyanate, TRITC, or Fluorescein Iso-Thiocyanate, FITC) in 1% BSA in PBS. The cells were then washed with PBS in three steps of 20 min, always in the dark. Two drops of citifluor were added to the slides, before examination under an inverted Zeiss 510 Laser Scanning Microscope.

FRET/FLIM ANALYSES

FRET analysis was performed by indirect YFP excitation. Confocal images were obtained using the microscope setups previously described and the interactions were quantitatively measured by FLIM.

A combination of a BIO-RAD Radiance 2100 MP system with a Nikon TE 300 inverted microscope was used to measure FLIM. The excitation source, a Ti:Sapphire laser (Coherent Mira) was pumped by a 5 W Coherent Verdi laser, resulting in the production of pulse trains of 76 MHz (150 fs pulse duration, 860 nm centre wavelength). The excitation light was directly coupled into the microscope and focused into the sample using a CFI Plan Apochromat 60x water immersion objective lens (N.A. 1.2) Detection of fluorescent light was done using the non-descanned single photon counting detection. The FLIM experiments were performed with the use of the Hamamatsu R3809U MCP PMT, which has a typical time resolution of around 50 ps. CFP fluorescence was selected using a 480DF30 nm band-pass filter. Images with a frame size of 64*64 pixels were acquired using the Becker and Hickl SPC 830 module (Borst *et al.*, 2003), with a duration of about 200 seconds. Complete fluorescence lifetime decays were calculated per pixel and fitted using a double exponential decay model. The lifetime of one component was fixed to the value found for N-CFP (2380 ps). The mean CFP lifetime was measured for every cell, allowing the calculation of the average lifetime decrease.

RESULTS

THE TSWV NUCLEOCAPSID PROTEIN FORMS CYTOPLASMIC AGGREGATES

Prior to analyzing the possible influence of the TSWV N protein on the localization and behavior of the viral glycoproteins, the N protein was studied upon single expression in protoplasts. For easy monitoring, N was fused at its C-terminus with a YFP fluorophore (Fig.1 II) and cloned downstream of a 35S promoter. *N. tabacum* protoplasts electroporated with this construct were sampled at different times (12-48 hours) post-transfection (p.t.) and analyzed by confocal fluorescence microscopy.

N-YFP was observed in large agglomerations spread throughout the cell (Fig. 2a), which differed in size and number. No clear differences in special distribution were observed between early and later times p.t. (results not shown)

To exclude that the C-terminal fusion of YFP would affect the N protein's behavior in plant cells, protoplasts were also transfected with a non-fused N construct and analyzed by immunolocalization. (Fig. 2b). No difference in the localization pattern between N and N-YFP was detected.

To more precisely define the cellular localization of the aggregates, N-YFP was co-expressed with the ER-marker GFP-HDEL (Fig. 3a-c) and no significant co-localization was observed. Similarly, using protoplasts prepared from plants stably transformed with Golgi marker ST-GFP, no co-localization was found (Fig. 3 d-f). Together with the fact that N is produced in the cytoplasm, these results suggest that this protein assumes the expected cytoplasmic distribution.
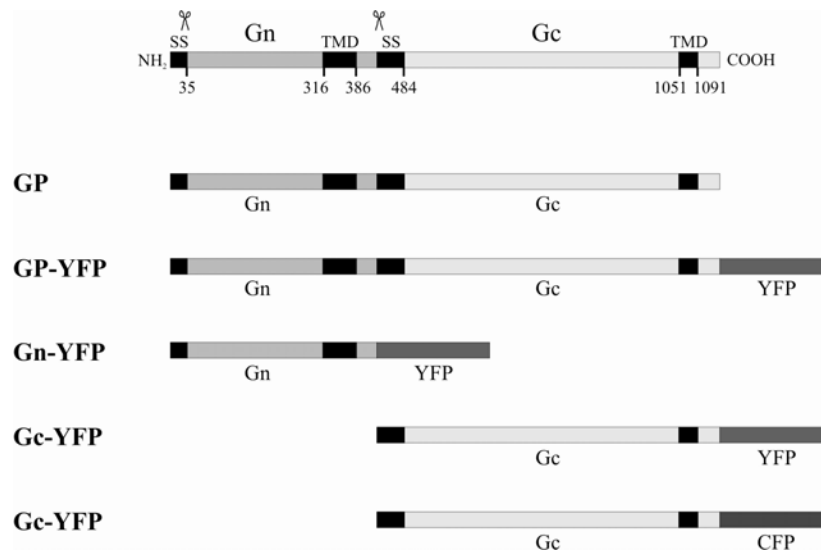
Figure 1: (I) Schematic representation of the topology of the TSWV glycoprotein precursor. (II) Constructs used for expression analysis (the glycoprotein constructs are aligned below the precursor). Predicted cleavage sites (scissor symbols), hydrophobic areas (black boxes) and aminoacid positions are indicated (SS stands for signal sequence; TMD stands for transmembrane domain). In all constructs, the YFP or CFP fluorophore was fused in frame at the position of the stop codon.
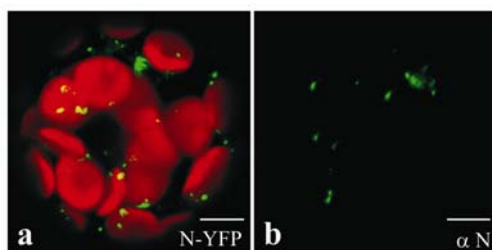
Figure 2: Localization and behavior of N in plant cells. (a) protoplast expressing N-YFP (in green) 24h p.t.; (b) protoplast expressing N 24h p.t. and immunolocalized with antibodies raised against N (FITC). Size bars represent 5 µm.

Figure 3: Localization of N in comparison with ER- and Golgi-markers. Panels a-c: protoplast transfected with N-YFP and GFP-HDEL 24h p.t.: (a) N-YFP, (b) GFP-HDEL, (c) merge image of a and b. Panels d-f: protoplast isolated from plants stably expressing ST-GFP, transfected with N-YFP 24h p.t.: (d) N-YFP, (e) ST-GFP, (f) merge image of d and e. Size bars represent 5 µm.
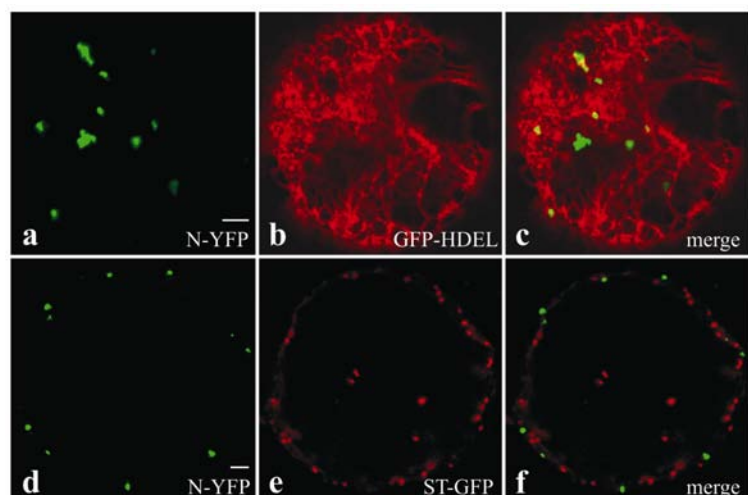
FRET/FLIM ANALYSES INDICATE STRONG HOMOTYPIC INTERACTIONS BETWEEN N PROTEINS

To analyze if the N aggregates were the result of N oligomerization, FRET and FLIM microscopy was applied. To this end, another construct was made in which the CFP was fused to the C-terminal of N (N-CFP, Fig. 1) and N-YFP and N-CFP were co-transfected into *N. tabacum* protoplasts. Confocal analysis (Fig. 4 I) showed a weaker N-CFP fluorescence in the presence of N-YFP (Fig. 4 I b), compared to the one observed upon single expression of N-CFP (data not shown). Furthermore, a high YFP fluorescence was detected upon excitation of CFP (Fig. 4 I c), suggesting the occurrence of FRET. However, this image may partially be a result of CFP crosstalk and also some YFP direct excitation, which does not allow us to accurately confirm the occurrence of an energy transfer. Hence, to further substantiate these results, FRET was measured by FLIM (Fig. 4 II). In protoplasts singly transfected with N-CFP, an average half-lifetime of 2380 picoseconds (ps) was measured, whereas in the additional presence of N-YFP, a decrease in CFP's fluorescence lifetime was observed ranging from 35 to 50 % (49% in Fig. 4 II), with an average of about 44%, confirming homodimerization of N, and N oligomerization in the large aggregates.

THE N PROTEIN CO-LOCALIZES WITH BOTH VIRAL GLYCOPROTEINS

Previous studies (Chapter 2) demonstrated that the TSWV glycoproteins, when co-expressed from their common precursor, are able to exit the ER and co-localize at the Golgi complex. To analyze whether the viral N protein would affect this translocation, GP-YFP (Fig. 1 and Chapter 2) was co-transfected with N-CFP into *N. tabacum* protoplasts. Due to processing of the precursor GP-YFP construct into mature Gc-YFP and Gn, the co-transfection allowed monitoring of Gc and N in the presence of Gn. The results showed a complete co-localization of Gc and N (Fig. 5 a-c) in structures which were smaller and with a more globular appearance than the regular cytoplasmic accumulations of N, and similar to those observed upon single GP-YFP expression (Chapter 2).

Immunolocalization experiments performed on protoplasts transfected with GP and N-YFP revealed similar results (Fig. 5 d-f), and confirmed the co-localization of Gn with Gc and N at these loci.
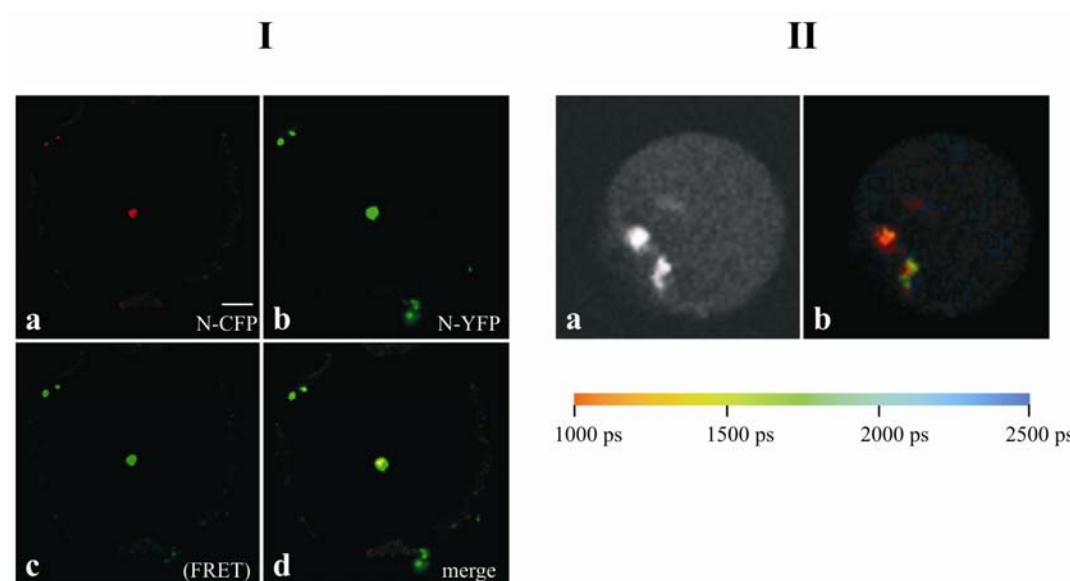
Figure 4: FRET and FLIM analysis of N homotypic interactions. (I) protoplast transfected with N-CFP and N-YFP 24h p.t.: (a) N-CFP, (b) N-YFP, (c) YFP fluorescence upon CFP excitation (indication of FRET); (d) merge image of a, b and c. (II) FLIM analysis of a protoplast transfected with N-CFP and N-YFP 24h p.t.: (a) N-CFP fluorescence image, (b) color-coded image of CFP lifetime. The colored legend indicates the CFP lifetime in ps. The CFP lifetime measured upon single N-CFP expression equals 2380 ps (results not shown). Size bar represents 5 µm.
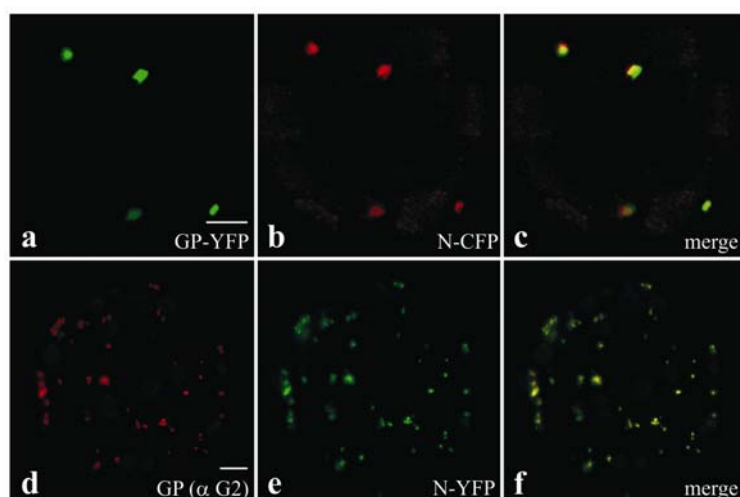
Figure 5: Localization and behavior of N co-expressed with GP in plant cells. Panels a-c: protoplast transfected with N-CFP and GP-YFP 24h p.t.: (a) GP-YFP (Gc-YFP), (b) N-CFP, (c) merge image of a and b. Panels d-f: protoplast transfected with N-YFP and GP and immunolocalized with antibodies against Gn 24h p.t.: (d) Gn (TRITC), (e) N-YFP, (f) merge image of d and e. Size bars represent 5 µm.

Gc AND N INTERACT IN THE PRESENCE OF Gn

To verify whether the co-localization of Gc and N, in the presence of Gn, was due to a direct interaction between these proteins, protoplasts were transfected with GP-YFP (producing free Gc-YFP and Gn) and N-CFP and analyzed by FRET/FLIM (Fig. 6).

Confocal analysis (Fig. 6 I) showed a weaker N-CFP fluorescence in the presence of GP-YFP (Fig. 6 I a), compared to the one observed upon single expression of N-CFP (data not shown). Furthermore, a high YFP fluorescence was detected upon excitation of CFP (Fig. 6 I c), suggesting the occurrence of FRET. However, as previously explained, this result does not allow us to accurately confirm the occurrence of an energy transfer. To further substantiate these observations and quantify this energy transfer, FLIM was performed. Repeated experiments revealed a 30-50% decrease of CFP lifetime with an average of about 38%. The example shown in figure 6 II revealed a decrease in CFP lifetime from 2380 ps to 1264 ps, corresponding to a 46.8% decrease. Altogether, these data pointed towards an interaction between Gc-YFP and N-CFP in the presence of Gn.

N CO-LOCALIZES AND INTERACTS WITH Gn, EXCEPT WITHIN THE PLEOMORPHIC MEMBRANE STRUCTURES

Since N co-localized with both glycoproteins, exhibiting an interaction with Gc, the question arose if and how N would affect the behavior of the glycoproteins when these would be singly expressed. To this end, *N. tabacum* protoplasts were co-transfected with fluorophore fusion constructs of Gn and N (Gn-YFP and N-CFP or Gn-CFP and N-YFP; Fig. 1) and analyzed by confocal microscopy. The results did not differ between these two combinations and are shown in Figure. 7. In Chapter 2 it was shown that upon single expression of Gn, this protein localized in the ER (at early times p.t.) or in the Golgi (at later times p.t.) either in small dense globular structures or in pleomorphic/circular (Gn-induced) membrane structures. Here it is shown that, in the presence of the N protein, this distribution pattern does not alter, and N co-localized with Gn either at the ER (Fig.7 a-c), or in the small Golgi-derived globular structures (Fig. 7 d-f). However, no co-localization was observed between N and Gn-induced pleomorphic membrane structures (Fig. 7 g-i), although N was mostly found in the proximity of these structures.

To analyze whether the observed co-localization between Gn and N was due to a direct interaction between these proteins, FRET and FLIM analyses were performed. FRET experiments suggested an interaction between Gn and N when co-localizing within the dense Golgi-derived globular structures (Fig. 8I). Subsequent FLIM analysis showed an approximate 12% decrease in the lifetime of CFP when Gn and N were co-expressed, suggesting an interaction. As expected, no positive FRET/FLIM results were obtained between these proteins, when Gn localized within the Golgi-derived pleomorphic membrane structures (results not shown).

Figure 6: FRET and FLIM analysis of N-Gc interactions in the presence of Gn. (I) protoplast transfected with N-CFP and GP-YFP 24h p.t.: (a) N-CFP, (b) GP-YFP (Gc-YFP), (c) YFP fluorescence upon CFP excitation (indication of FRET); (d) merge image of a, b and c. (II) FLIM analysis of a protoplast transfected with N-CFP and GP-YFP 24h p.t.: (a) N-CFP fluorescence image, (b) color-coded image of CFP lifetime. The colored legend indicates the CFP lifetime in ps. The CFP lifetime measured upon single N-CFP expression equals 2380 ps (results not shown). Size bar represents 5 µm.
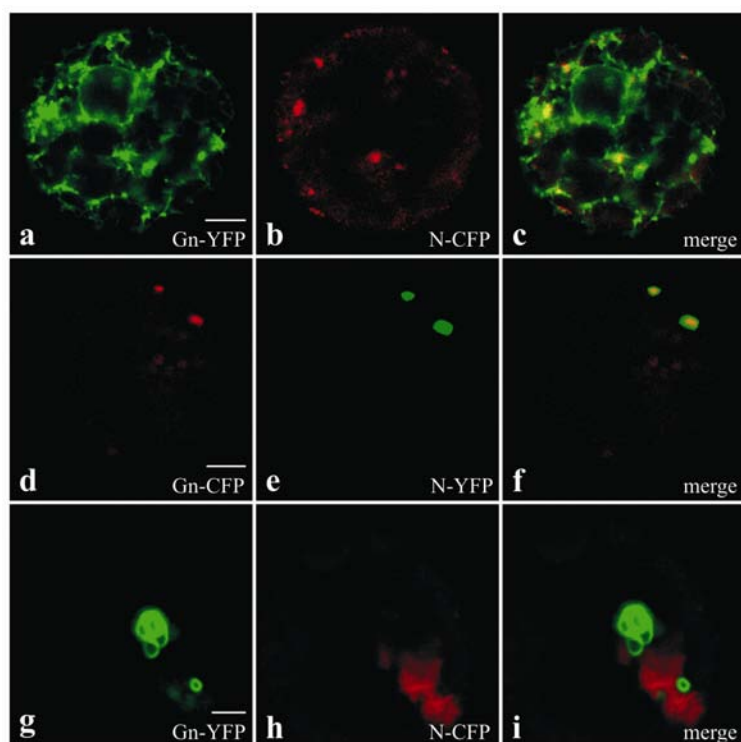
Figure 7: Localization and behavior of N co-expressed with Gn in plant cells. Panels a-c: protoplast transfected with Gn-YFP and N-CFP 24h p.t.: (a) Gn-YFP, (b) N-CFP, (c) merge image of a and b. Panels d-f: protoplast transfected with Gn-CFP and N-YFP at 48h p.t.: (d) Gn-CFP, (e) N-YFP, (f) merge image of d and e. Panels g-i: protoplast transfected with Gn-YFP and N-CFP at 48h p.t.: (g) Gn-YFP, (h) N-CFP, (i) merge image of g and h. Size bars represent 5 µm.
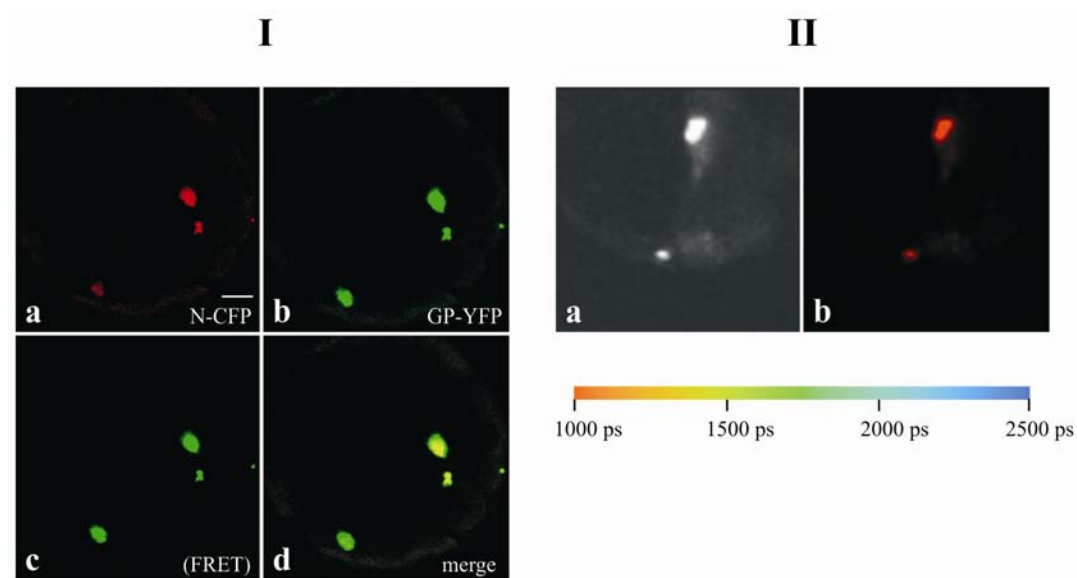
Figure 8: FRET and FLIM analysis of N-Gn interaction. (I) protoplast transfected with Gn-CFP and N-YFP 24h p.t.: (a) Gn-CFP, (b) N-YFP, (c) YFP fluorescence upon CFP excitation (indication of FRET); (d) merge image of a, b and c. (II) FLIM analysis of a protoplast transfected with N-CFP and Gn-YFP 24h p.t.: (a) N-CFP fluorescence image, (b) color-coded image of CFP lifetime. The colored legend indicates the CFP lifetime in ps. The CFP lifetime measured upon single N-CFP expression equals 2380 ps (results not shown). Size bar represents 5 µm.
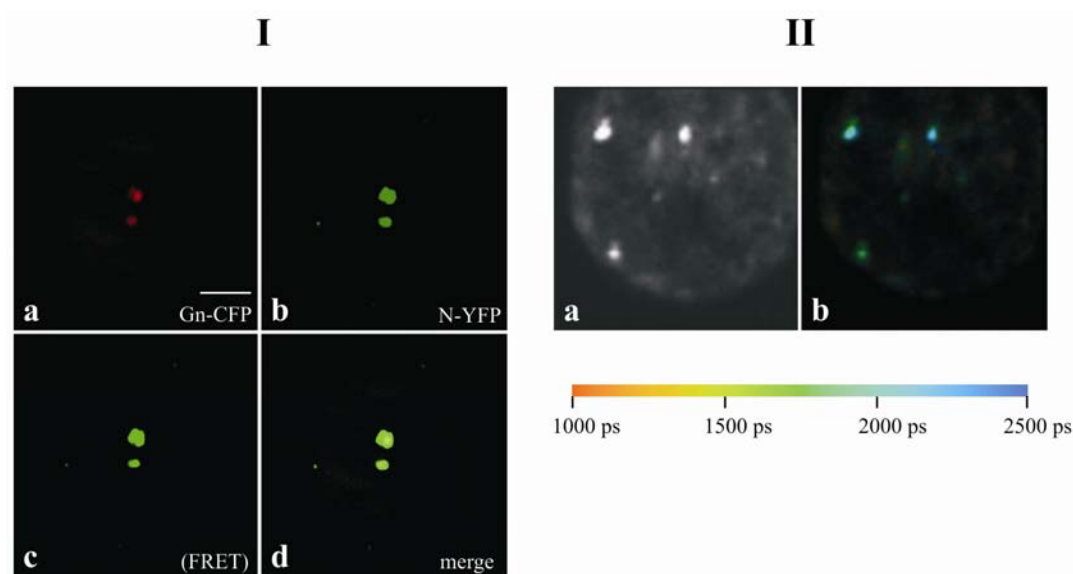
N INTERACTS WITH SINGLY EXPRESSED Gc AND DRASTICALLY ALTERS ITS SPATIAL DISTRIBUTION WITHIN THE ER

In analogy to Gn, the behavior of singly expressed Gc in the presence of N was analyzed. To this end, *N. tabacum* protoplasts were co-transfected with Gc-YFP (Fig. 1) and N-CFP. Unfortunately, in several independent experiments both proteins were never observed in the same cell, most likely due to a quenching phenomenon resulting from the interaction between these two proteins. In these experiments, the fluorophore fused to the N could always be observed but not the one fused to Gc (both reciprocal fluorophore fusion constructs were tested, results not shown). Since no quenching was observed (and a clear interaction was measured) between Gc and N when co-expressed in the presence of Gn, the quenching is maybe due to a different folding of Gc in the absence of Gn. Altogether, these observations strongly point towards the occurrence of an interaction between Gc and N, even in the absence of Gn.
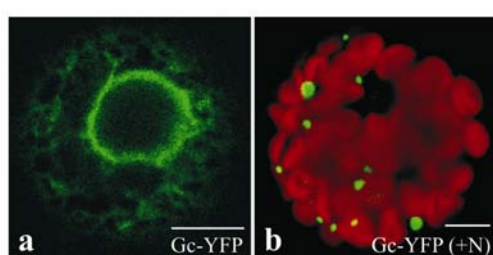

Figure 9: Distribution pattern of Gc's localization in the absence and presence of N. (a) protoplast transfected with Gc-YFP 24h p.t., (b) protoplast transfected with Gc-YFP (in green) and N 24h p.t.. Size bars represent 5 µm.

In order to avoid quenching and enable visualization of Gc's cellular distribution in the presence of N, Gc-YFP was co-expressed with a non-fused N protein. Surprisingly, a dramatic change in the localization of Gc was observed (Fig. 9). Whereas, when individually expressed, Gc was found spread all over the ER (Fig. 9a and Chapter 2) and, in some cases, in ER-derived Gc-induced pleomorphic membrane structures (Chapter 2), in the presence of N the glycoprotein was observed entirely concentrated in specific clusters, independent of the time p.t. (Fig. 9b). Immunolocalization analysis showed that N co-localized with Gc in all those clusters (Fig. 10 a-c). Furthermore, upon co-expression with N, the expression level of Gc (based on the percentage of cells in which the glycoprotein could be detected) increased about 10 fold, apparently due to a stabilizing interaction between these proteins.

To analyze whether Gc and N co-localized at Golgi-derived globular structures similar to those observed upon co-expression of Gn and N, protoplasts of plants stably transformed with ST-GFP Golgi marker were transfected with Gc-YFP and N. No co-localization between Gc-YFP and the Golgi-marker was observed (Fig. 10 d-f) suggesting that Gc-YFP was still located within the ER. To verify this hypothesis, protoplasts were co-transfected with Gc-YFP, N and an ER marker GFP-HDEL (Fig. 10 g-i) and some co-localization could be observed. This dramatic change of Gc's localization within the ER in the presence of N, together with their co-localization, strongly indicates an interaction between these two proteins.

N SEEMS TO PREFERENTIALLY INTERACT WITH Gn

Since the N protein appears to be able to interact separately with both Gn and Gc, a competition experiment was designed to identify the difference in affinity between the glycoproteins for the interaction with N. Earlier studies aimed to map the Golgi retention signal in the cytoplasmic tail of Gn (Snippe *et al.*, 2007a) and rendered a mutant, denoted Gn-408 (Fig. 1), that was still able to target to the Golgi but lacked the capacity to interact with Gc and thereby redirect this protein to the Golgi. Co-expression of N-fluorophore, Gc-CFP (Fig. 1) and Gn-408 would then result in the presence of Gc in the ER, Gn-408 in the Golgi. In this situation, the preference for interaction with any of these glycoproteins could be judged by the localization of N. However, this experiment could not be performed due to the quenching observed when Gc-CFP was co-expressed with a fluorophore-fused N. Hence, the co-transfection experiment was performed with a non-fused N gene construct and the interaction between Gc-CFP and (non-fused-) N was monitored by the occurrence of the previously described dramatic change in the distribution of Gc from reticular to punctate spots. The expression levels (based on the percentage of cells in which the glycoproteins could be detected) of both Gc-CFP and Gn-408 (YFP) were very low upon single expression. However, their expression level dramatically raised in the additional presence of N, likely due to stabilization upon interaction (data not shown). Since no fluorophore could be fused to N during the triple expression experiments (due to the previously described quenching of Gc-CFP) the visualization of the results would imply an immunolocalization procedure. However, the strong increase on the glycoproteins' expression levels upon co-expression with N could be considered, by itself, as an indication of interaction and stabilization. Indeed, upon co-transfection of *N. tabacum* protoplasts with all three constructs, Gc-CFP, Gn-408 (YFP) and N, to our surprise 95% of the observed cells hardly showed Gc-CFP

fluorescence but only a clear and strong Gn-408 YFP signal (Fig. 10) (the expression levels resulting form this combination reach 75%), suggesting that the N-Gn interaction may to be favored.
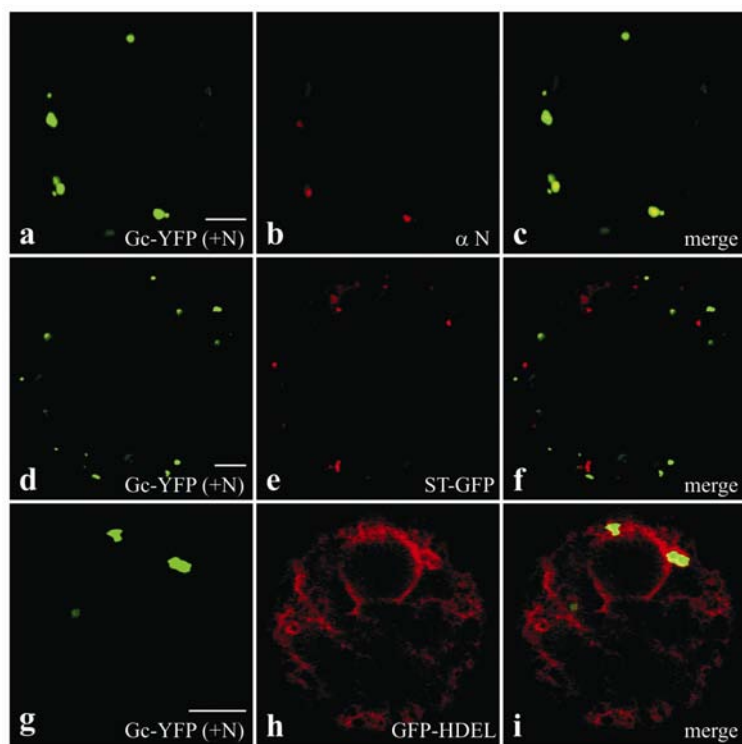
Figure 10: Localization and behavior of Gc co-expressed with N in plant cells. Panels a-c: protoplast transfected with Gc-YFP and N and immunolocalized with antibodies against N 24h p.t.: (a) Gc-YFP, (b) N (TRITC), (c) merge image of a and b. Panels d-f: protoplast isolated from plants stably expressing ST-GFP, transfected with Gc-YFP and N 24h p.t.: (d) Gc-YFP, (e) ST-GFP, (f) merge image of d and e. Panels g-i: protoplast transfected with Gc-YFP, N and GFP-HDEL 24h p.t.: (g) Gc-YFP, (h) GFP-HDEL, (i) merge image of g and h. Size bars represent 5 µm.
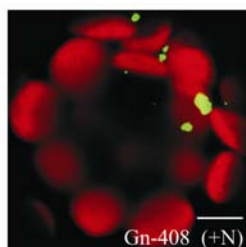
Figure 11: *N. tabacum* protoplast transfected with the Gn-408 mutant (in green) and N, 24h p.t.. Size bar represents 5 µm

DISCUSSION

In this Chapter, the influence of the TSWV N protein on the localization and behavior of the viral envelope glycoproteins in plant cells was analyzed. In Chapter 2 it was shown that Gc, expressed in the absence of any other viral protein, is retained in the ER and is only able to migrate to the Golgi complex upon co-expression with Gn, whereas Gn on its own is able to migrate from the ER to the Golgi. Furthermore, both glycoproteins were shown to induce the formation of ER- or Golgi-derived circular/pleomorphic membrane structures.

Here it is shown that co-expression of the Gc and Gn glycoproteins in the presence of N (thereby better resembling a situation similar to the natural viral assembly) did not change their localization patterns and a complete co-localization between these three proteins was observed and postulated to occur at the Golgi complex, the natural assembly locus for virus particle formation. Furthermore, by FRET/FLIM analysis a direct interaction and a very close proximity between Gc and N in the presence of Gn (with donor lifetime decrease up to 38%) was confirmed. N also did not influence the localization profile of Gn. When expressed by itself, Gn localizes in the ER and later in the Golgi in small dense globular structures or in pleomorphic Gn-induced Golgi-derived membrane structures (Chapter 2). Here, it is demonstrated that N and Gn co-localize whenever Gn is present in the ER or in dense globular structures in the Golgi. However, N does not co-localize with Gn when this glycoprotein is found at the Golgi-derived pleomorphic membrane structures, although being always present in very close proximity. Coherently, FRET/FLIM analyses indicate an interaction between Gn and N, except when Gn is present in the pleomorphic membrane structures. The measured interactions ranged around 12% of donor's lifetime decrease which is significantly lower than what was measured for N-N and Gc-N (in the presence of Gn), indicating a larger distance between the fluorophores associated with Gn and N. These results were quite surprising as previous studies (Snippe *et al.*, 2007b) performed in mammalian cells did not reveal the occurrence of this interaction.

One of the most surprising observations obtained in the present study resulted from the co-expression of N and Gc. Whereas upon single expression, Gc localizes all over the ER (Chapter 2), co-expression with N caused a major relocalization of Gc to specific regions within this organelle where both proteins co-localized. In the context of viral assembly, in which the three structural proteins (Gc, Gn and N) eventually have to concentrate in the Golgi complex, it is tempting to hypothesize that these specific ER regions correspond to ER export sites, discrete ER domains where the COPII coated membranes and/or vesicles responsible for the ER to Golgi transport are concentrated (Hanton *et al.*, 2006). This possibility would also explain the observed non-complete co-localization between Gc-YFP (in the presence of N) and the ER marker, since this is also often observed between ER and ERES markers. In this situation, N could be responsible for concentrating the glycoproteins at these areas, aiding on their route to the Golgi complex.

Unfortunately, no FRET/FLIM analyses could be performed to study the interaction between Gc and N, due to a quenching of the fluorophore fused to the glycoprotein, suggesting a change in the folding of Gc upon interaction with N. In the presence of Gn (as a third protein) this quenching was somehow overcome, likely due to a conformational change in Gc.

Although we could not apply FRET/FLIM to prove Gc-N interaction in the absence of Gn, the dramatic change in the distribution (and expression level) of Gc within the ER in the presence of N, their co-localization, the clear interaction detected between these proteins in the additional

presence of Gn and the previous results on mammalian cells that positively identified this interaction (Snippe *et al.*, 2007b), strongly indicate an interaction between these two proteins.

Single expression of the N protein resulted in the formation of agglomerations randomly distributed throughout the cytoplasm. These agglomerations were due to oligomerization of N monomers, involving a clear interaction as demonstrated by FLIM, where up to 50% decrease in donor lifetime was observed. This oligomerization capacity of the nucleocapsid protein has also been demonstrated for several animal-infecting bunyaviruses (Alfadhli *et al.*, 2001; Kaukinen *et al.*, 2001; Leonard *et al.*, 2005). For TSWV, it was also shown to occur *in vitro* (Uhrig *et al.*, 1999) and *in vivo* (Snippe *et al.*, 2005b) in mammalian cells. However, in the latter case a much lower decrease in lifetime of the donor fluorophore was reported (~20%). How N is able to translocate from its random cytoplasmic distribution to eventually co-localize with Gn and/or Gc at ER and Golgi, is still unclear and remains to be investigated.

Also very surprising were the results from a competition experiment in which N was offered the possibility to interact with either Gc and/or Gn-408, a mutant containing a C-terminal truncation that rendered this Gn-derivative incompetent to interact with and thereby rescue Gc from the ER to the Golgi (Snippe *et al.*, 2007a). The idea was that once all three constructs were co-transfected, N would either show up co-localizing with Gc (changing its localization from a reticular pattern into punctate spots) or with Gn and thereby exhibit its preference for one of the two glycoproteins. Due to the quenching problem denoted earlier, a non fluorophore-fused N construct was co-expressed with Gc-CFP and Gn-408 (YFP). Since the latter two proteins normally expressed in very low levels (often almost undetectable) but in the presence of N appeared to highly stabilize, the presence of a CFP or YFP signal would betray the preference of N for Gc or Gn-408, respectively. Unexpectedly, co-transfection of all three constructs showed an increase in the expression of Gn-408 from 2-5% to more than 80%, while almost no Gc-CFP could be observed. This indicated a strong preference of N for Gn-408, and additionally demonstrated that the C-terminal 20 aa of Gn are not required for the interaction with N. Whether the truncation of Gn-408 stabilized the interaction with N in comparison to wild type Gn remains to be investigated.

As mentioned before, similar interactions and co-localization studies have been earlier performed in mammalian cells (Snippe, 2006). Interestingly, some similarities but also some differences were observed between plant and mammalian cell systems. The main difference observed is the occurrence of an interaction between N and Gn in plants cells. A poor co-localization and FRET/FLIM analyses between N and Gn (Snippe *et al.*, 2007b), have clearly shown that these proteins do not interact in mammalian cells. Another striking difference is the dramatic change in Gc distribution within the plant ER in the presence of N (from reticular to punctate spots). In mammalian cells, a change in Gc's distribution within the ER is also observed but does not result in punctate loci. In mammalian cells, Gc (when singly expressed) is found in the ER, all over the cell. Upon co-expression with N, its localization changes to a perinuclear area where these two proteins co-localize. Also differences in protein folding are found between these two types of cells: the quenching phenomenon observed in plant cells upon co-expression of fluorophore-fused Gc and N does not occur in mammalian cells.

These marked differences may reflect the different virus particle assembly mechanisms occurring in plant and insect (animal) cells. In plant cells, this process involves enwrapment of (a part of) a (viral glycoproteins-containing) Golgi stack around the viral RNPs, forming doubly enveloped virus particles that will ultimately become singly enveloped by fusion with other membranes and accumulate in large vesicles within the cytoplasm. This phenomenon does not

occur in insect cells where, similarly to the animal bunyaviruses in their mammalian hosts, the virus particles are secreted. These different fates of assembled TSWV particles, together with the differences in cellular architecture and organization of the endomembrane system of plant and animal cells, may explain the encountered results, reflecting an adaptation of the virus to the replication and particle formation in the two distinct types of cells.

ACKNOWLEDGEMENTS

CHAPTER 4
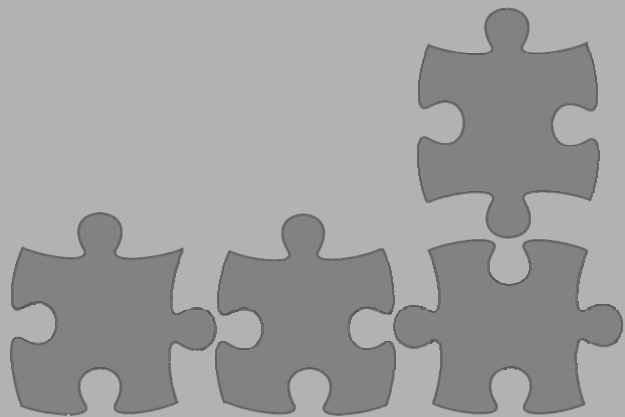
LIMITED INVOLVEMENT OF CYTOSKELETON ELEMENTS IN THE CLUSTERING OF TSWV STRUCTURAL PROTEINS

ABSTRACT

Expression studies in plant protoplasts have shown that upon co-expression of the Tomato spotted wilt virus (TSWV) structural proteins, the cytoplasmic nucleocapsid (N) protein co-localizes and interacts with both viral glycoproteins (Gn and Gc) at the endoplasmic reticulum (ER) and/or Golgi complex (Chapter 3). Furthermore, in the absence of Gn, N was shown to induce the redistribution of Gc within the ER, inducing its concentration at specific ER domains. In this study we have applied specific inhibitors to analyze the possible involvement of microtubules and actin filaments in these processes. The formation of large cytoplasmic agglomerations of N was found to be actin-dependent but microtubule-independent. In contrast, the trafficking of N to the ER and Golgi to interact with the glycoproteins, as well as the re-distribution of Gc within the ER, was not affected by interference with the microtubule- or actin network. The results indicate that the cytoskeleton does not play a major role during TSWV particle formation in plant cells.

INTRODUCTION

For many enveloped viruses, various steps within the process of particle assembly remain an enigma. Enveloped viruses usually obtain their lipid membranes by budding into one of the cellular membranes. Viruses of the large family of arthropod-borne *Bunyaviridae*, whose members are primarily restricted to animal-infecting viruses (Elliott, 1990, 1996; Goldbach and Peters, 1996), obtain their lipid envelop from the Golgi complex, and the virus particles are secreted from the cell by transport from the Golgi to the plasma membrane (Elliott, 1996; Griffiths and Rottier, 1992; Petterson and Melin, 1996).

During Tomato spotted wilt virus (TSWV, a plant-infecting member of the *Bunyaviridae)* particle assembly in plant cells, ribonucleoproteins (RNPs) are enwrapped by Golgi cisternae that contain the two viral glycoproteins (denoted Gn and Gc), giving rise to doubly enveloped virus particles (DEVs). These fuse with each other and ER-derived membranes and lead to the accumulation of mature singly enveloped virus particles (SEVs) clustered inside large vesicles that retain in the cytoplasm until uptake by its insect vector (Kikkert *et al.*, 1997; Kikkert *et al.*, 1999; Kikkert *et al.*, 2001; Petterson and Melin, 1996). In insect cells, enwrapment of RNPs has never been observed, but mature virus particles are being secreted from the salivary gland cells (the primary site of replication) into the salivary gland ducts. Hence, TSWV particle assembly in insect cells resembles that of the animal-infecting bunyaviruses, where secretion of mature virus particles from the cell is also observed (Elliott, 1996; Griffiths and Rottier, 1992; Petterson and Melin, 1996).

Since the viral glycoproteins are the key mediators in the process of particle assembly and release, they have been the focus of intense studies for different animal-infecting bunyaviruses. These studies revealed that (for most bunyaviruses) Gc is arrested in the ER but upon co-expression with Gn becomes redirected to the Golgi, likely due to heterodimerisation (Chen *et al.*, 1991; Lappin *et al.*, 1994; Matsuoka *et al.*, 1988). Their accumulation and retention in the Golgi is due to the presence of a Golgi retention signal in Gn (Andersson *et al.*, 1997b; Gerrard and Nichol, 2002; Shi *et al.*, 2004) and budding of RNPs into the lumen of the Golgi is assumed to be triggered by a specific interaction between the cytoplasmic tail of one of the glycoproteins (Andersson *et al.*, 1997a) and a structural component of the RNPs, likely the nucleocapsid protein. Prior to this, RNPs have to concentrate at glycoprotein-containing loci in the Golgi complex. For several bunyaviruses, RNPs were observed to accumulate in a perinuclear region and co-localize with interferon-induced MxA, which led to the suggestion that perinuclear RNP sequestering might be the result of an antiviral defense response (Andersson *et al.*, 2004a). On the other hand, in animal cells, the Golgi complex localizes in a perinuclear region, thus constituting a perfect site for particle assembly to take place.

The TSWV glycoproteins exhibit a similar trafficking behavior in mammalian cells, and a Golgi retention signal was mapped at the cytoplasmic tail and transmembrane domain of Gn (Snippe *et al.*, 2007a). An interaction between N and Gc was suggested to trigger Golgi-membrane envelopment of RNPs based on the occurrence of an interaction measured *in vivo* by Förster Resonance Energy Transfer (FRET) and Fluorescence Lifetime Imaging Microscopy (FLIM) (Snippe *et al.*, 2007b). Furthermore, in mammalian cells, transiently expressed TSWV N has been shown to accumulate as large aggregates in a non-Golgi perinuclear region, and this perinuclear accumulation required active microtubules and actin filaments (Snippe *et al.*, 2005b). Upon co-expression of N and Gc, both proteins similarly accumulate in a

perinuclear region, likely also in a microtubules/actin dependent way (Snippe *et al.*, 2007b).

In Chapter 2 was shown that, in plant cells, transiently expressed TSWV glycoprotein Gc is retained in the ER, unless upon co-expression with Gn which renders its co-translocation to the Golgi complex. Furthermore, the results indicated that Gc and Gn have the capability to induce, respectively, ER and Golgi membrane deformation, forming (pseudo-) circular and pleomorphic membrane structures (Chapter 2). Also in plant cells, the N protein gives rise to the formation of large aggregates. These do not accumulate in a perinuclear region as in mammalian cells, nor co-localize with ER or Golgi but are found randomly scattered throughout the cytoplasm (Chapter 3). Interactions were demonstrated by FRET- FLIM between both glycoproteins and N at ER and Golgi and, upon co-expression with N, a redistribution of Gc within the ER, from reticular to punctate spots was also observed (Chapter 3).

Not much is known on how TSWV N is able to move through the cytoplasm of plant cells to form agglomerations and to reach the glycoproteins in the ER and/or Golgi complex. Elements of the cytoskeleton, specifically actin and microtubules, have earlier been demonstrated to be involved in the intracellular trafficking of RNPs or N from animal-infecting bunyaviruses (Andersson *et al.*, 2004b; Ramanathan *et al.*, 2007; Ravkov *et al.*, 1998). Also for plant viruses, the cytoskeleton has been reported to play an important role (Ashby *et al.*, 2006; Boyko *et al.*, 2000; Laporte *et al.*, 2003; Reichel *et al.*, 1999; Seemanpillai *et al.*, 2006; Wright *et al.*, 2007). Since TSWV N forms large perinuclear accumulations (near the Golgi) in a microtubule- and actin-dependent manner in mammalian cells (Snippe *et al.*, 2005b) the question arose whether this dependency would also occur in plant cells.

Whereas in previous Chapters (2 and 3) transient expression of the viral structural proteins (N, Gc, Gn) in plant protoplasts have helped to reconstruct the initial part of the particle assembly mechanism, in this Chapter, the involvement of cytoskeleton elements in the intracellular trafficking and clustering of these proteins at the organelles involved in particle assembly are analyzed. To this end, specific inhibitors of microtubules and actin polymerization have been employed to study the role of these cytoskeleton elements in the N protein's distribution within the cytoplasm of the plant cell, as well as in its trafficking to the elements of the secretory pathway where interaction with the viral glycoproteins occurs. Furthermore, FRET-FLIM (Borst *et al.*, 2003; Gadella, 1999; Gadella *et al.*, 1999; Hink *et al.*, 2002) has been applied to investigate the occurrence of protein interactions in the absence of actin or microtubules.

MATERIALS AND METHODS

PLANT MATERIAL, TRANSIENT EXPRESSION AND TREATMENTS

Tobacco plants (*Nicotiana tabacum* cv Petit Havana) (Maliga *et al.*, 1973) were grown in Murashige and Skoog medium (Murashige and Skoog, 1962) and 2% sucrose in controlled sterile conditions at 25°C with a 16 hours period of light per day. Tobacco leaf protoplasts preparation and transfection were performed as described by Denecke and Vitale (1995), with some minor modifications. In short, leaves of fully-grown plants were pierced and digested overnight in TEX [B5 salts, 500 mg/l MES, 750 mg/l $CaCl_2 \cdot 2H_2O$, 250 mg/l NH_4NO_3, 0.4 M sucrose, pH 5.7]

containing 0.2% Macerozyme and 0.4% Cellulase. Protoplasts were recovered by filtration and washed by multiple centrifugations with Electroporation Buffer (EB) [0.4 M sucrose, 2.4 g/l HEPES, 6 g/l KCl, 600 mg/l $CaCl_2·2H_2O$, pH 7.2]. Healthy living protoplasts were recovered and ressuspended in the proper EB volume. A hundred µl of the plasmids (30 µg of each) in EB is added to 500 µL of the protoplast suspension and this mixture is subjected to electroporation (160V, 925µF, ∞Ω) in 4 mm cuvettes using a BIO-RAD X-cell electroporator. After 10 min recovery, the treatments were applied and the protoplasts were incubated in 2 mL TEX in the dark (the incubation times differed per experiment, ranging between 24 and 48 hours). Several concentrations of colchicine (Duchefa) and cytochalasin D (Sigma) were applied and time-course analyses were performed in order to establish an optimal concentration for this specific type of cells and conditions. In the experiments presented in this chapter, the final concentrations of 100 µM of colchicine and 20 µM of cytochalasin D were applied.

The fluorescent proteins used in this study were the pH-insensitive forms of EYFP, ECFP and mGFP5 (Haseloff *et al.*, 1997). The spectral properties of mGFP5 allow efficient spectral separation from YFP (Brandizzi *et al.*, 2002b).

In these experiments we made use of GFP-α-tubulin, a marker of the microtubule network) (Kumagai *et al.*, 2001).

SAMPLING AND IMAGING

Twenty four to forty eight hours post-transfection (p.t.), the living protoplasts were isolated by centrifugation and confocal sections images were obtained using an inverted Zeiss 510 Laser Scanning Microscope and a 40x oil or 63x oil and water immersion objective.

For the imaging of the single expression of YFP-fused viral proteins, excitation lines of an argon ion laser of 488 nm were used with a 505/530 nm bandpass filter in the single-track facility of the microscope. For the imaging of the co-expressing YFP-fused and CFP-fused (as well as YFP-fused and GFP-fused) proteins, excitation lines of an argon ion laser of 458 nm for CFP (and GFP) and 514 nm for YFP were alternately used with line switching using the multi-track facility of the microscope. Fluorescence was detected using a 458/514 nm dichroic beam splitter and a 470/500 nm bandpass filter for CFP (and GFP) and a 535/590 nm bandpass filter for YFP. Appropriate controls were performed to exclude possible crosstalk and energy transfer between fluorochromes.

QUANTITATIVE AND STATISTICAL ANALYSIS

The quantitative analysis of the number and size of N agglomerations present in protoplasts upon treatment with the inhibitor and in non-treated cells was performed on a total of 70 cells per treatment. The sizes of the agglomerations were divided into 4 categories: 0-1 µm, 1-3 µm, 3-4 µm and > 4 µm. The number of N-YFP agglomerations per protoplast were counted and divided into 5 categories: 1-5, 6-10, 11-15, 16-20 and >20. The Mann-Whitney U test was applied and the significance level was set at 0.05 (Ott and Longnecker, 2001)

FRET/FLIM ANALYSES

FRET analysis was performed by indirect YFP excitation. Confocal images were obtained using the microscope setups previously described and the interactions were quantitatively measured by FLIM.

A combination of a BIO-RAD Radiance 2100 MP system in with a Nikon TE 300 inverted microscope was used to measure FLIM. The excitation source, a Ti:Sapphire laser (Coherent Mira) was pumped by a 5 W Coherent Verdi laser, resulting in the production of pulse trains of 76 MHz (150 fs pulse duration, 860 nm centre wavelength). The excitation light was directly coupled into the microscope and focused into the sample using a CFI Plan Apochromat 60x water immersion objective lens (N.A. 1.2) Detection of fluorescent light was done using the non-descanned single photon counting detection. The FLIM experiments were performed with the use of the Hamamatsu R3809U MCP PMT, which has a typical time resolution of around 50 ps. CFP fluorescence was selected using a 480DF30 nm band-pass filter. Images with a frame size of 64*64 pixels were acquired using the Becker and Hickl SPC 830 module (Borst *et al.*, 2003), with a duration of about 200 seconds. Complete fluorescence lifetime decays were calculated per pixel and fitted using a double exponential decay model. The lifetime of one component was fixed to the value found for N-CFP (2380 ps). The mean CFP lifetime was measured for every cell, allowing the calculation of the average lifetime decrease.

RESULTS

N PROTEIN'S DISTRIBUTION WITHIN THE CYTOPLASM IS ACTIN-DEPENDENT BUT MICROTUBULE-INDEPENDENT

To investigate a possible dependence of TSWV N protein trafficking and behavior on cytoskeleton elements, N. tabacum protoplasts were co-transfected with YFP-fused N (N-YFP, Chapter 3 and Fig. 1) and GFP-α-tubulin (a marker of the microtubule network) (Kumagai *et al.*, 2001).

The cells were incubated in the presence of colchicine, an inhibitor of microtubule polymerization (Guha and Bhattacharyya, 1997; Morejohn and Fosket, 1991), or cytochalasin D, an inhibitor of actin polymerization (Goddette and Frieden, 1986). Several control experiments were performed in order to determine the optimal drug concentration to be used while maintaining the viability of the cells. Furthermore, time course experiments on cells expressing GFP-α-tubulin under influence of the drugs were performed in order to determine the earliest time point where an effect could be observed. Complementing these experiments with immunolocalizations using anti α-tubulin antibodies, it was observed that, 3 hours after the application of either drug, the microtubule network had already been disrupted (results not shown).
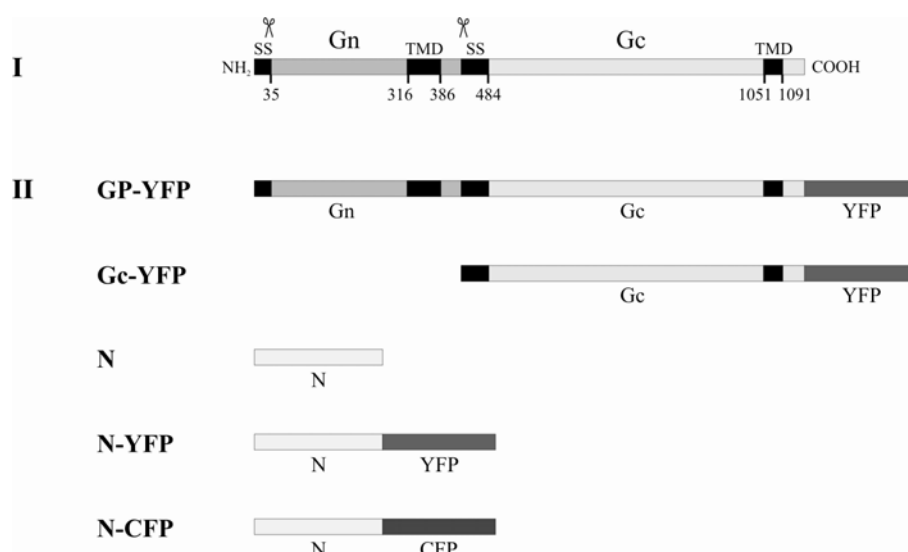
Figure 1: (I): Schematic representation of the topology of the TSWV glycoprotein precursor. (II): viral protein constructs used for expression analysis (the glycoprotein constructs are aligned below the precursor). Predicted cleavage sites (scissor symbols), hydrophobic areas (black boxes) and aminoacid positions are indicated (SS stands for signal sequence; TMD stands for transmembrane domain). In all constructs, the YFP or CFP fluorophores were fused in frame at the position of the stop codon.

Next, the effects of these inhibitors on the behavior of the N protein were analyzed by confocal microscopy 24-48 hours post-transfection (p.t.). Cytochalasin D also affected the microtubule network (results not shown), possibly due to the tight association of microtubules with actin filaments. Hence, the depolymerization of microtubules could also be used as an indirect marker to monitor the effect of the actin polymerization inhibitor.

When N was expressed and analyzed in non-treated cells, no co-localization was observed between the N agglomerations and microtubules (Fig. 2 a-c). Upon colchicine treatment, the microtubule network was still disturbed after 24h (Fig. 2e), but no change could be observed in the distribution of N agglomerations, i.e. N agglomerates were formed in similar number (Mann-Whitney U test: $U_{number\ of\ agglomerations}$= 2329.0; N= 70; Sig.= 0.613) and size (Mann-Whitney U test: $U_{size\ of\ agglomerations}$= 153647.5; N= 70; Sig.= 0.990) compared to non-treated cells (Fig. 2d). In contrast, 24 hours after cytochalasin D treatment, the number of agglomerations increased (Mann-Whitney U test: $U_{number\ of\ agglomerations}$= 567.5; N= 70; Sig.= 0.000) and their size became significantly smaller (Mann-Whitney U test: $U_{size\ of\ agglomerations}$= 92599.5; N= 70; Sig.= 0.000) (Fig. 2g). In both cases, no co-localization was observed between N and the depolymerized α-tubulin (Fig. 2 d-i). These observed differences were quantified and are graphically presented in Fig. 3. These results indicate that in plant cells N protein behaves in a microtubule-independent but actin-dependent manner.
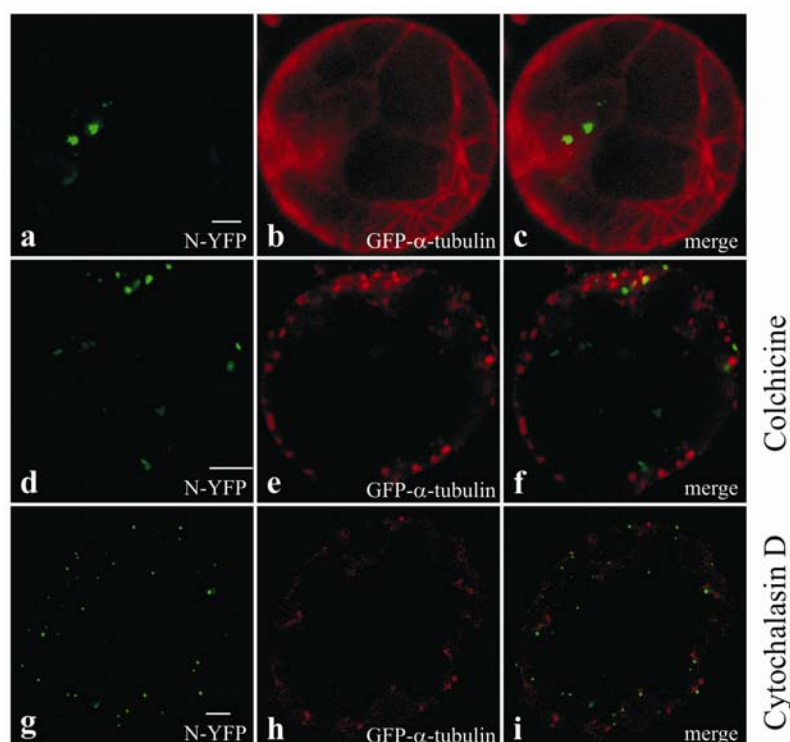
Figure 2: Cellular distribution of transiently expressed N protein under the influence of cytoskeleton inhibitors. Panels a-c: protoplast transfected with N-YFP and GFP-α-tubulin 24h p.t.: (a) N-YFP, (b) GFP-α-tubulin; (c) merge image of a and b. Panels d-f: protoplast transfected with N-YFP and GFP-α-tubulin and treated with colchicine 24h p.t.: (d) N-YFP, (e) GFP-α-tubulin, (f) merge image of d and e. Panels g-i: protoplast transfected with N-YFP and GFP-α-tubulin and treated with cytochalasin D 24h p.t.: (g) N-YFP, (h) GFP-α-tubulin, (i) merge image of g and h. The images were taken 24 hours p.t.. Size bars represent 5 µm.

CLUSTERING OF THE TSWV STRUCTURAL PROTEINS AT THE ER AND/OR GOLGI IS CYTOSKELETON-INDEPENDENT

Previous protoplast expression studies have shown a co-localization and interaction between N and the viral glycoproteins at ER and Golgi (Chapter 3). To investigate the requirement of actin filaments and/or microtubules for the migration of the cytoplasmic N to these sites, protoplasts were co-transfected with a fluorophore-fused glycoprotein precursor construct GP-YFP, which allowed the monitoring of Gc-YFP in the presence of Gn, (Chapter 2) and N-CFP (Chapter 3 and Fig. 1). Similar to what was observed in non-treated cells (Fig. 4 a-c), 24h after colchicine application (and even 48 hours, results not shown) the N protein still co-localized with the glycoproteins (Fig. 4 d-f). Surprisingly, similar results were obtained upon treatment with cytochalasin D (Fig. 4 g-i). However, the number of sites where the glycoproteins and N co-localized increased in number and decreased in size (Fig. 4a and g), in analogy to what was previously observed for N-YFP in cells treated with the same drug. Hence, it was tempting to assume that the spatial distribution pattern observed for the co-localizing glycoproteins and N in

the presence of cytochalasin D, originated from the influence of actin filament disruption on N protein agglomerations.

Figure 3: Graphical representations of the influence of colchicine and cytochalasin D on the number and size of cytoplasmic N aggregations. (I): distribution of the number of N agglomerations per cell; (II): distribution of the size of N agglomerations.
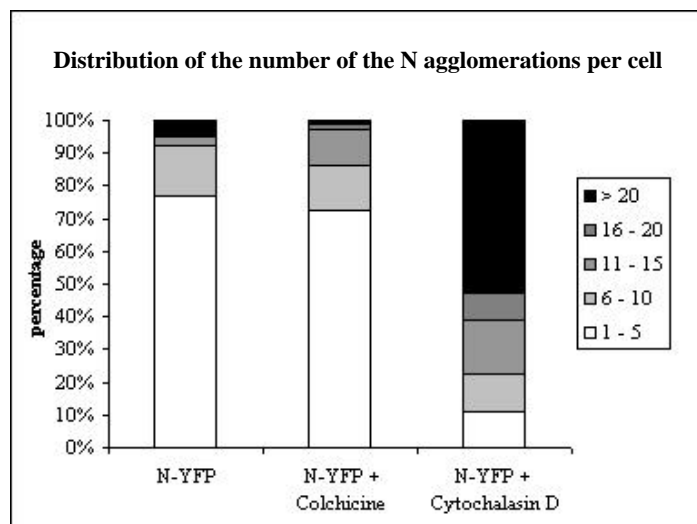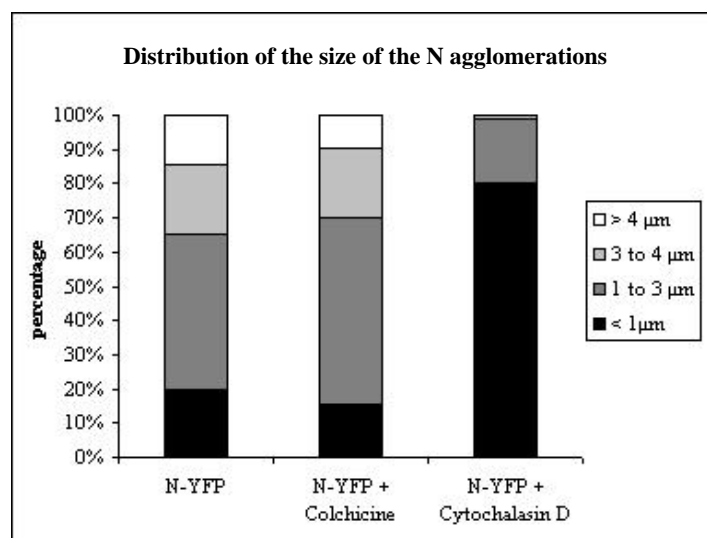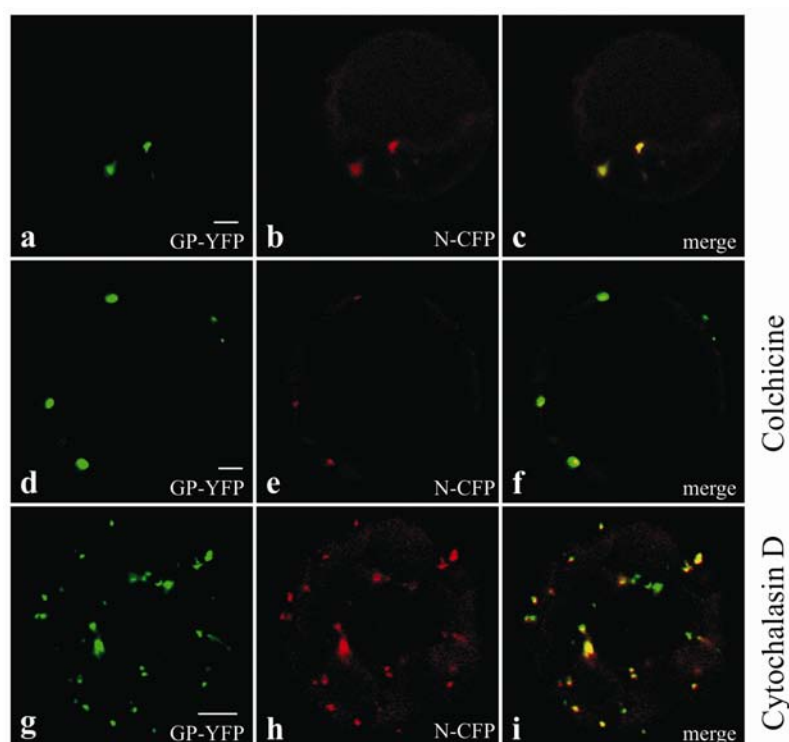
Figure 4: Cellular distribution of N and the viral glycoproteins under the influence of cytoskeleton inhibitors. Panels a-c: protoplast transfected with GP-YFP and N-CFP 24h p.t.: (a) GP-YFP (Gc-YFP), (b) N-CFP; (c) merge image of a and b. Panels d-f: protoplast transfected with GP-YFP and N-CFP and treated with colchicine 24h p.t.: (d) GP-YFP (Gc-YFP), (e) N-CFP, (f) merge image of d and e. Panels g-i: protoplast transfected with GP-YFP and N-CFP and treated with cytochalasin D 24h p.t.: (g) GP-YFP (Gc-YFP), (h) N-CFP, (i) merge image of g and h. Size bars represent 5 μm.

THE INTERACTION BETWEEN THE N PROTEIN AND THE GLYCOPROTEINS IS NOT AFFECTED UPON DISRUPTION OF THE MICROTUBULE OR ACTIN NETWORKS

Due to the observation that a disruption of microtubules and actin filaments did not avoid co-localization of N protein with the glycoproteins, it was likely that their interaction was also not affected. In order to verify this hypothesis, FRET/FLIM analyses were performed on protoplasts co-expressing GP-YFP and N-CFP, and treated with either colchicine or cytochalasin D (Fig. 5).

Confocal imaging (Fig. 5 Ia-d and IIa-d) showed a weaker N-CFP fluorescence in the presence of N-YFP in cells treated with colchicine (Fig. 5 Ib) as well as in cells treated with cytochalasin D (Fig. 5 IIb), compared to the one observed upon single expression of N-CFP (data not shown). A high YFP fluorescence was detected upon excitation of CFP (Fig. 5Ic and 5IIc), suggesting the occurrence of FRET. However, this image may also be partially composed of CFP crosstalk and also some YFP direct excitation, which does not allow accurate confirmation of the occurrence of energy transfer. Hence, to further substantiate this, FLIM was performed, revealing a strong decay in the lifetime of the donor fluorophore after cells were treated with either colchicine (Fig. 5 Ie) or cytochalasin D (Fig. 5 IIe). In previous studies (Chapter 3) the interaction between Gc and N in the presence of Gn revealed a decrease of 30-50% (an average of 38%) in the life time of the donor fluorophore. Here, in cells treated with colchicine, still a 33-58%

decrease in CFP lifetime was observed with an average of about 45%. The example in Figure 5 Ie shows an average lifetime decrease from 2380 ps to 1271 ps, corresponding to 46.5%. Similar results were obtained for the cells treated with cytochalasin D, where a 39-62% decrease was observed, with an average of 47%. The example in Figure 5 IIe shows an average lifetime decrease from 2380 ps to 1424 ps, corresponding to 40%. Altogether, these results indicated that, even upon disturbance of the microtubules and/or actin networks, the viral N protein is still able to localize to the site where the glycoproteins are concentrated (ER and Golgi) and to interact with them in similar conformations as in non-treated cells.

N PROTEIN-MEDIATED REALLOCATION OF GC DOES NOT REQUIRE ACTIN FILAMENTS OR MICROTUBULES

Whereas co-expression of N with both glycoproteins rendered a clear co-localization of all three structural proteins at the Golgi complex, co-expression of N with only Gc caused a dramatic chance of Gc distribution within the ER (Chapter 3) from reticular to punctate spots. Upon colchicine treatment of protoplasts transfected with Gc-YFP and N (Fig. 6b), no change was observed compared to non-treated cells (Fig. 6a). However, when cells were treated with cytochalasin D, the number of punctate spots of Gc increased (Fig. 6c) whereas their size decreased, similarly to what was previously observed in the presence of Gn, or for N only. Co-expression experiments showed a co-localization between Gc-YFP (and N) and the GFP-HDEL ER-marker and not with the ST-GFP Golgi-marker (Chapter 3).
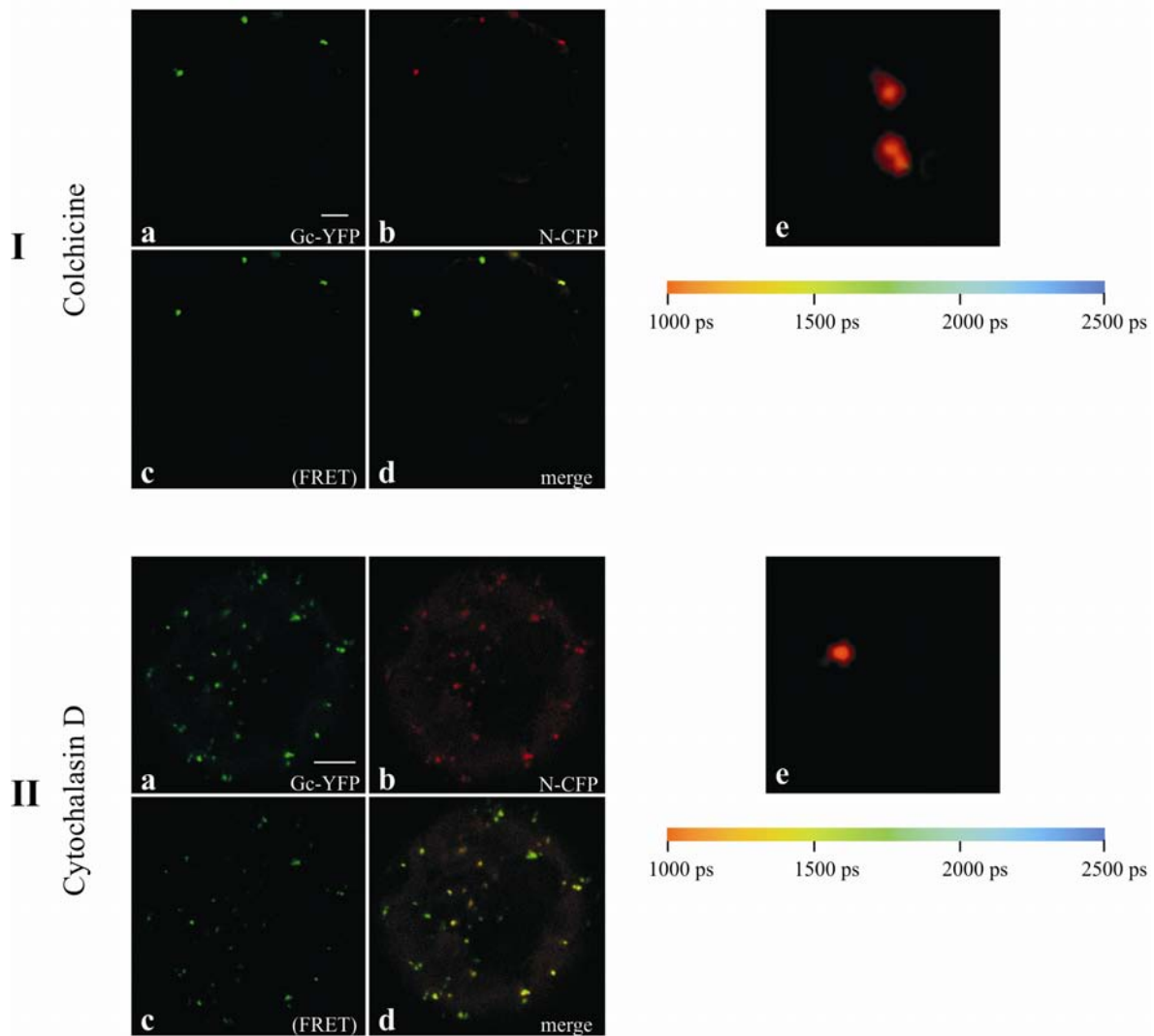
Figure 5: FRET and FLIM analysis of N-Gc interactions in the presence of Gn and cytoskeleton inhibitors. (I) protoplasts transfected with N-CFP and GP-YFP treated with colchicine 24h p.t.: (a) GP-YFP (Gc-YFP), (b) N-CFP, (c) YFP fluorescence upon CFP excitation (indication of FRET) and (d) merge image of a, b and c; (e) color-coded image of CFP lifetime (different protoplast). (II) protoplasts transfected with N-CFP and GP-YFP treated with cytochalasin D 24h p.t.: (a) GP-YFP (Gc-YFP), (b) N-CFP, (c) YFP fluorescence upon CFP excitation (indication of FRET) and (d) merge image of a, b and c; (e) color-coded image of CFP lifetime (different protoplast). The color legends indicate the CFP lifetime in ps. The CFP lifetime measured upon single N-CFP expression equals 2380 ps. Size bars represent 5 µm.

Figure 6: Behavior and localization of Gc in the presence of N, under the influence of cytoskeleton inhibitors. Panels a-c: protoplasts transfected with Gc-YFP (in green) and N: (a) non-treated cell, (b) cell treated with colchicine; (c) cell treated with cytochalasin D. The images were taken 24 hours p.t.. Size bars represent 5 µm.
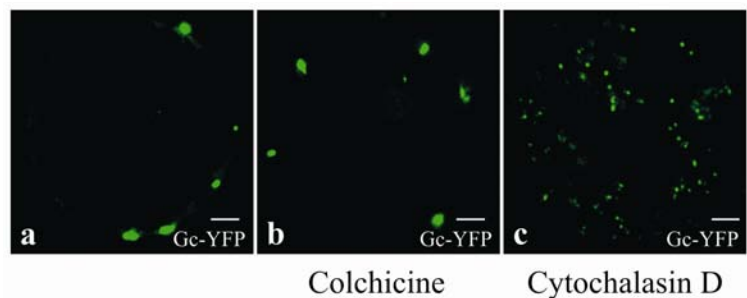
DISCUSSION

Membrane bound particles of the plant-infecting bunyavirus TSWV arise as a result of RNP enwrapment with glycoprotein-containing Golgi membranes (Kikkert *et al.*, 1999). To better understand this process, the structural proteins of TSWV have been singly or co-expressed in protoplasts. These studies have shown that the structural protein N is able to interact with both Gc and Gn glycoproteins in the ER and/or Golgi complex and that the N protein re-directs Gc within the ER to specific punctate spots (Chapters 2 and 3)

In this chapter we aimed at investigating the influence of cytoskeleton elements on some of the steps prior to viral assembly, by analyzing the cytoplasmic trafficking of the N protein. It is shown that the formation of N agglomerations throughout the cytoplasm is independent of the microtubules but somehow dependent on actin filaments. Indeed, upon disruption of the latter, cytoplasmic N agglomerations appeared much smaller and larger in number, which suggested that transport of individual (or small clusters of) N molecules through the cytoplasm to form larger agglomerations takes place along the actin network.

Surprisingly, none of the inhibitors interfered with the transport of N through the cytoplasm to line up along ER and Golgi membranes where the glycoproteins were located. Similarly to what was observed in the absence of the inhibitors (Chapter 3), there was still a very clear co-localization of the proteins. The interaction between N and the glycoproteins also did not change in the presence of colchicine or cytochalasin D, as demonstrated by FRET/FLIM. This indicates that microtubules and actin filaments are not involved in the transport of N to the loci of glycoprotein accumulation and their disruption does not affect in the interaction between the proteins.

Similarly, relocation of Gc by N from a reticular ER distribution, to punctate spots (Chapter 2) still occurred in the presence of either colchicine or cytochalasin D, apparently not requiring microtubules or actin filaments.

Whereas colchicine or cytochalasin D did not keep N from targeting to and co-localizing with Gc or both glycoproteins, cytochalasin D in all cases did affect the number and size of the protein complexes. Agglomerations in general were significantly higher in number and smaller in size. Since this effect was already observed when only N was expressed, it is not unlikely that a change in appearance of glycoprotein-N complexes is the consequence of the primary effect of cytochalasin D on the number and size of N agglomerations. In the presence of this drug, a larger number of smaller N agglomerations become targeted in a microtubule- and actin-independent manner to ER or Golgi membranes were the glycoproteins reside. As a logical consequence more and smaller loci with N-glycoprotein complexes occur, as depicted in figure 7.

The observation that N does not depend on microtubules for its behavior in plant cells is intriguing when compared with earlier studies in mammalian BHK21 cells where N was observed to accumulate in a non-Golgi, perinuclear region and assumed to be present at the microtubule organizing centre (MTOC) (Snippe *et al.*, 2005b). In the presence of colchicine, N was shown to end up as smaller aggregates and more dispersed in the cytoplasm, a phenomenon that often applies to proteins destined to oligomerize/aggregate at the MTOC in mammalian cells (Snippe *et al.*, 2005b). These proteins require the dynactin complex involved in minus-end directed motor activities of cytoplasmic dynein along the microtubules (Heath *et al.*, 2001). The organization of the microtubule network differs in high extent between plant and mammalian cells (Luders and Stearns, 2007). While animal cells only contain one or two MTOCs, plant cells contain many

more microtubule nucleation sites, although not much is known yet about these structures. These differences may, to some extent, justify the distinct behavior exhibited by the viral proteins, in adaptation to the different cellular architectures.
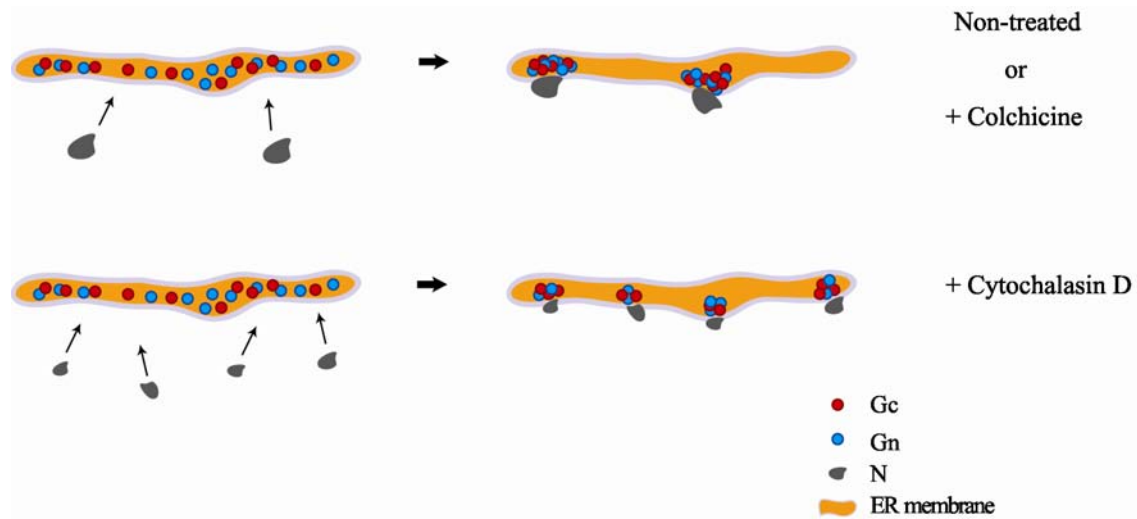
Figure 7: Schematic model for the migration of N agglomerations to glycoprotein-containing ER membranes and association between the viral proteins upon treatment with cytoskeleton inhibitors. Cytochalasin D causes the formation of smaller agglomerations that migrate to the vicinity of ER membranes and consequently originate smaller N/glycoproteins agglomerations.

On the other hand, it is also possible that the perinuclear accumulation of N in mammalian cells is a genuine antiviral defense response to avoid, by sequestering, N from taking part in the viral replication cycle, as was observed and suggested for other bunyaviruses (Andersson *et al.*, 2004a; Kochs *et al.*, 2002). In this case, a dependency of N on microtubules would not be an intrinsic property of the protein and microtubules may not be required for the movement of N in plant cells, as part of the particle assembly process.

The involvement of cytoskeleton elements in protein trafficking during virus assembly has been demonstrated for several bunyaviruses (Andersson *et al.*, 2004b; Ramanathan *et al.*, 2007; Ravkov *et al.*, 1998), but the knowledge is still quite limited.

Our results show that both the cytoplasmic translocation of N as well as the glycoprotein trafficking within the ER are cytoskeleton-independent. Since the other trafficking phenomenon observed during assembly, the ER-to-Golgi transport of the glycoproteins, also shows this independency in plant cells, the results from this study seem to indicate that the first steps of TSWV particle assembly occur independently of cytoskeleton elements. However, the independency on these networks for the process of Golgi membrane enwrapment around the RNPs and DEVs fusion, remains to be investigated.

ACKNOWLEDGEMENTS

CHAPTER 5
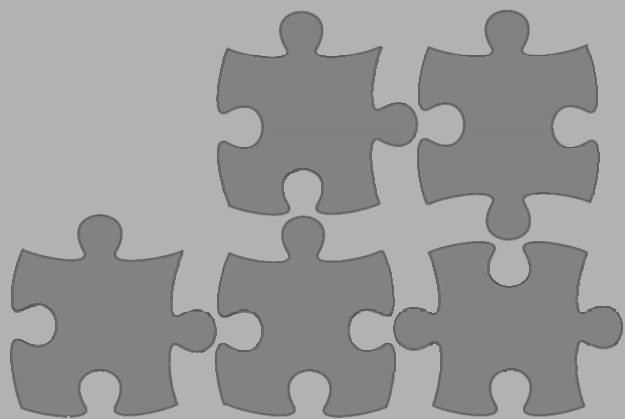
TOMATO SPOTTED WILT VIRUS GC AND N PROTEINS ACCUMULATE AT ER EXPORT SITES

ABSTRACT

During maturation of the Tomato spotted wilt virus (TSWV) structural proteins, the glycoprotein Gc localizes in the ER and is only able to migrate to the Golgi complex upon co-expression with the second viral glycoprotein Gn. In the presence of the viral N protein, Gc remains arrested in the ER, although concentrated in specific areas of this organelle. Here it is shown that these loci correspond to ER export sites (ERES), distinct ER domains where protein cargo concentrates prior to transport to the Golgi. Apparently, the presence of the cytoplasmic N protein induced the concentration of Gc at ERES. A chimeric calnexin protein, provided with the cytoplasmic tail (CT) of Gc, was also targeted to ERES upon co-expression with N protein, indicating that N-Gc binding through the CT domain of Gc is crucial for this targeting.

INTRODUCTION

The Golgi complex has been determined as the major virus particle assembly site for members of the *Bunyaviridae*. For the animal-infecting bunyaviruses, this process occurs by budding of viral ribonucleoproteins (RNPs) into enlarged lumen of Golgi cisternae, leading to the formation of enveloped virus particles that are ultimately secreted for further viral spread (Elliott, 1996; Griffiths and Rottier, 1992; Petterson and Melin, 1996). For the plant-infecting bunyavirus Tomato spotted wilt virus (TSWV), particle assembly involves wrapping of RNPs by Golgi cisternae giving rise to doubly enveloped virus particles (DEVs) as intermediates (Kikkert *et al.*, 1999; Kitajima *et al.*, 1992a). These subsequently fuse with each other and with ER-derived membranes, leading to the formation of large cytoplasmic vesicles containing mature virus particles (Kikkert *et al.*, 1999), which accumulate until uptake by insect vector thrips (Whitfield *et al.*, 2005).

Transient expression of the two TSWV glycoproteins (Gc and Gn) in plant protoplasts have shown that both ultimately localize at the Golgi complex (Chapter 2). However, when singly expressed, the glycoprotein Gc is not able to migrate to this organelle, being retained in the ER, while Gn, on the other hand, is able to translocate by itself from the ER to the Golgi (Chapter 2).

Using FRET-FLIM technologies, it was shown that the cytoplasmic N protein interacts with both viral glycoproteins (Chapter 3) at the ER and/or Golgi in a microtubule- and actin-independent manner (Chapter 4). No change was observed in the behavior of Gn due to the interaction with N (Chapter 3). However, a dramatic change in the localization of Gc was observed upon interaction with this cytoplasmic protein. Although still in the ER, Gc is no longer spread throughout this organelle, but becomes concentrated in specific areas where it co-localizes with N (Chapter 3).

In this study the identity of these Gc-N accumulation sites has been investigated. Since previous studies have shown that Gn is able to induce the concentration of Gc at ER export sites (ERES) prior to exit to the Golgi (Chapter 2), it was tempting to hypothesize that the loci where Gc-N accumulates might also correspond to these ER domains.
Furthermore the role of the cytoplasmic tail (CT) of Gc in Gc-N binding and subsequent targeting within the ER has been investigated, by fusing this domain to a non-related ER-resident chaperone protein, calnexin, which normally localizes randomly through the ER (da Silva *et al.*, 2005; da Silva *et al.*, 2006).

MATERIALS AND METHODS

PLASMID CONSTRUCTION AND ORGANELLE MARKERS

Plasmids encoding the GFP-fused transmembrane domain of *Arabidopsis* calnexin and cytoplasmic tail of Gc (GFP-CNX-CTGc) mutant were obtained by assembly PCR. A PCR fragment containing the cauliflower mosaic virus 35S (CaMV35S) promoter, GFP and the transmembrane domain of calnexin, flanked on its 3'-end with 24 nucleotides (nts) that overlap with the first 24 nts at the 5'-terminal end of the cytoplasmic tail of Gc, was amplified from a

GFP-CNX construct (da Silva *et al.*, 2005; da Silva *et al.*, 2006) (with primers 35SFwd, GGGCACTATCCTTCGCAAGACC and TMDCNXGcRvs, TTATAAGATTCATTCTTTAC ATATCGCCTTTTTGCCACCAAAGAT). Another PCR fragment containing the cytoplasmic tail of Gc, flanked on its 3'-end with a SpeI restriction site, was amplified from a construct that encodes Gc (pMONGc, prepared from the previously established pSFVGc (Kikkert *et al.*, 2001), subjected to a restriction enzyme digestion with BamHI, which resulted in the isolation of a cloning cassette which was inserted in the previously digested and defosforilated pMON999 vector, through the BamHI multiple cloning site) with the primers CTGcFwd, ATATGTAAA GAATGAATCTTATTA, and CTGcRvs, GGGTCAGACAAGGTGA GAGAAATCCAT. Both PCR fragments were fused by assembly PCR and the product was digested with NcoI and SpeI and ligated to a predigested (with NcoI and XbaI) GFP-CNX construct (da Silva *et al.*, 2005; da Silva *et al.*, 2006), leading to the final product.

The fluorescent proteins used in this study for fusion to the viral glycoproteins were a pH-insensitive form of YFP, CFP and mGFP5 (Haseloff *et al.*, 1997). The spectral properties of mGFP5 allow efficient spectral separation from YFP (Brandizzi *et al.*, 2002b).

As ER export sites-marker, the YFP-Sec24 (Stefano *et al.*, 2006) was used.

PLANT MATERIAL, TRANSIENT EXPRESSION AND TREATMENTS

Tobacco plants (*Nicotiana tabacum* cv Petit Havana) (Maliga *et al.*, 1973) were grown in Murashige and Skoog medium (Murashige and Skoog, 1962) and 2% sucrose in controlled sterile conditions at 25°C with a 16 hours period of light per day. Tobacco leaf protoplasts were prepared and transfected as described by Denecke and Vitale (1995), with some minor modifications. In short, leaves of fully-grown plants were pierced and digested overnight in TEX (B5 salts, 500 mg/l MES, 750 mg/l $CaCl_2 \cdot 2H_2O$, 250 mg/l NH_4NO_3, 0.4 M sucrose, pH 5.7) containing 0.2% Macerozyme and 0.4% Cellulase. Protoplasts were recovered by filtration and washed by multiple centrifugations with Electroporation Buffer (EB) (0.4 M sucrose, 2.4 g/l HEPES, 6 g/l KCl, 600 mg/l $CaCl_2 \cdot 2H_2O$, pH 7.2). Viable protoplasts were recovered and resuspended in proper EB volume. A volume of 100 µl containing plasmids (30 µg of each) in EB was added to 500 µL of protoplast suspension and this mixture was subjected to electroporation (160V, 925µF, $\infty\Omega$) in 4 mm cuvettes using a BIO-RAD X-cell electroporator. After 10 min recovery, treatments (inhibitors) were applied and protoplasts were incubated in 2 mL TEX in the dark (the incubation times differed per experiment, ranging between 24 and 48 hours). A final concentration of 100 µM of colchicine (Duchefa) or 20 µM of cytochalasin D (Sigma) was applied, according to tests performed in Chapter 4.

SAMPLING AND IMAGING

Twenty four to forty eight hours post-transfection, the living protoplasts were isolated by centrifugation and confocal sections images were obtained using an inverted Zeiss 510 Laser Scanning Microscope and a 40x oil or 63x oil and water immersion objective.

For the imaging of the single expression of YFP-fused (and GFP-fused) proteins, excitation lines of an argon ion laser of 488 nm were used with a 505/530 nm bandpass filter in

the single-track facility of the microscope. For the imaging of the co-expressing YFP-fused and the CFP-fused proteins (as well as for YFP- and GFP-fused proteins), excitation lines of an argon ion laser of 458 nm for CFP (and GFP) and 514 nm for YFP were alternately used with line switching using the multi-track facility of the microscope. Fluorescence was detected using a 458/514 nm dichroic beam splitter and a 470/500 nm bandpass filter for CFP (and GFP) and a 535/590 nm bandpass filter for YFP. Appropriate controls were performed to exclude possible crosstalk and energy transfer between fluorochromes.

RESULTS

THE PRESENCE OF THE TSWV N PROTEIN INDUCES GC ACCUMULATION AT ER EXPORT SITES

Previous studies have shown that the TSWV glycoprotein Gc interacts with the cytoplasmic N protein, leading to a change in its distribution within the ER, accumulating at specific areas of this organelle (Chapter 3). Furthermore, it was also shown that Gn is able to redirect Gc to ER export sites, prior to their migration to the Golgi complex (Chapter 2).

In order to test the hypothesis that N, like Gn, is able to induce accumulation of Gc at the ERES, tobacco protoplasts were transfected with Gc-CFP (Chapter 2), N (Chapter 3) and ERES-marker YFP-Sec24 (Stefano *et al.*, 2006). The results showed that indeed, in the presence of N, Gc-CFP localized to ERES (Fig. 1 a-c).

It has previously been shown that actin filaments were not involved in the cytoplasmic transport of the N protein to the ER, prior to its interaction with Gc (Chapter 4). However, when these filaments were disrupted, more and smaller spots of Gc-N complexes were observed, likely due to the previous effect of actin filament disruption on the formation of N agglomerations (Chapter 4). To test whether, under these conditions, the (more abundant and smaller) agglomerations of Gc-N also localized to ERES, protoplasts were transfected with Gc-CFP, N and YFP-Sec24 and incubated in the presence of cytochalasin D (an inhibitor of actin polymerization; Chapter 4). Still, Gc-CFP co-localized with the ERES-marker (Fig. 1 d-f), indicating an increase of the number of ERES and suggesting their *de novo* formation upon cargo-protein accumulation. To exclude the possibility that the increase in ERES number was triggered by depolymerization of the actin filaments, protoplasts singly transfected with the YFP-Sec24 ERES marker were incubated in the presence of the same concentration of cytochalasin D and analyzed at the same time point. Repeated experiments in which 40 cells were observed (20 of which treated with cytochalasin D) and the number of ERES presented by the marker was quantified did not reveal any significant difference in ERES number due to the presence of the drug (results not shown).
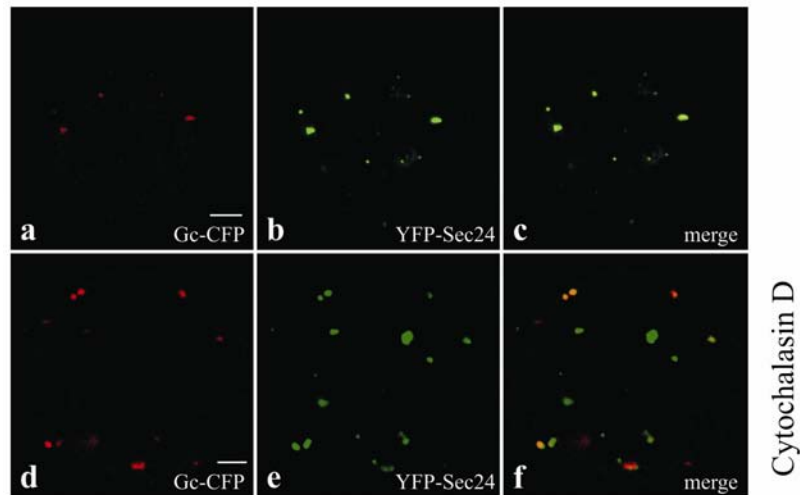
Figure 1: Localization of TSWV Gc/N complexes within the ER. Panels a-c: protoplast transfected with Gc-CFP, N and YFP-Sec24, 24h p.t., (a) Gc-CFP, (b) YFP-Sec24, (c) merge of a and b. Panels d-f: protoplast transfected with Gc-CFP, N and YFP-Sec24 and incubated in the presence of cytochalasin D, 24h p.t., (d) Gc-CFP, (e) YFP-Sec24, (f) merge image of d and e. Size bars represent 5 μm.

THE CYTOPLASMIC TAIL OF GC IS CRUCIAL FOR ITS REDIRECTION TO ERES BY N PROTEIN

Since N is a cytoplasmic protein, the recruitment of Gc to ERES was likely due to an interaction between these two proteins via the cytoplasmic tail of the glycoprotein. To test this hypothesis, a calnexin mutant GFP-CNX-CTGc (Fig. 2 I) was constructed. This mutant originated from a calnexin derivate (named GFP-CNX; Fig. 2 I, IIa) in which the luminal domain was exchanged by GFP, not altering its reticular localization pattern (da Silva *et al.*, 2005; da Silva *et al.*, 2006). GFP-CNX-CTGc was constructed from this derivate by substitution of the cytoplasmic tail of GFP-CNX by the one of Gc, which similarly did not have any effect on its localization pattern (Fig. 2 IIb)
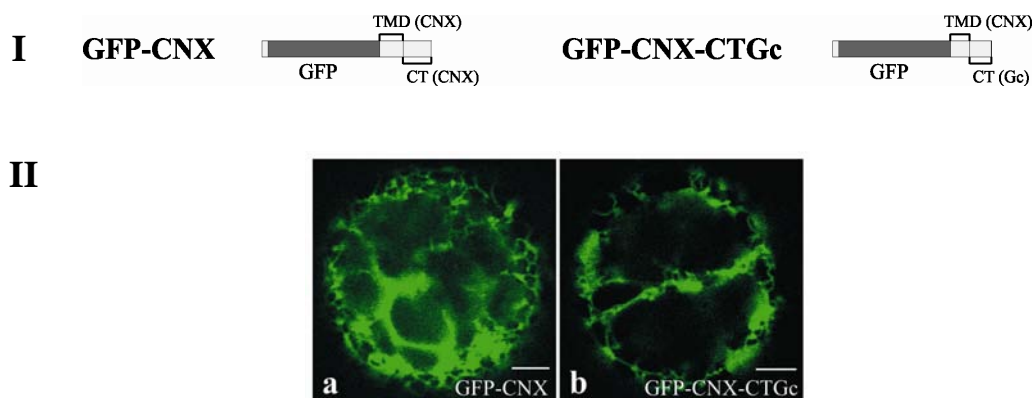
Figure 2 : (I) Schematic representation of the calnexin mutants used in this study. TMD_{CNX} and CT_{CNX} refer to calnexin's transmembrane domain and cytoplasmic tail, respectively. CTGc refers to the cytoplasmic tail of Gc. (II) Localization analysis of the two calnexin mutants. (a) Protoplast transfected with GFP-CNX 24h p.t.; (b) protoplast transfected with GFP-CNX-CTGc 24h p.t.. Size bars represent 5 μm.

Upon co-expression of N-YFP (Chapter 3) with GFP-CNX-CTGc, both proteins concentrated and co-localized at punctate spots (Fig. 3 d-f), similarly to what had previously been described for Gc-N. As control, GFP-CNX was co-expressed with N-YFP but these results showed no change in the localization of GFP-CNX or any co-localization with N (Fig. 3 a-c). To exclude the possibility that the observed change in localization was due to the deletion of the calnexin CT, another mutant equivalent to GFP-CNX but lacking its CT (denoted GFP-CNXΔCT (da Silva *et al.*, 2006)), was also expressed and showed a clear reticular ER localization (results not shown). Co-expression of GFP-CNX-CTGc, N and YFP-Sec24 (Fig. 3 g-i) demonstrated that these punctate spots corresponded to ERES, indicating that N was able to redirect this chimeric calnexin within the ER to ERES. Furthermore, these results confirm that the cytoplasmic domain of Gc is both necessary and sufficient for the interaction with the N protein.

DEPOLYMERIZED Α-TUBULIN APPEARS TO CONCENTRATE AT ERES

Previous experiments (Chapter 4) studying the translocation of the N protein to the ER in order to interact with Gc, not only demonstrated an independency of active microtubule and actin-filaments for this interaction, but also revealed that the Gc-N complexes seemed to co-localize with depolymerized α-tubulin (results not shown in Chapter 4). Since in this chapter it was demonstrated that these Gc-N complexes localize at ERES, these results became even more intriguing as they seem to indicate a correlation between microtubules and ERES.

These experiments were here repeated, i.e. protoplasts were transfected with Gc-YFP, N and GFP-α-tubulin and incubated in the presence of colchicine (an inhibitor of microtubule polymerization). As previously observed, Gc-YFP co-localized with the α-tubulin agglomerations (Fig. 4 a-c)

Protoplasts were also transfected with YFP-Sec24 and GFP-α-tubulin in the presence of colchicine and indeed the agglomerations of depolymerized GFP-α-tubulin co-localized with the ERES (Fig. 4 d-f). The same experiment was performed in the presence of cytochalasin D (as shown in Chapter 4, this drug has an indirect effect on the polymerization of GFP-α-tubulin) and the obtained results were similar (Fig. 4 g-i), altogether strongly suggesting a connection between microtubule elements and ERES.
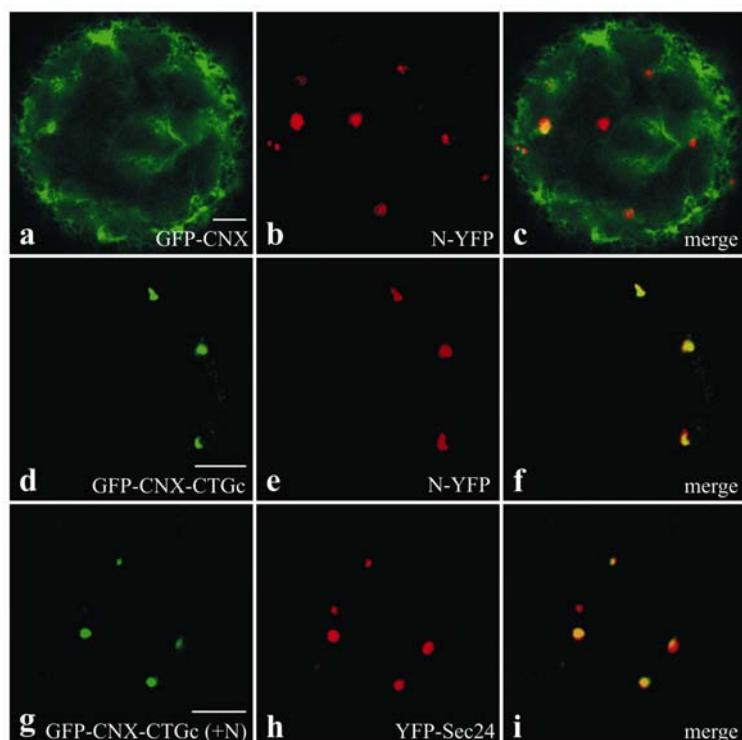
Figure 3: Influence of N protein on the localization of a calnexin mutant containing the CT of Gc. Panels a-c: protoplast transfected with GFP-CNX and N-YFP, 24h p.t., (a) GFP-CNX, (b) N-YFP, (c) merge of a and b. Panels d-f: protoplast transfected with GFP-CNX-CTGc and N-YFP, 24h p.t., (d) GFP-CNX-CTGc, (e) N-YFP, (f) merge of d and e. Panels g-i: protoplast transfected with GFP-CNX-CTGc, N and YFP-Sec24, 24h p.t., (g) GFP-CNX-CTGc, (h) YFP-Sec24, (i) merge of g and h. Size bars represent 5 μm.

Figure 4: Localization analysis of Gc-N complexes, ERES and depolymerized α-tubulin. Panels a-c: protoplast transfected with Gc-YFP, N and GFP-α-tubulin treated with colchicine 24h p.t., (a) Gc-YFP, (b) GFP-α-tubulin, (c) merge image of a and b. Panels d-f: protoplast transfected with YFP-Sec24 and GFP-α-tubulin treated with colchicine 24h p.t., (d) YFP-Sec24, (e) GFP-α-tubulin, (f) merge image of d and e. Panels g-i: protoplast transfected with YFP-Sec24 and GFP-α-tubulin treated with cytochalasin D 24h p.t., (g) YFP-Sec24, (h) GFP-α-tubulin, (i) merge image of g and h. Size bars represent 5 μm.
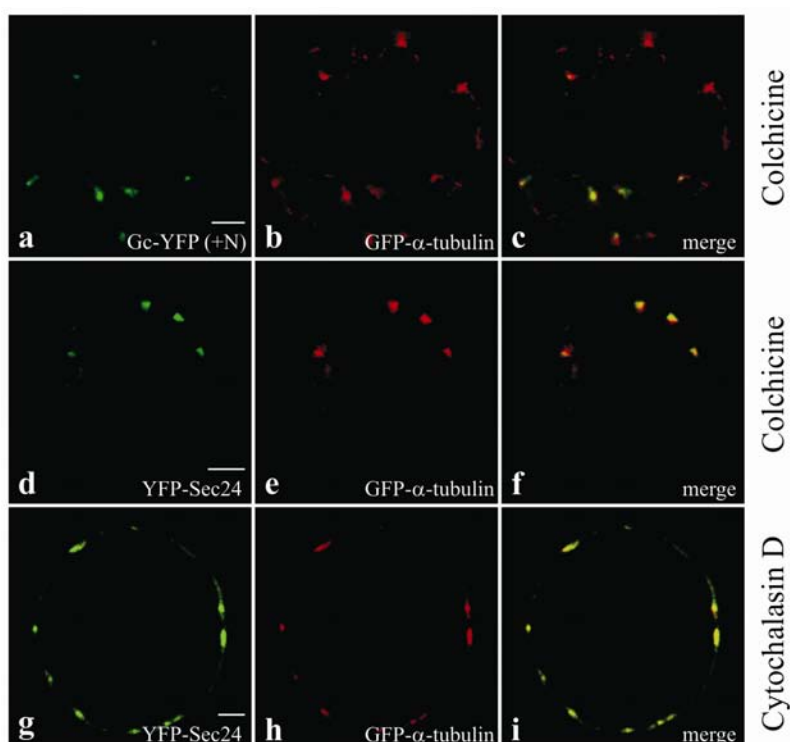
DISCUSSION

The TSWV glycoprotein Gc was previously shown to localize at specific loci in ER upon co-expression with the viral N protein (Chapter 2). Here, we report evidence that these loci represent ER export sites. ERES are discrete domains of the ER where the machinery responsible for the formation of COPII vesicles is assembled (reviewed by Hanton *et al.* (2006)). In mammalian and yeast cells, the COPII-coat components (the GTPase Sar1 and two heterodimeric complexes Sec23/24 and Sec13/31) are thought to be sequentially recruited at ERES (Aridor *et al.*, 2001; Barlowe *et al.*, 1994; Matsuoka *et al.*, 2001). However, the characteristics and function of the plant ERES are less understood and may differ from the other biological systems, mainly due to the unique motile nature of its early secretory pathway. Different models have been proposed for the protein transport occurring between ER and Golgi in plant cells (Hanton *et al.*, 2006). According to the "vacuum cleaner model" (Boevink *et al.*, 1998), the Golgi stacks move over the ER, constantly collecting cargo at ERES, suggesting that the whole ER surface is capable of forming these export sites. On the other hand, the "stop-and-go" model (Nebenfuhr *et al.*, 1999) suggests that the Golgi stacks temporarily stop at defined ERES. A third model was also proposed according to which cargo transport from the ER to the Golgi occurs in a continuous manner, suggesting that Golgi stacks move with (and not over) the surface of the ER as a "mobile secretory unit" (Brandizzi *et al.*, 2002b; da Silva *et al.*, 2004; Stefano *et al.*, 2006). Finally, the "kiss-and-run" model, demonstrated to occur in tobacco BY-2 cells, postulates that several ERES can interact with a single Golgi stack and these associations continuously change in number and position (Hanton *et al.*, 2006; Yang *et al.*, 2005).

The mechanism and regulation of ERES formation as well as cargo recruitment in plant cells are not yet well understood. It is possible that the cargo is recruited to defined ERES, as was observed to occur in mammalian cells (Aridor *et al.*, 2001), but, alternatively, the cargo molecules themselves may recruit the COPII components to ERES (da Silva *et al.*, 2004). A recent study has shown that cargo transport can not only be mediated by recruitment of COPII components to existing ERES, but also by *de novo* formation of new ERES (Hanton *et al.*, 2007).

The role of the N protein in the accumulation of Gc at ERES is quite surprising, subject to different interpretations and raises several questions. The first one concerns the mechanism by which this phenomenon occurs. It may happen by random movement of N agglomerations in the vicinity of the ER-surface, collecting (by interaction with their cytoplasmic tail) Gc proteins and redirecting them to existing ERES or to a location where new ERES can be formed upon recruitment of COPII components. A slightly different explanation involves a (signal-mediated) concentration of N agglomerations at certain loci on the surface of ER membranes (that may correspond to existing ERES or places where new ERES can be formed), and interaction with Gc proteins that (possibly by oligomerization) become recruited to the same location.

Another interesting question arising from these studies concerns the reason why these Gc-N complexes would localize at ERES, since Gc is not able to translocate by itself to the Golgi (Chapter 2) and interaction with N does not overcome this ER-arrest. Perhaps a change in the folding of Gc due to this interaction, changes its affinity to COPII components or other proteins causing this accumulation at ERES.

Our results have also demonstrated that the cytoplasmic tail of Gc is sufficient for the interaction with N to occur and for Gc-N complex concentration at ERES. This was shown by exchanging the CT of a previously studied (da Silva *et al.*, 2006) calnexin mutant with the one of

Gc and subsequent co-expression with N, yielding an accumulation at these specific ER domains.

The accumulation of the N and Gc proteins at ERES may indicate that, in the natural case (virus infection), the interaction between the glycoproteins and the RNPs may occur prior to transport to the Golgi complex, shedding some more light on one of the steps involved in the TSWV particle assembly mechanism in plant cells.

It was known already (Chapter 4) that, upon actin filaments disruption, Gc and N concentrate at a higher number of agglomerations within the ER. This was thought to occur due to a previous effect of this drug on the formation of the cytoplasmic agglomerations of N that, under these conditions, are also present in higher number (Chapter 4). Here we show that, also upon actin disruption, the Gc-N agglomerations in the ER correspond to ERES, suggesting the *de novo* formation of ERES (Hanton *et al.*, 2007) by recruitment of COPII components to these areas where the viral proteins are concentrated. The presented data also suggest that recruitment to ERES does not necessarily guarantee ER-export.

It was shown in Chapter 4 that the interaction between Gc and N is microtubule- and actin-independent. However, when performing control experiments (to check the efficiency of the applied inhibitors) it was observed that the Gc-N complexes co-localized with the depolymerized α-tubulin. The current results show that, even in the absence of any viral proteins, depolymerized α-tubulin co-localizes at ERES. In mammalian cells, it has been demonstrated that microtubules are involved in the transport of proteins from the ER to the Golgi (Murshid and Presley, 2004; Watson *et al.*, 2005). However, cytoskeleton elements appear not to be required for ER-to-Golgi transport in plant cells (Boevink *et al.*, 1998; Brandizzi *et al.*, 2002b; Saint-Jore *et al.*, 2002), although the actin network is involved in the maintenance of the organization of the Golgi apparatus and movement of the ER network (Boevink *et al.*, 1998; Nebenfuhr *et al.*, 1999). Hence, our results are quite intriguing since they point to a direct correlation between ERES and microtubules, which has (to our knowledge) never been reported in plant cells. This phenomenon may reflect a possible role of the microtubules in the transport of cytoplasmic proteins to ERES. The relevance and biological function of this suggested correlation between microtubules and ERES remains to be investigated.

ACKNOWLEDGEMENTS

CHAPTER 5

CHAPTER 6
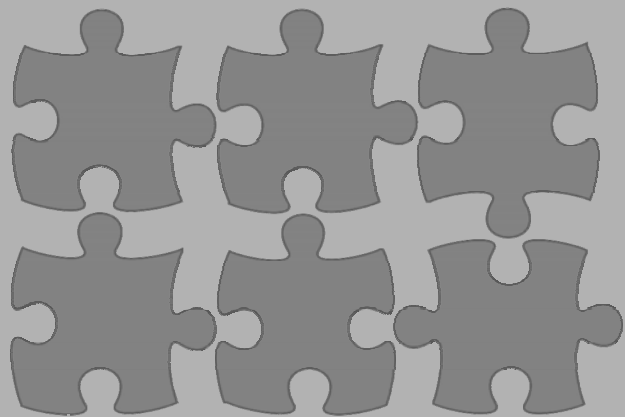
TRAFFICKING OF TOMATO SPOTTED WILT VIRUS GN AND GC GLYCOPROTEINS: REQUIREMENTS FOR ER-ARREST AND EXIT TO THE GOLGI

ABSTRACT

The envelope glycoproteins Gn and Gc are major determinants in the assembly of Tomato spotted wilt virus (TSWV) particles at the Golgi complex. In this chapter the ER-arrest of singly expressed Gc and transport to the Golgi of both Gn and Gc upon co-expression have been analyzed. Arrest of Gc at the ER didn't appear to result from improper folding, as ER-resident chaperone proteins Bip, calnexin and calreticulin did not seem to bind to this protein upon its expression. Instead, transient expression of chimeric Gc, in which the transmembrane domain (TMD) and/or cytoplasmic tail were swapped with those from Gn, showed that the TMD of Gn was sufficient to allow ER-exit and transport to the Golgi. Expression of both glycoproteins in the presence of overexpressed Sar1p-specific guanosine nucleotide exchange factor Sec12p, resulted in ER-retention demonstrating that the viral glycoproteins are transported to the Golgi in a COPII-dependent manner. Inhibition of ER-Golgi transport by brefeldin A (BFA), had a similar effect on the localization of Gn. However, inhibition of ER to Golgi transport of co-expressed Gc and Gn by overexpression of Sec12p or by BFA revealed distinct localization patterns, i.e. diffuse ER localization versus concentration at specific spots. It is furthermore shown that, upon ER retention of Gn, this protein is able to induce ER membrane deformation, a phenomenon previously shown to occur only at Golgi membranes.

INTRODUCTION

Tomato spotted wilt virus (TSWV) is a plant-infecting counterpart of the animal-infecting viruses within the arthropod-borne *Bunyaviridae* (Goldbach and Peters, 1996). Viruses of this family obtain their lipid membrane at the Golgi complex. Instead of ribonucleoproteins (RNPs) budding into enlarged lumen of the Golgi as regularly observed for the animal-infecting bunyaviruses, TSWV particles arise within the infected plant cell from RNPs becoming enwrapped by Golgi cisternae (Kikkert *et al.*, 1999). The resulting doubly enveloped virus particles (DEVs) fuse with each other and ER-membranes, leading to the accumulation of singly enveloped virus particles (SEVs) in large cytoplasmic vesicles where they retain until uptake by its insect vector (thrips) upon feeding (Kikkert *et al.*, 1999; Kitajima *et al.*, 1992a).

The viral glycoproteins Gn and Gc (where n and c refer to the amino- and carboxy-terminal topology within the precursor protein) are generally assumed to play a key role in bunyavirus particle assembly and release. Previous transient expression studies in plant cells have shown that TSWV Gn is able, by itself, to migrate from the ER to the Golgi complex. On the other hand, Gc on its own retains in the ER, unless Gn is co-expressed, enabling their co-migration to the Golgi complex (Chapter 2).

Other studies have shown that the viral nucleocapsid (N) protein (the major protein component of viral RNPs) interacts with both glycoproteins at ER and/or Golgi (Chapter 3) in a microtubule- and actin-independent manner (Chapter 4). In contrast, the formation of large N agglomerations did require active actin filaments (Chapter 4). Furthermore, N has been shown to influence the localization of Gc within the ER (Chapter 3), recruiting it to ER export sites (ERES) (Chapter 5). When co-expressed, Gn and Gc were also found to partially localize at the ERES, indicating that also Gn is able to recruit Gc to these specific ER-domains, while trafficking to the Golgi complex. ERES are specialized regions of the ER involved in the sorting of proteins for COPII-mediated ER-to-Golgi transport (Aridor *et al.*, 1999). The sequential action of COPII and COPI coat complexes is a widely accepted model for ER-to-Golgi transport of proteins in different organisms (Hanton *et al.*, 2006; Matheson *et al.*, 2006; Sato and Nakano, 2007). COPII vesicles are involved in the anterograde cargo transport and COPI vesicles, although mainly responsible for the retrograde transport, have been suggested to take part in both directions (reviewed by Barlowe (2002)). During COPII vesicle formation, Sec12p, an integral ER membrane protein, acts as a specific GTP/GDP exchange factor for the activation of the small GTP binding protein Sar1p (Barlowe and Schekman, 1993). This causes the exposure of the N-terminal amphipatic α-helix of Sar1p that constitutes a membrane anchor to the ER (Huang *et al.*, 2001), and an additional increase in the affinity for the Sec23/24p complex, leading to the formation of a prebudding complex. The binding of other components to this coat complex and its polymerization ultimately give rise to the formation of COPII vesicles (Barlowe *et al.*, 1994; da Silva *et al.*, 2004).

Throughout this thesis, several specific steps involved in the TSWV particle assembly mechanism have been analyzed. In this chapter, attention was paid to the steps involved in ER-exit and transport to the Golgi of the viral glycoproteins. More specifically, the ER-arrest of Gc has been analyzed by investigating possible interactions with ER chaperones and analyzing the influence of the protein's transmembrane and cytoplasmic domains in this retention. Furthermore, we have also analyzed the ER-to-Golgi transport of the viral glycoproteins by using two distinct interference strategies: overexpression of Sec12p and application of brefeldin A

(BFA). Overexpression of Sec12p is known to inhibit COPII vesicle formation, likely due to a titration of Sar1p (Phillipson *et al.*, 2001), while the fungal metabolite brefeldin A (BFA) causes, among others, the loss of *cis*-Golgi cisternae thereby leading to a redistribution of Golgi membrane proteins to the ER (Boevink *et al.*, 1998; Brandizzi *et al.*, 2002b; Ritzenthaler *et al.*, 2002).

MATERIALS AND METHODS

PLASMID CONSTRUCTION AND ORGANELLE MARKERS

The plant expression vectors containing the chimeric Gc with the cytoplasmic tail of Gn (p2GW7.0Gc(CTn) and with the cytoplasmic tail and transmembrane domain of Gn (p2GW7.0Gc(TMDnCTn) were obtained using the GATEWAY^{TM} system (Invitrogen), following the manufacturer's instructions. The primers GcFwdGW (GGGGACAAGTTTGTACAAAA AAGCAGGCTGGATGAGTGTACTAAAGTCTGCATTTC) and CTnRvsGW (GGGGAC CACTTTGTACAAGAAAGCTGGGTGTCAT TCCATGCTAGTCCACT) were used to PCR amplify Gc(CTn) and Gc(TMDnCTn) from the previously established pSFVss-Gc-TMc-CTn and pSFVss-Gc-TMn-CTn constructs, respectively (Snippe *et al.*, 2007a). The PCR fragments were introduced into pDonr207 by BP recombination and subsequently into the p2GW7.0 (Karimi *et al.*, 2002) destination vector by LR recombination.

The plant expression vector (with a 35S-driven promotor) containing the YFP-fused chimeric Gc with the transmembrane domain of Gn (pMONGc(TMDn)-YFP) was obtained by assembly PCR. A PCR fragment containing the transmembrane domain of Gn flanked by the SphI and XhoI restriction sites (amplified with the TMDnFwd –GGGGCATC TGCATCAATTTTTCTTGG- and TMDnRvs - GGGCTCGAGATGTGTGACTATGCACAG- primers from pMON Gn-YFP, Chapter 2) was fused with another PCR fragment containing the complete sequence of pMON Gn-YFP with the exception of the transmembrane domain of Gc, flanked by the same restriction sites (amplified with the LDcRvs – GGGGCATG CACTCTTAATATAATCCC and CTcFwd - GGGCTCGAGATATGTAAAGAATGAAT- primers from pMONGc-YFP, Chapter 2).

The fluorescent proteins used in this study for fusion to the viral glycoproteins were a pH-insensitive form of YFP and mGFP5 (Haseloff *et al.*, 1997). The spectral properties of mGFP5 allow efficient spectral separation from YFP (Brandizzi *et al.*, 2002b).

In these experiments we made use of the GFP-HDEL ER-marker (Carette *et al.*, 2000) and the ST-GFP Golgi-marker (Boevink *et al.*, 1998) and the YFP-Sec24 ER export sites-marker (Stefano *et al.*, 2006).

PLANT MATERIAL, TRANSIENT EXPRESSION AND TREATMENT

Tobacco plants (*Nicotiana tabacum* cv Petit Havana) (Maliga *et al.*, 1973) were grown in Murashige and Skoog medium (Murashige and Skoog, 1962) and 2% sucrose in controlled sterile conditions at 25°C with a 16 hours light period per day. Tobacco leaf protoplasts were prepared and transfected as described by Denecke and Vitale (1995), with some minor modifications. In short, leaves of fully-grown plants were pierced and digested overnight in TEX [B5 salts, 500 mg/l MES, 750 mg/l $CaCl_2 \cdot 2H_2O$, 250 mg/l NH_4NO_3, 0.4 M sucrose, pH 5.7] containing 0.2% Macerozyme and 0.4% Cellulase. Protoplasts were recovered by filtration and washed 3 times after centrifugation in Electroporation Buffer (EB) [0.4 M sucrose, 2.4 g/l HEPES, 6 g/l KCl, 600 mg/l $CaCl_2 \cdot 2H_2O$, pH 7.2]. Healthy living protoplasts were recovered and resuspended in a proper EB volume. A volume of 100 µl EB containing plasmid DNA (30 µg each) was added to 500 µl of protoplast suspension and subjected to electroporation (160V, 925µF, $\infty\Omega$) in 4 mm cuvettes using a BIO-RAD X-cell electroporator. After a 10 min recovery, protoplasts were incubated in 2 ml TEX in the dark (the incubation times differed per experiment, ranging between 24 and 48 hours). When applicable, BFA (Sigma) was added immediately after recovery, at a final concentration of 50 µg/mL. This amount was found to be most optimal for our studies, resulting in the expected effects in control samples, while maintaining the cells' viability.

Nicotiana tabacum plants stably expressing the Golgi-marker ST-GFP (kindly provided by Prof. Chris Hawes) were grown under the previously described conditions and the analyses were conducted in protoplasts isolated and transfected according to the previously described methodology.

SAMPLING AND IMAGING

Twenty four to forty eight hours post-transfection, the living protoplasts were isolated by centrifugation and confocal sections images were obtained using an inverted Zeiss 510 Laser Scanning Microscope and a 40x oil or 63x oil and water immersion objective.

For the imaging of the single expression of YFP-fused proteins, excitation lines of an argon ion laser of 488 nm were used with a 505/530 nm bandpass filter in the single-track facility of the microscope. For the imaging of the co-expressing YFP-fused and the GFP-fused proteins, excitation lines of an argon ion laser of 458 nm for GFP and 514 nm for YFP were alternately used with line switching using the multi-track facility of the microscope. Fluorescence was detected using a 458/514 nm dichroic beam splitter and a 470/500 nm bandpass filter for GFP and a 535/590 nm bandpass filter for YFP. Appropriate controls were performed to exclude possible crosstalk and energy transfer between fluorochromes. For the imaging of FITC, excitation lines of an argon ion laser of 488 nm were used with a 505/530 nm bandpass filter in the single-track facility of the microscope.

INDIRECT FLUORESCENCE ANALYSIS

Living protoplasts were selected as previously described and carefully placed on a microscope slide previously coated with 0.05% poly-L lysine. Approximately 5 min after, the

slides are submerged in 96% ethanol where the fixation occurred for about 20 min. After a 20 min wash in PBS (0.137 M NaCl, 1.5 mM KH_2PO_4, 8.1 mM Na_2HPO_4, 2.7 mM KCl, 3.1 mM NaN_3), the protoplasts are blocked with 5% BSA in PBS for 45 min. The cells were subsequently incubated for one hour in a 1:1000 dilution of the polyclonal antibodies against Gc (raised in rabbit) (Kikkert *et al.*, 1997) in 1% BSA in PBS. Three washing steps of 20 min in PBS preceded one hour incubation in the dark, in a 1:100 dilution of the secondary antibody (swine anti-rabbit conjugated with Fluorescein Iso-Thiocyanate, FITC) in 1% BSA in PBS. The cells were then washed with PBS in three steps of 20 min, always in the dark. Two drops of citifluor were added to the slides, before examination under an inverted Zeiss 510 Laser Scanning Microscope.

IMMUNOPRECIPITATION ANALYSIS

After transfection, the protoplasts were incubated for about two hours and the cells were recovered by centrifugation. Fifty to a hundred μL of 35-S methionine were added to the cells to reach a total of 100-200 μCi/mL in the labeling solution. After about 16 hours, the cells were 10 times diluted in 250 mM NaCl. After centrifugation, the cells were resuspended in 500 μL homogenization buffer (200 mM Tris-HCl, pH 8.0, 300 mM NaCl, 1% Triton X-100, and 1 mM EDTA) followed by 5 minutes centrifugation at 4°C. The cell extract was precipitated in NET gel buffer (50 mM Tris-HCl, pH 7.5, 150 mM NaCl, 1 mM EDTA, 0.1% IGEPAL CA-630, 0.02% NaN_3, and supplemented with 0.25% gelatin), containing anti-GFP antiserum. After 1h incubation on ice and centrifugation, the supernatant was added to a tube containing 2.5 mg of hydrated Protein A-Sepharose (Sigma-Aldrich) in NET buffer. The samples were incubated for 2h at 4°C with slow rotation. Protein A-Sepharose was then pelleted by 10 min centrifugation at 8000*g*, and the supernatant was discarded. The pellet was washed twice with NET buffer. Thirty microliters of SDS-PAGE sample buffer were added to the final pellet, and the suspension was incubated at 95°C for 5 min and analyzed by SDS-PAGE. Labeled proteins were detected by phosphor imaging (Fuji Film FLA 500).

RESULTS

THE TRANSMEMBRANE DOMAIN OF GN IS SUFFICIENT TO ENABLE ER-EXIT AND GOLGI TARGETING OF GC

The viral glycoprotein Gc is retained in the ER, only being able to exit this compartment upon co-expression with Gn (Chapter 2). On the other hand, Gn has all the necessary characteristics to render its exit from the ER and transport to the Golgi (Chapter 2). In order to investigate a possible role of the transmembrane domain (TMD) and cytoplasmic tail (CT) of Gc in its ER-retention, chimerical constructs were made that involved substitutions of the TMD and/or CT of Gc for those of Gn (Fig. 1).
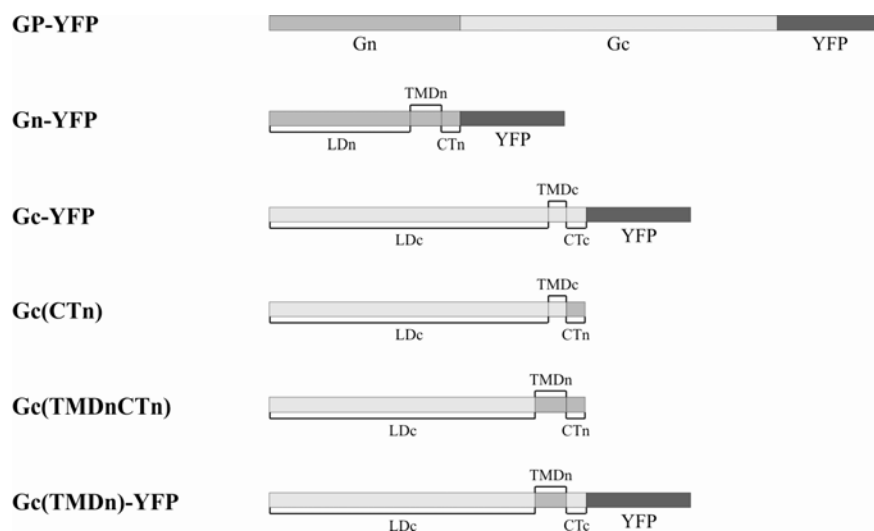
Figure 1: Schematic representation of the viral protein constructs used in this study. TMD, CT and LD refer to, respectively, transmembrane domain, cytoplasmic tail and luminal domain. CTn and CTc refer to the CT of, respectively, Gn and Gc. TMDn and TMDc refer to the TMD of, respectively, Gn and Gc. LDn and LDc refer to the LD of, respectively, Gn and Gc.

The constructs were electroporated into *N. tabacum* protoplasts and the cells were subjected to immunolocalization (except the ones expressing Gc(TMDn)-YFP, which could directly be monitored by confocal microscopy) with antibodies raised against Gc. As control, YFP-fused Gc (Fig. 1) was expressed and, as expected (Chapter 2), revealed a clear reticular pattern that co-localized with ER-marker GFP-HDEL (Fig. 2 a-c).

When the construct Gc(CTn) (containing the CT of Gn, Fig. 1) was expressed, a similar ER pattern was observed 24 (Fig. 2d-f) and 48 (results not shown) hours post-transfection (p.t.), as confirmed by its co-localization with GFP-HDEL. These results indicated that the CT of Gn was not sufficient for release of Gc from ER. In contrast, expression of Gc(TMDnCTn) (which contains both the TMD and CT of Gn, Fig. 1) in protoplasts from plants stably transformed with Golgi-marker ST-GFP, showed that the TMD and CT of Gn allowed Gc to exit from the ER and traffic to the Golgi, as confirmed by its co-localization with ST-GFP (Fig. 2 g-i).

To investigate whether a concerted action of the TMD and CT was required to allow ER-release of Gc, a third (YFP-fused) chimeric construct was made in which only the TMD of Gc was substituted by the one of Gn, and referred to as Gc(TMDn)-YFP (Fig. 1). Expression of this construct surprisingly showed that the TMD of Gn was sufficient to enable ER-exit and Golgi targeting of Gc, as confirmed by co-localization with the Golgi-marker ST-GFP (Fig. 2 j-l).
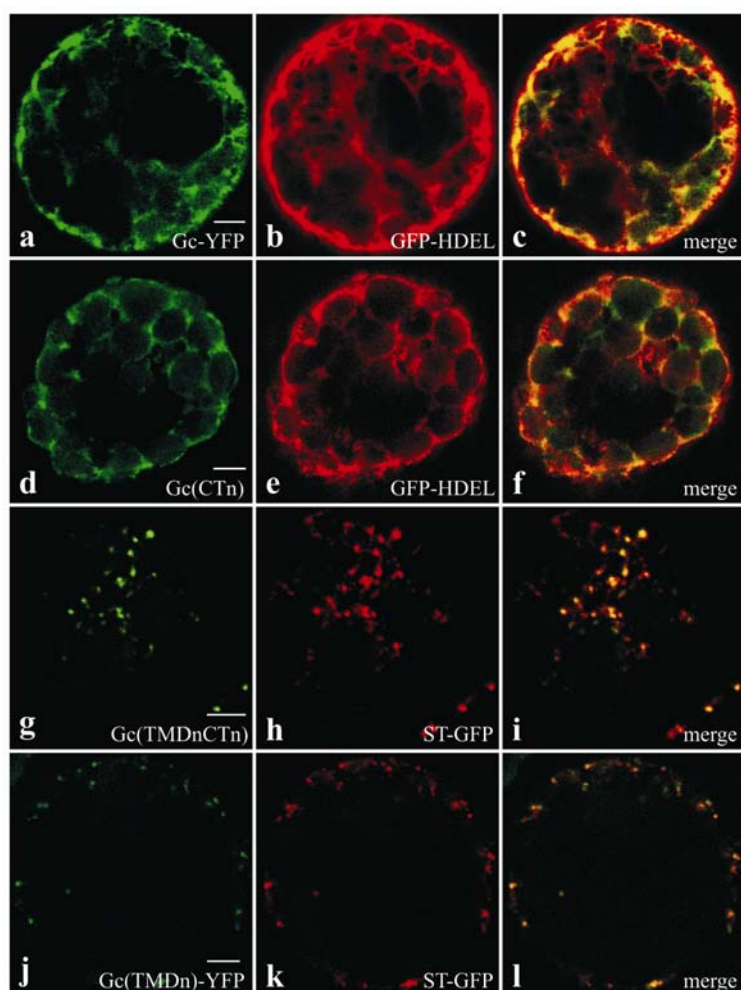
Figure 2: Analysis of the influence of the TMD and/or CT of Gn on ER retention of Gc. Panels a-c: protoplast transfected with Gc-YFP and ER marker GFP-HDEL 24 hours p.t., (a) Gc-YFP, (b) GFP-HDEL, (c) merge of a and b. Panels d-f: protoplast transfected with Gc(CTn) and GFP-HDEL, 24 hours p.t., (d) Gc(CTn), (e) GFP-HDEL, (f) merge of d and e. Panels g-i: protoplast from plants stably transformed with ST-GFP and transfected with Gc(TMDnCTn), 24 hours p.t., (g) Gc(TMDnCTn), (h) ST-GFP, (i) merge of g and h. Panels j-l: protoplast from plants stably transformed with ST-GFP and transfected with Gc(TMDn)-YFP, 24 hours p.t., (j) Gc(TMDn)-YFP, (k) ST-GFP, (l) merge of j and k. Size bars represent 5 μm.

THE TMD AND CT OF GN ARE NOT SUFFICIENT FOR THE INTERACTION WITH GC, NECESSARY FOR ITS RESCUE FROM THE ER

The glycoprotein Gn is able to rescue Gc from the ER (Chapter 2) and studies performed in mammalian cells have shown that the last 20 amino acids of the CT of Gn were essential for their co-translocation to the Golgi complex (Snippe *et al.*, 2007a). These results seemed to
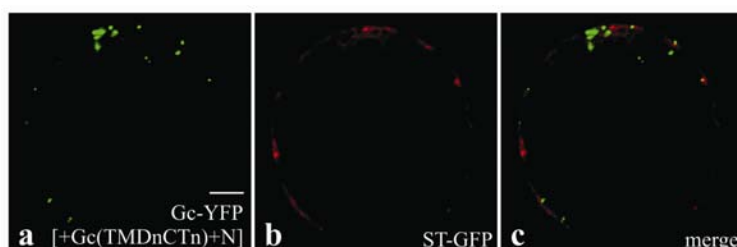

Figure 3: Analysis of the influence of the TMD and CT of Gn on the interaction with Gc. Panels a-c: protoplast from plants transformed with Golgi marker ST-GFP and transfected with Gc-YFP, Gc(TMDnCTn) and N, 24 hours p.t.. (a) Gc-YFP, (b) ST-GFP, (c) merge of a and b. Size bar represents 5 μm.

indicate that the interaction between these two glycoproteins would occur through their cytoplasmic tails. Hence, since Gc(TMDnCTn) was efficiently targeted to the Golgi complex, it was questioned whether this chimera would be able to rescue Gc-YFP to the Golgi complex. To this end, protoplasts from plants stably transformed with the Golgi marker ST-GFP were co-transfected with both constructs. However, the level of expression of Gc-YFP was very low (results not shown), constituting a first indication for the lack of interaction between these two proteins since, normally, interaction with Gn significantly boosts the level of expression of Gc (Chapter 2). The viral N protein was earlier shown to interact with and to greatly increase the expression levels of Gc-YFP (Chapter 3), while simultaneously redirecting it to ERES (Chapter 5). Hence, a construct expressing N (Chapter 3) was co-transfected with Gc-YFP and Gc(TMDnCTn) in the ST-GFP expressing protoplasts, in order to boost the expression of Gc-YFP. In several independent experiments, surprisingly, no co-localization was observed between Gc-YFP and ST-GFP (Fig. 3 a-c), not even after extended periods of expression (48 hours p.t., results not shown). The observed punctate localization of Gc-YFP corresponds to its localization at the ERES, due to the presence of N.

These results indicate that both the TMD and CT of Gn are not sufficient for the interaction with Gc in plant cells resulting in its rescue from the ER, suggesting that the luminal domains of the glycoproteins may be determinant for this interaction.

ER-ARREST OF GC DOES NOT SEEM TO BE DUE TO INTERACTION WITH CHAPERONE PROTEINS

Although exchange of the TMD of Gc by that of Gn was sufficient to render its export from the ER, we also investigated whether the ER-retention of this glycoprotein could be due to misfolding and interaction with ER chaperone proteins. To test this hypothesis, protoplasts were transfected with Gc-YFP (Fig. 1 and Chapter 2), and subjected to immunoprecipitation analysis with an antibody raised against GFP. As controls, non-transfected protoplasts and protoplasts transfected with Gn-YFP were included. The results (Fig. 4) showed that next to Gc-YFP (98 kDa, lane B) or Gn-YFP (78 kDa, lane C), no additional bands indicative for the presence of the main ER-resident chaperone proteins BiP (75 kDa) (Crofts *et al.*, 1998), calnexin (64 kDa) (Huang *et al.*, 1993) or calreticulin (60 kDa) (Crofts *et al.*, 1998) were observed.
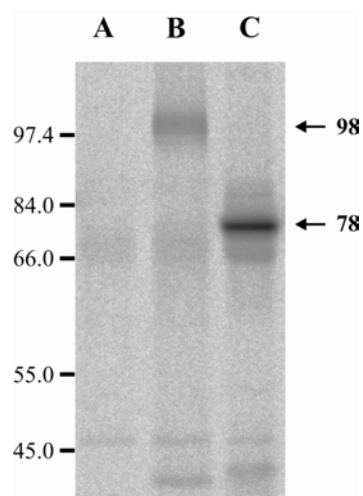
Figure 4: Immunoprecipitation analyses of Gc-YFP and Gn-YFP using specific antibodies against GFP. (A) non-transfected protoplasts, (B) protoplasts transfected with Gc-YFP and (C) protoplasts transfected with Gn-YFP. Molecular weights are indicated in kDa.. Arrows indicate bands corresponding to Gc-YFP and Gn-YFP.

If Gc would be retained in the ER due to an interaction with chaperone proteins, the presence of one or more of these proteins would be expected. Their absence, thus, constitutes an indication that arrest of Gc in ER was likely not due to improper folding. As expected, the non-transfected protoplasts (Fig. 4 lane A) did not show any relevant signal. However, to further confirm these preliminary results, experiments must be performed with specific antibodies directed against the chaperone proteins

ER-TO-GOLGI TRANSPORT OF THE VIRAL GLYCOPROTEINS IS COPII-DEPENDENT

The previously observed localization of the viral glycoproteins at ERES (Chapters 2 and 5) suggested that ER-exit to the Golgi likely involved COPII vesicles. To test this COPII-dependency, a YFP-fused Gn construct (Gn-YFP) (Fig. 1 and Chapter 2) was co-transfected to *N. tabacum* protoplasts with a construct coding for the Arabidopsis homolog of protein Sec12p (Phillipson *et al.*, 2001). Overexpression of this protein provokes inhibition of COPII vesicle budding from the ER surface thereby inhibiting, consecutively, COPII-dependent ER to Golgi transport (Phillipson *et al.*, 2001).

As control, protoplasts were transfected with Gn-YFP and the ER marker GFP-HDEL. Protoplasts from plants stably transfected with the ST-GFP Golgi marker were also transfected with Gn-YFP. As previously shown (Chapter 2) Gn localized in the ER (Fig. 5 a-c) and, at later times p.t. (here, after 48h), in the Golgi complex (Fig. 5 d-f), either in small dense globular structures or in pleomorphic Gn-induced membrane structures.

Upon co-expression of Gn-YFP, Sec12p and the ER marker GFP-HDEL (Fig. 5 g-i), Gn retained in the ER in all the cells analyzed, even beyond 48 hours p.t. (results not shown). These data suggested that ER-to-Golgi transport of Gn is COPII-dependent.

Since Gn was shown to be depended on COPII vesicles for its movement to the Golgi complex, it was expected that both viral glycoproteins Gn and Gc, when co-expressed, would also show this dependency.

Gc-YFP and Gn (processed from GP-YFP) localize as punctate spots that were earlier found to co-localize with a Golgi marker and, in some cases, with an ERES-marker (Chapter 2), and do not co-localize with the ER-marker HDEL-GFP (Fig. 6 a-c)

However, when protoplasts were co-transfected with GP-YFP, GFP-HDEL and Sec12p (Fig. 6 d-f), the glycoproteins localized in a reticular pattern and show an almost complete co-localization with the ER marker, indicating that the ER-to-Golgi transport of Gc and Gn glycoproteins is COPII-dependent. The glycoproteins were also (in lower amount) observed in punctate spots that did not co-localize with HDEL-GFP (Fig. 6 d-f) and likely correspond to ERES, where the glycoproteins are normally also found.

Figure 5: Effect of Sec12p overexpression on transport of Gn to the Golgi complex. Panels a-c: protoplast transfected with Gn-YFP and GFP-HDEL 24 hours p.t., (a) Gn-YFP, (b) GFP-HDEL, (c) merge of a and b. Panels d-f: protoplast from plants stably transformed with ST-GFP and transfected with Gn-YFP, 48 hours p.t., (d) Gn-YFP, (e) ST-GFP, (f) merge of d and e. Panels g-i: protoplast transfected with Gn-YFP, Sec12p and GFP-HDEL, 48 hours p.t., (g) Gn-YFP, (h) GFP-HDEL, (i) merge of g and h. Size bars represent 5 μm.

Figure 6: Effect of overexpression of Sec12p on transport of Gc and Gn (co-expressed from their common precursor GP) to the Golgi complex. Panels a-c: protoplast transfected with GP-YFP and GFP-HDEL 24 hours p.t., (a) GP-YFP (Gc-YFP), (b) GFP-HDEL, (c) merge of a and b. Panels d-f: protoplast transfected with GP-YFP, Sec12p and GFP-HDEL, 24 hours p.t., (d) GP-YFP (Gc-YFP), (e) GFP-HDEL, (f) merge of d and e. Size bars represent 5 μm.

To further substantiate the previous results and, with a different approach, investigate the dependency on the vesicular transport route for ER-to-Golgi trafficking of the viral glycoproteins, protoplasts were transfected with Gn-YFP (Fig. 1 and Chapter 2) and immediately incubated in the presence of BFA, a fungal metabolite that, among others, causes the loss of *cis*-Golgi cisternae, leading to a redistribution of Golgi membrane proteins to the ER (Boevink *et al.*, 1998; Brandizzi *et al.*, 2002b; Ritzenthaler *et al.*, 2002). After 24 to 48 hours protoplasts were checked for viability (results not shown) prior to confocal microscopy analysis. In the absence of BFA, Gn-YFP was found at the ER and (at later p.t.) at the Golgi and Golgi-derived (pseudo)-circular/pleomorphic membrane structures (Fig. 5 a-f and Chapter 2). In the presence of this drug, however, (at all analyzed time points) Gn entirely co-localized with the ER marker GFP-HDEL, even when present in pleomorphic/circular membrane structures (Fig. 7 a-c).

When, as a control to check the effectiveness of the drug, Gn-YFP was co-expressed with the Golgi-marker ST-GFP (which, under these conditions, retained in ER) in the presence of BFA, both proteins also completely co-localized in a similar fashion, i.e. in a reticular pattern (Fig. 7 d-f) or in pleomorphic membrane structures (Fig. 7 g-i). All these results demonstrated that the transport of Gn to the Golgi is BFA-sensitive.

Additionally, these results demonstrate that Gn is also able to induce the deformation/circularization of ER membranes (Fig. 7 a-c and g-i) (a phenomenon previously observed to occur only at Golgi membranes), suggesting that this capability is intrinsic to the glycoprotein and independent on the membrane where it localizes.

Similarly, both Gc and Gn glycoproteins were co-expressed (from the precursor GP-YFP gene, Fig. 1) in the presence of BFA. Surprisingly, the glycoproteins did not localize in a reticular pattern (indicative of ER-retention), but in punctate spots similarly to what has been observed in the absence of the drug (Fig. 6 a-c, and Chapter 2). Upon co-expression with HDEL-GFP, only partial or no co-localization was observed (Fig. 8 a-c). As co-localization was neither observed with the (ER-retained) ST-GFP Golgi marker (Fig. 8 d-f), these results seemed to indicate that the ER exit of Gc and Gn had not been affected by the presence of the drug. However, in the absence of the drug, as previously explained, some of the GP-YFP was found to localize at the ERES (Chapter 2). Hence, it was tempting to consider the possibility that the observed punctate spots upon incubation with BFA did not correspond to Golgi stacks, but to ERES, which would indicate ER-retention due to sensitivity to BFA. This hypothesis is further supported by the BFA-sensitivity of transport of singly expressed Gn to the Golgi, since this glycoprotein is the responsible for the ER-to-Golgi transport of the Gn-Gc complex.

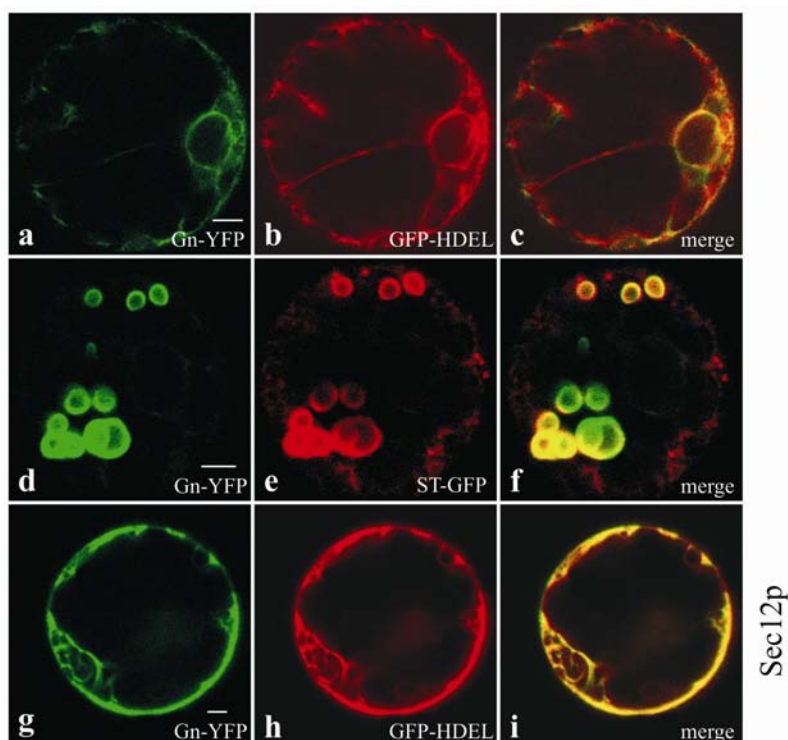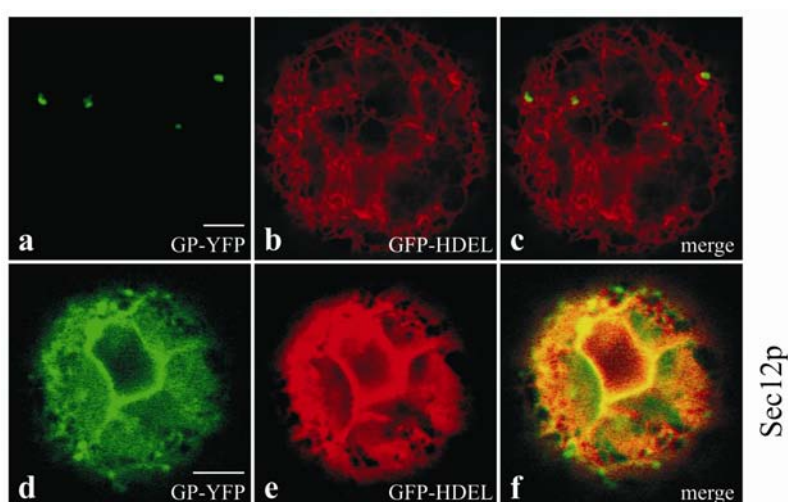**Figure 7:** Effect of BFA on transport of Gn to the Golgi complex. Panels a-c: protoplast transfected with Gn-YFP and GFP-HDEL, incubated 24 hours in the presence of BFA, (a) Gn-YFP, (b) GFP-HDEL, (c) merge of a and b. Panels d-f: protoplast transfected with Gn-YFP and ST-GFP, incubated for 24 hours in the presence of BFA, (d) Gn-YFP, (e) ST-GFP, (f) merge of d and e. Panels g-i: protoplast transfected with Gn-YFP and ST-GFP, incubated for 24 hours in the presence of BFA, (g) Gn-YFP, (h) ST-GFP, (i) merge of g and h. Size bars represent 5 μm.

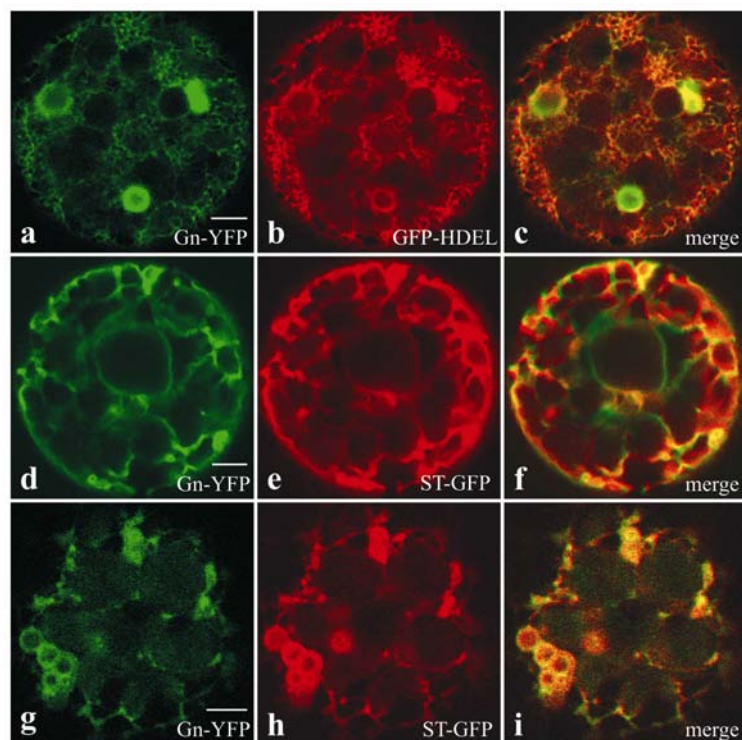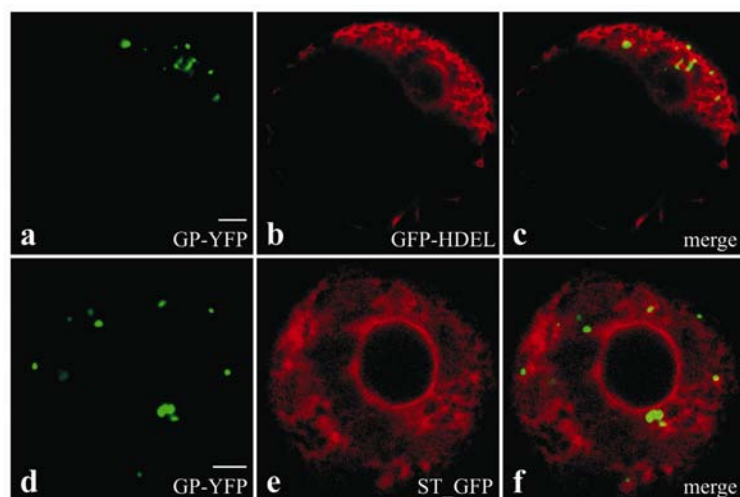**Figure 8**: Effect of BFA on the transport of GP (Gn-Gc) to the Golgi complex. Panels a-c: protoplast transfected with GP-YFP and GFP-HDEL, incubated 24 hours in the presence of BFA, (a) GP-YFP, (b) GFP-HDEL, (c) merge of a and b. Panels d-f: protoplast transfected with GP-YFP and ST-GFP, incubated for 24 hours in the presence of BFA, (d) GP-YFP, (e) ST-GFP, (f) merge of d and e. Size bars represent 5 μm.

DISCUSSION

Previous studies (Chapter 2) have shown that the TSWV glycoprotein Gc retains in the ER and is only able to escape and migrate to the Golgi complex in the presence of Gn. Several reports have demonstrated that the transmembrane domain and cytoplasmic tail dictate the ER-export and translocation of type I membrane-spanning proteins in plant cells (Brandizzi *et al.*, 2002a; Hanton *et al.*, 2005; Moreau *et al.*, 2007). Hence, the influence of these two domains on the ER-arrest of Gc has here been studied by constructing chimeric Gc proteins where its TMD and/or CT were exchanged with those of Gn (which is, by itself, able to exit the ER and migrate to the Golgi; see Chapter 2). The results have shown that the transmembrane domain of Gn is sufficient to render Gc's export from the ER. The cytoplasmic tail of Gn, however, does not affect the localization of Gc.

One of the main differences between the TMDs of Gc and Gn is their length (40 and 70 amino acids (aa), respectively). It has been shown (Brandizzi *et al.*, 2002a) that the TMD length of type I membrane proteins plays an important role in their final destination within the secretory pathway (shorter TMDs restricting the proteins to the ER and longer TMDs allowing their migration to other locations). These observations supported the model for protein translocation within the secretory pathway by means of diffusion: a protein migrates within the secretory pathway until is able to find a membrane with the right thickness to mask its hydrophobic transmembrane domain (Brandizzi *et al.*, 2002a; Moreau *et al.*, 2007). In this way, one could consider that the ER membrane would likely have insufficient thickness to harbour the TMD of Gn. However, although smaller, the 40 aa TMD of Gc is still significantly longer that the 23 aa TMD suggested to be necessary for ER-release (Brandizzi *et al.*, 2002a). Analysis of the aa composition of the TMD of Gn did not show any specific combination that might cause this ER-export. Hence, the specific characteristics of the TMD of Gn that may cause the ER-release of Gc in the presence of Gn were not yet identified.

Since it had been previously reported (in mammalian cells) that, next to the TMD, an additional stretch of 10 aa within the CT of Gn is required for Golgi-localization of this protein (Snippe *et al.*, 2007a) it was quite surprising to observe that the CT of Gn did not seem to be crucial for ER-export in plant cells. Unless such cell sorting signals act differently in these two types of cells, it is possible that ER-export is the result of a concerted action of the TMD of Gn and the cytoplasmic tail (of Gn or Gc) to which it is attached. However, the CTs of Gn and Gc would have to share a functional similarity, which was not directly revealed by primary or secondary sequence analyses.

As the chimera Gc(TMDnCTn) harbors all the suggested requirements for ER-exit and migration to the Golgi, we were interested in investigating whether it would be able to interact with Gc and overcome its ER-arrest. The results showed that Gc was still not able to migrate to the Golgi complex in the presence of this chimera and demonstrated that the TMD and CT of Gn are not sufficient for interaction with Gc. It had previously been shown that the last 20 aa of the CT of Gn are essential for the interaction with Gc in mammalian cells (Snippe *et al.*, 2007a). Since it is not expectable that the interacting domains differ between these two different cell types, it can be suggested that, together with the cytoplasmic tail, also the luminal domain of Gn may be required for interaction with Gc.

Besides the influence of the TMD of Gc on it's ER-arrest, the possibility that this phenomenon would result from a misfolding of the glycoprotein and interaction with

ER-chaperone proteins (Crofts *et al.*, 1998; Crofts and Denecke, 1998; Denecke *et al.*, 1991; Pimpl and Denecke, 2000) was also investigated. Interaction with Gn would induce its proper folding, enabling the co-migration as a protein complex to the Golgi complex. Interactions of viral proteins with ER-chaperones have previously been shown to occur for the newly synthesized Gn and Gc glycoproteins from Uukuniemi phlebovirus (Veijola and Pettersson, 1999). However, preliminary experiments involving co-immunoprecipitation of singly expressed TSWV Gc did not reveal a bound status with any of these three main ER-resident chaperone proteins, suggesting that misfolding is not the cause of the ER-arrest of Gc. Further experiments using specific antibodies directed against these proteins should be performed to substantiate this preliminary result.

The presence of Gn renders Gc capable to migrate to the Golgi complex (Chapter 2), the viral assembly locus. Export of proteins from the ER to the Golgi complex in plants cells has been shown to occur through different routes. In addition to a COPII-dependent mechanism, alternatives have been suggested (Hanton *et al.*, 2006; Oufattole *et al.*, 2005; Takahashi *et al.*, 2005; Tormakangas *et al.*, 2001) that are mostly thought to be involved in the transport of proteins to the protein storage vacuole. Our results showed that Gn and the Gn-Gc complex migrate to the Golgi complex by COPII-vesicles, as overexpression of Sec12p (that causes the titration of Sar1p, resulting in the inhibition of COPII-vesicles formation (Phillipson *et al.*, 2001)) aborted glycoprotein trafficking to the Golgi.

Golgi targeting was also blocked by the fungal metabolite BFA, a drug that, among others, causes the loss of *cis*-Golgi cisternae, leading to a redistribution of Golgi membrane proteins to the ER (Boevink *et al.*, 1998; Brandizzi *et al.*, 2002b; Ritzenthaler *et al.*, 2002). However, whereas Gn-Gc localized mainly in a reticular (ER) pattern upon overexpression of Sec12p, in the presence of BFA these proteins concentrated at specific punctate spots. A first analysis of this result would suggest that the transport of Gn-Gc from the ER to the Golgi would not be affected by BFA. However, this hypothesis is very unlikely since Gn (whose single migration is sensitive to this drug) is the protein within this complex that guides this translocation. Furthermore, the presence of Gn-Gc at the ER in a punctate appearance was previously shown to occur in the absence of any drug. Indeed, upon expression of the glycoprotein precursor, the two mature proteins were found at the Golgi complex but also at specific locations within the ER, the ERES (Chapter 2). Hence, it is likely that, in the presence of BFA, the ER-to-Golgi transport of the glycoproteins was indeed blocked, rendering accumulation of the glycoproteins at ERES and explaining the observed (glycoproteins-containing) punctate spots. It has been suggested that the BFA effects on protein secretion and the block of ER-to-Golgi transport in plant cells would be a consequence of an inhibition of elements responsible for the recruitment of the components of the COPI coats, causing their loss from the Golgi apparatus (reviewed by Nebenfuhr *et al.* (2002)). The breakdown of the physical separation between ER and Golgi, allowing membrane fusion, has also been suggested (Nebenfuhr *et al.*, 2002). Only few reports have shown a direct interference of this drug with the ERES formation in plant cells. However, da Silva *et al.* (2004) have demonstrated that the presence of BFA inhibited the accumulation of Sar1p at the ERES, suggesting an influence of this drug on the functionality of these domains. Contradictory, in BY-2 cells, it was demonstrated that LeSec13 concentration at ERES is independent of BFA (Yang *et al.*, 2005). Failure of BFA to prevent recruitment of cargo to the ERES has also previously been demonstrated in animal cells (Ward *et al.*, 2001). Independently of the BFA effect on ERES and COPII vesicle formation, our results seem to indicate that this drug has no influence on the glycoprotein's concentration at specific areas within the ER. Whether these areas correspond to

functional ERES still needs to be determined. However, the results obtained upon co-expression of Sec12p suggest that this concentration of Gn and Gc at specific loci is dependent on the functionality of the ERES. Indeed, under these conditions, the glycoproteins localize mostly in a reticular pattern, which may be explained by the fact that this overexpression directly interferes with the COPII-vesicle formation (Phillipson *et al.*, 2001), affecting the functionality of the ERES.

Last but not least, our studies revealed that, when Gn was arrested in ER due to BFA, part of these membranes were modified into (pseudo)-circular/pleomorphic membrane structures, as previously reported to occur in Golgi-derived membranes (Chapter 2). Apparently, this membrane deformation is an intrinsic property of Gn (and not membrane-specific) and may reflect some stage of membrane curvature required for the enwrapment of viral RNPs (Chapter 2). TSWV particle maturation upon enwrapment of ER membranes around the viral RNPs has never been observed but the Punta Toro virus (an animal infecting counterpart of TSWV within the *Bunyaviridae* family) was found to be able to adapt to the transport blockage by BFA by assembling in different intracellular membranes, producing infectious virions, although these were never released from the cells (Chen *et al.*, 1991). Whether the application of BFA would block the assembly of TSWV particles during a natural infection remains to be investigated.

ACKNOWLEDGEMENTS

CHAPTER 6

CHAPTER 7

GENERAL DISCUSSION
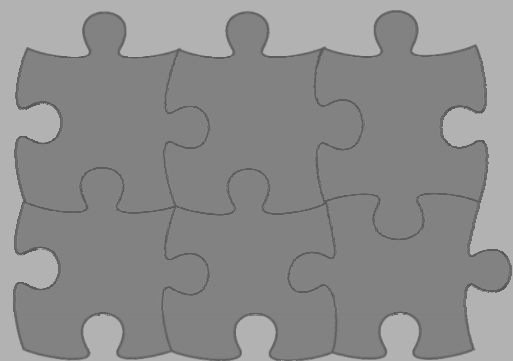
The work presented in this thesis aimed at obtaining more insight into the process of TSWV particle assembly in plants by studying the structural proteins Gc, Gn and N upon transient expression in protoplasts and their relation to elements of the plant endomembrane system and cytoskeleton. The use of fluorophore-fused proteins allowed monitoring of their *in vivo* behavior by confocal microscopy as well as the application of FRET/FLIM technologies for the analysis of possible protein-protein interactions. The additional use of specific organelle marker proteins allowed the identification of their specific cellular localization.

The results obtained, in combination with previous observations made in infected plant protoplasts (Kikkert *et al.*, 1999) and cells from naturally infected plant tissue (Kitajima *et al.*, 1992b), led to the proposed current model for TSWV particle assembly in plant cells, as schematically presented in Figure 1.
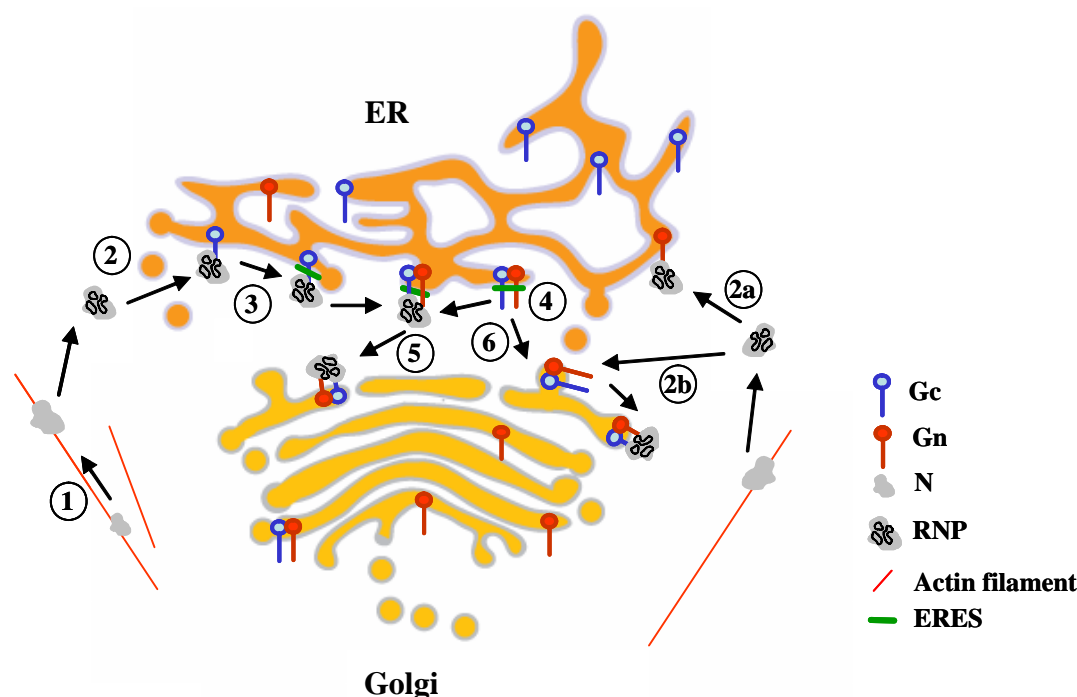
Figure 1: Proposed model for TSWV particle assembly in plant cells. The figure and the sequential steps indicated by numbers are explained in the text.

This model proposes that the viral nucleocapsid protein (N) oligomerizes along actin filaments (Fig. 1 step 1) while encapsidating the viral RNA genome together with small amounts of the RNA-dependent RNA polymerase, forming the infectious ribonucleoproteins (RNPs). These move in a cytoskeleton-independent manner to the ER where the RNPs, by means of N, interact with the cytoplasmic tail of Gc (Fig. 1 step 2) (or Gn, figure 1 step 2b), and subsequently accumulate at ER export sites ERES (Fig. 1 step 3). Meanwhile, Gn interacts with Gc (Fig. 1 step 4), relocating it to ERES, and both co-migrate to the Golgi complex via COPII vesicles. The viral protein complexes that exit from ERES may consist of Gc, Gn and RNPs (Fig. 1 step 5) or Gc and Gn (Fig. 1 step 6) that upon arrival in the Golgi may interact with RNPs (Fig. 1 step 2b).

Once all structural components have reached and concentrated in the Golgi, its membranes wrap around RNPs forming doubly enveloped virus particles (DEVs) that fuse with each other and ER membranes forming singly enveloped virus particles (SEVs) that retain in large cytoplasmic vesicles until uptake by the insect vector (Kikkert *et al.*, 1999; Kitajima *et al.*, 1992a).

In the remainder of this chapter, the proposed model and the results that led to its formulation will be discussed in light of the plant cell's architecture and in a comparison to previous results obtained on TSWV and other members of the Bunyavirus family during (transient expression) studies in animal cells.

RNP FORMATION AND MOVEMENT

Formation of RNPs requires N protein's oligomerization and simultaneous encapsidation of genomic RNA. Once synthesized, the viral N protein localizes in the the cytoplasm in agglomerations that are formed as a result of homotypic interactions (Chapter 3). The occurrence of these interactions had already been shown *in vitro* (Uhrig *et al.*, 1999) and *in vivo* in mammalian cells (Snippe *et al.*, 2005b), and FRET-FLIM techniques helped us to ultimately verify that this also takes place in the "real world", i.e. within the living plant cell. Microtubules were shown not to be involved in the transport of N through the cytoplasm to form these agglomerations in plant cells, since their number and appearance did not change in the presence of a microtubule polymerization inhibitor (Chapter 4). However, when an inhibitor of actin polymerization was applied, a significant increase in the number of these agglomerations was observed, together with a reduction in their size (Chapter 4). Hence, actin filaments seem to be involved in the cytoplasmic transport of N. Besides the requirement of the transport of N along actin filaments for the formation of large N agglomerations, this protein must also be transported to the vicinity of ER and/or Golgi complex, in order to interact with the glycoproteins. In this study we have shown that this transport does not seem to occur by means of microtubules or actin, since the disruption of these networks did not seem to affect these interactions (Chapter 4). These results were quite surprising since both cytoskeleton elements have been shown to be involved in the behavior of N/RNPs of several animal-infecting members of the *Bunyaviridae* family (Andersson *et al.*, 2004b; Ramanathan *et al.*, 2007; Ravkov *et al.*, 1998). Also for TSWV, the localization of transiently expressed N was affected in mammalian cells, upon application of microtubule and actin depolymerizing drugs (Snippe *et al.*, 2005b). The unexpected result that, in plant cells, the cytoskeleton does not seem to be involved in the transport of N to ER and/or Golgi may be due to the differences in the cellular organization and function of cytoskeleton elements between plant and mammalian cells (Fig. 2) (Alberts, 2002). In animal cells, the microtubules emerge from one or two microtubule organizing centers (MTOC) (Chapman *et al.*, 2000; Joshi, 1993), which are located in a perinuclear region, in close proximity to the Golgi apparatus (Fig. 2). The MTOC gathers the (static) minus ends of the microtubules into a centralized location, from where, in a dynamic mode, the (+)-ends of microtubules constantly polymerize and depolymerize. In contrast, in plants, no distinct MTOC has been described. The minus and plus ends are distributed throughout the cell cortex to which they tightly associate (Ehrhardt and Shaw, 2006). Although not much is yet known concerning the characteristics of microtubule

nucleation sites in plants, recent studies have suggested their presence at the nuclear surface and close to the cell membrane (Ehrhardt and Shaw, 2006; Erhardt *et al.*, 2002).
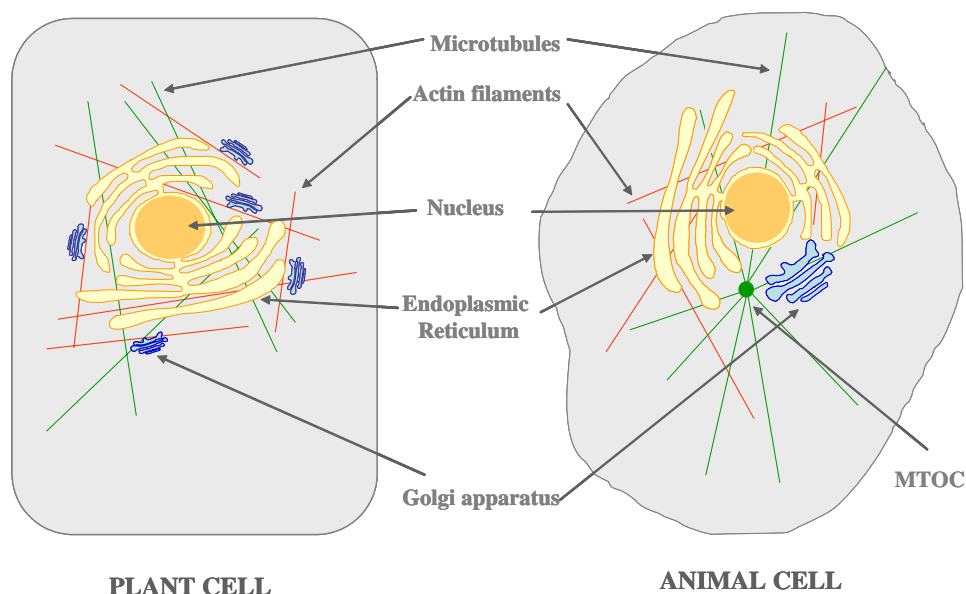
Figure 2: Schematic representation of the cellular architecture of plant and animal cells, highlighting the differences in the microtubule network and Golgi apparatus organization.

It has been demonstrated that the N protein of several bunyaviruses engages in a cytoskeleton-dependent movement to a perinuclear region (Andersson *et al.*, 2004b; Kochs *et al.*, 2002). This localization has been suggested to correspond to aggresomes, accumulation sites for misfolded proteins, that are related to the MTOC (Johnston *et al.*, 1998). A similar pattern was also observed for TSWV N protein when expressed in mammalian cells (Snippe *et al.*, 2005b). This localization is justified in animal cells, since the MTOC is in close proximity to the Golgi complex, the virus assembly locus. Indeed, it has been suggested that this location might be exploited by viruses to concentrate their structural proteins in vicinity of the particle assembly site (Heath *et al.*, 2001). However, in plant cells, the N protein did not localize either at a perinuclear region, or at any specific spot in the cell, which may be explained by the lack of a single MTOC (Fig. 2). Also the organization of the secretory pathway differs between these two cell types. While in mammalian cells the Golgi complex localizes in the perinuclear region, close to the MTOC, this organelle, in plant cells, is composed by several motile stacks distributed all over the cell (Fig. 2) (Ward and Brandizzi, 2004). Hence, the perinuclear localization of N would not bring it to the required proximity of the glycoprotein-containing Golgi cisternae. One might speculate that agglomerations of N could still localize in close proximity to Golgi stacks in plant cells, perhaps in a location that would correspond to the plant microtubule nucleation sites. However, this seems unlikely since no proximity between N agglomerations and the Golgi was observed upon transient expression (Chapter 3) and the nucleation sites seem to concentrate mainly at the nuclear envelope and cortex regions of the cell. Surprisingly, during our studies, a co-localization between depolymerized α-tubulin and ERES was observed. Although

microtubules are not involved in the ER-to-Golgi vesicular transport in plant cells (Boevink *et al.*, 1998; Brandizzi *et al.*, 2002b; Saint-Jore *et al.*, 2002), it is tempting to speculate that microtubules might be connected to ERES, allowing e.g. cytoplasmic proteins to actively move and direct towards ERES.

The driving force for transport of N to ER and Golgi in plant cells is still unknown. Since actin is involved in cytoplasmic streaming (Foissner and Wasteneys, 2007; Shimmen, 2007), it seems more likely that N agglomerations would move by diffusion, or would be formed in the vicinity of the glycoprotein-containing ER or Golgi, facilitating the interaction.

INTERACTION BETWEEN RNPS AND VIRAL GLYCOPROTEINS

Once in the vicinity of the ER membranes, N is able to interact with the Gc glycoprotein, in the presence or absence of Gn (Chapter 3). N is responsible for a dramatic change in the localization of Gc (Chapter3), inducing its concentration at ERES, discrete domains within ER where the machinery responsible for the formation of the COPII vesicles is assembled (reviewed by Hanton *et al.* (2006)). The mechanisms involved in the formation of ERES in plant cells are currently subject of many studies, since not much is known concerning their formation and regulation. A recent study has shown that cargo transport can be mediated not only by existing ERES, but also by the *de novo* formation of new ERES (Hanton *et al.*, 2007). In any case, it is likely that interaction with N increases the affinity of Gc to COPII components or other proteins that facilitate either their transport to existing ERES, or the recruitment of proteins that stimulate the formation of new ERES at the places where Gc-N complexes concentrate.

The mechanism through which N is able to find and subsequently concentrate Gc at these sites is not yet understood. The independence of cytoskeleton-directed movement seems to indicate that N agglomerations may randomly get in contact with the cytoplasmic tails of Gc at the ER surface, redirecting them to specific ER areas. On the other hand, it can not be excluded that a signal-mediated transport takes N to specific areas within the ER where this interaction occurs and further homodimerization between Gc proteins may be responsible for their redistribution and concentration at ERES. Our results have shown that the property of recruitment to ERES is not a phenomenon restricted to Gc, but can be transferred to other ER-arrested proteins by substitution of their cytoplasmic tail by the one of Gc, as demonstrated in Chapter 5. Hence, it seems likely that this concentration at ERES is due to a concerted action between N and Gc's tail, perhaps involving the recruitment of cytosolic COPII-components.

The concentration of Gc and N at ERES was shown to occur in the absence of intact microtubule- or actin- networks (Chapter 5), suggesting once more that the viral structural proteins' behavior is independent of cytoskeleton elements. However, disruption of actin filaments leads to an increase in the number of ERES containing Gc-N. This seems to be due to the fact that, under these conditions, a larger number of smaller agglomerations of N are formed. Hence, more agglomerations reach the ER and interact with Gc at a higher number of dispersed sites, leading to the observed increase in the number of Gc-N containing ERES. Interestingly, these observations seem to support the model that describes the formation of new ERES upon cargo concentration (Hanton *et al.*, 2007).

Although N is able to concentrate Gc at ERES, it is not able to overcome the

glycoprotein's ER-arrest and support its export to the Golgi. Only in the presence of Gn, Gc is allowed to exit via ERES to the Golgi (Chapter 2). Our studies suggested that this arrest was not due to misfolding, since no chaperone proteins were co-immunoprecipitated with Gc after single transfection (Chapter 6). On the other hand, the transmembrane domains (TMDs) of the glycoproteins were shown to play a key-role in ER-export (Chapter 6), since exchange of the TMD of Gc by the one of Gn (which by itself can exit ER and migrate to the Golgi (Chapter 2)) rendered its efficient transport to the Golgi. The exchange of the cytoplasmic tails did not have any effect on the localization of Gc. The importance of the size of the TMD for the ER-exit of type I membrane proteins has previously been demonstrated (Brandizzi *et al.*, 2002a). According to the model of protein translocation through diffusion, a protein migrates through the secretory pathway until it finds a membrane with a certain thickness that is able to mask its hydrophobic TMD (Brandizzi *et al.*, 2002a; Moreau *et al.*, 2007). Since the size of the TMD of Gc is 30 residues smaller than the one of Gn, it is possible that the size increase is responsible for the observed localization change. However, according to the reported data (Brandizzi *et al.*, 2002a), the 40 aminoacids length of Gc's TMD would theoretically be enough to allow its ER-exit and translocation to the Golgi (unless its effective length would differ from the one assumed based on the number of residues). Obviously, the composition of the TMD may also be crucial for this ER-release. However, until now, no specific sequence or residue was identified that might confer this translocation ability.

The observation that the cytoplasmic tail (CT) of Gn did not confer to Gc the capability of moving to the Golgi (Chapter 6) was quite surprising, since earlier results had indicated that this domain was required for Gn's localization at the Golgi complex in mammalian cells (Snippe *et al.*, 2007a). It is possible, though, that the CT of Gc has some similarity to the CT of Gn and, in concert with the TMD of Gn, allows ER-export and targeting to the Golgi. However, careful analyses of the aminoacid composition of both CTs did not show any significant similarity.

ER-to-Golgi transport

Similarly to N, also Gn is able to concentrate Gc at ERES (Chapter 2). Furthermore, this protein is also able to transport Gc to the Golgi complex (Chapter 2), rescuing it from the ER. Previous studies have shown that the last 20 aa of the CT of Gn are essential for the interaction with Gc in mammalian cells (Snippe *et al.*, 2007a). The results from Chapter 6 have shown, however, that the TMD and CT of Gn are not sufficient to allow interaction with Gc (Chapter 6), suggesting the involvement of the proteins' lumenal domains.

In contrast to the observation made in mammalian cells that N solely interacts with Gc (Snippe *et al.*, 2007b), the current results in plant cells show that N is able to interact with both viral glycoproteins and even seemed to exhibit a preference for interaction with Gn (Chapter 3). These observations raise several questions regarding the interaction between N and the viral glycoproteins and the order of these events during ER-to-Golgi transport of viral proteins. At least three models can be proposed that may explain the observations made (Fig. 3).
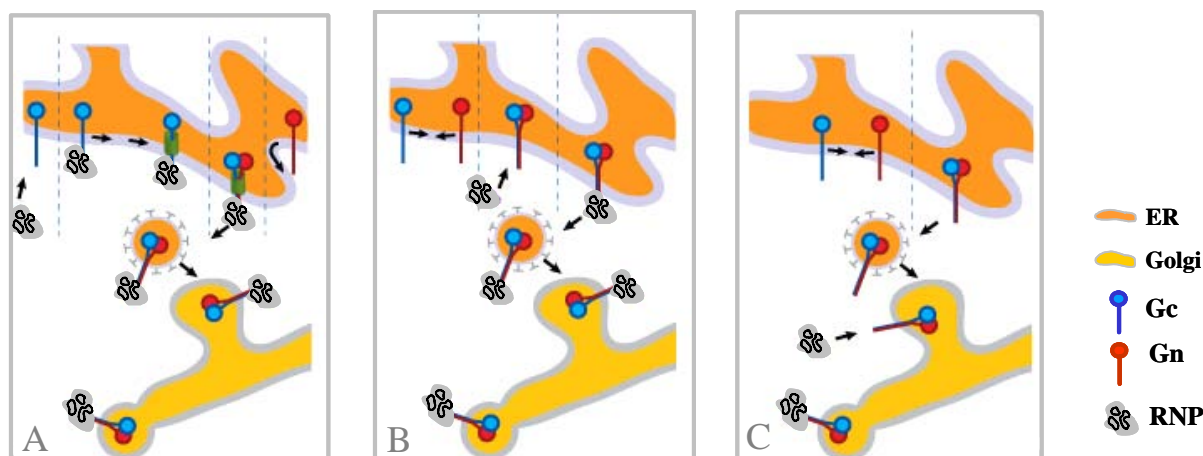
Figure 3: Schematic representation of three models (A, B and C), presenting different possibilities concerning the order of viral proteins interactions and transport to the Golgi complex, prior to TSWV particle assembly in plant cells. The figure is explained in the text.

One of the possibilities (Fig. 3A) is that N/RNPs interact with Gc prior to interaction with Gn. In this case, Gc-Gn and/or N-Gn interactions could occur before or after the concentration at the ERES. In this model, the three proteins exit together from the ER and migrate to the Golgi complex. The second model (Fig. 3 B) involves the heterodimerization of Gc and Gn and simultaneous or sequential interaction with N/RNPs during their maturation in the ER, prior to their joint relocation to ERES. Similar to the first model, the proteins would then migrate as a triple complex to the Golgi complex. The third model (Fig. 3 C) involves the heterodimerization of the glycoproteins at ER and their joint relocation to ERES by means of Gn, in order to exit to the Golgi complex where the interaction with RNPs takes place. Based on the results presented in this thesis, any of these three options is considerable. However, the very specific phenomenon of Gc's concentration at ERES due to interaction with N, seems to favor the hypothesis that the Gc-N interaction occurs at the ER.

The transport of proteins from ER to Golgi in plant cells has been the subject of many recent studies (Hanton *et al.*, 2006; Matheson *et al.*, 2006; Moreau *et al.*, 2007). Although both Golgi and ER move and organize along actin filaments (Boevink *et al.*, 1998; Nebenfuhr *et al.*, 1999), the cargo transport between these two organelles is cytoskeleton independent (Boevink *et al.*, 1998; Brandizzi *et al.*, 2002b; Saint-Jore *et al.*, 2002), contrarily to what is observed in animal cells, where this transport occurs along microtubules (Murshid and Presley, 2004; Watson *et al.*, 2005), reflecting the structural differences between the cells of these two types of organisms (Fig. 2).

Several models have been suggested to explain the ER-to-Golgi transport in plant cells. The "vacuum cleaner model" (Boevink *et al.*, 1998) suggests the movement of Golgi stacks along the ER surface, constantly collecting cargo at ERES. Another model, the "stop-and-go", suggests that Golgi stacks temporarily stop at defined ERES (Nebenfuhr *et al.*, 1999). A third, more recent model proposes a continuous transport between ER and Golgi, in which Golgi stacks move with (and not over) the surface of the ER as a "mobile secretory unit" (Brandizzi *et al.*, 2002b; da Silva *et al.*, 2004; Stefano *et al.*, 2006). A fourth, the "kiss-and-run" model was demonstrated in BY-2 cells and proposes the interaction between several ERES and a single Golgi stack,

suggesting that these associations continuously change in number and position (Hanton *et al.*, 2006; Yang *et al.*, 2005). Independently of the model, the sequential action of COPII and COPI coat complexes is a widely accepted model for the transport of proteins between the ER and the Golgi (Hanton *et al.*, 2006; Matheson *et al.*, 2006). Whereas COPII vesicles are required for anterograde cargo transport, COPI vesicles, although mainly responsible for the retrograde transport, have been suggested to take part in both directions (reviewed by Barlowe (2002)). Our studies have shown that Gn also moves from the ER to the Golgi in COPII-coated vesicles, and strongly suggest that the same is valid for the Gc-Gn complex (Chapter 6).

MEMBRANE ENVELOPMENT

A peculiar and unexpected observation was the ability of the TSWV glycoproteins to induce membrane curvature/deformation. For Gc, this was observed at ER membranes and for Gn at both ER and Golgi membranes (Chapter 2). This phenomenon has never been observed in mammalian cells or reported for any other animal-infecting member of the *Bunyaviridae*. It is tempting to assume that this phenomenon is related to the observed Golgi membrane curving (paired parallel membranes, PPM) during enwrapment of RNPs in naturally infected plant cells (Kikkert *et al.*, 1999). Indeed, as previously mentioned, Gc and Gn-containing Golgi stacks enwrap around the RNPs (Fig. 4 step 1), forming doubly enveloped virus particles (DEVs). These fuse with each other and ER-derived membranes (Fig. 4 step 2), forming singly enveloped virus particles (SEVs) that retain in large accumulations in the cytoplasm (Fig. 4) (Kikkert *et al.*, 1999). Hence, the observed phenomenon may reflect an intrinsic property of both glycoproteins required to assist in the final stages of RNP membrane envelopment.
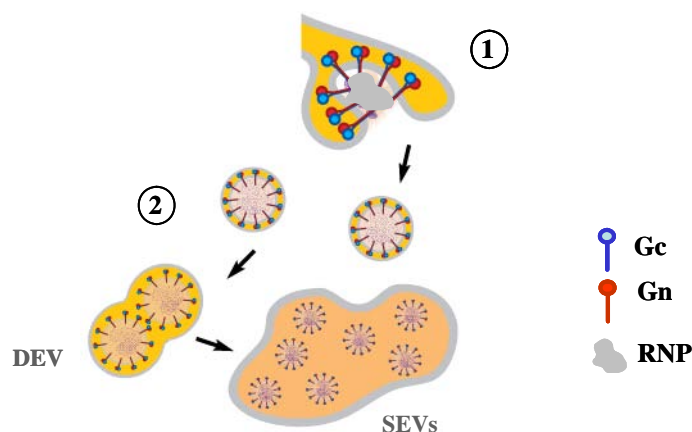
Figure 4: Schematic representation of the final steps during TSWV particle assembly. The figure and numbering are explained in the text.

It should be noted that the observed pleomorphic/circular membrane structures are larger in size than the observed PPM curvings (Kikkert *et al.*, 1999). This may be due to the transient expression of the glycoproteins in the absence of any other viral protein and/or RNA that normally would lead to an accumulation and concentration at a few sites within ER/Golgi membranes. Perhaps, the structures observed with light microscopy reflect the curving of (enlarged) entire Golgi stacks, resulting from the excessive (and not concentrated at certain areas) presence of the glycoproteins. Hence, this larger size of these structures may be an "artifact" resulting from the experimental system used. The possibility that these (pseudo)circular/pleomorphic membrane structures might also reflect the formation of virus-like particles (VLPs), as previously reported for several other membrane enveloped (animal-infecting) viruses upon transient expression of viral glycoproteins (Kolesnikova *et al.*, 2004; Latham and Galarza, 2001; Shaw *et al.*, 2003), remains to be investigated.

In summary, the studies described in this thesis have provided more insight into the behavior of the structural proteins of TSWV in relation to virus particle assembly. The presented work has also demonstrated that this virus may represent a valuable tool to study and compare the functional protein trafficking routes in mammalian and plant cells, with specific emphasis on the involvement of the endomembrane system therein.
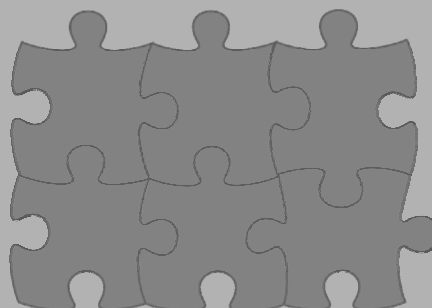
SUMMARY

At the onset of the studies presented in this thesis, it was already known that the assembly of the enveloped particle of Tomato spotted wilt virus (TSWV; family *Bunyaviridae*) in the infected plant cell was featured by a number of interesting phenomena. This process involves enwrapment of the viral ribonucleoparticles (RNPs) by Golgi membranes. As a consequence, doubly enveloped virus particles (DEVs) are formed which, by fusion with each other and ER-derived membranes, give rise to large cytoplasmic vesicles that contain accumulating amounts of mature singly enveloped virus particles (SEVs), which are not secreted from the cell. Furthermore, since TSWV also replicates in its insect vector (thrips), viral assembly should be compatible with the membranous organelles and intracellular transport pathways present in both plant and insect cells.

To gain more insight into the sequential steps that eventually lead to particle assembly, and on the longer term be able to identify the key factors involved in the observed differences in intracellular targeting between plant and insect cells, the behavior of the viral structural proteins, i.e. the nucleocapsid (N) protein and the two envelope glycoproteins Gc and Gn, was studied in plant cells. To this end a *N. tabacum* protoplast system was established that supported efficient transient expression of these proteins. By using fluorophore-fusions of these proteins, the interactions between one-another as well as their co-localization with specific elements of the endomembrane system and/or cytoskeleton could be monitored by confocal microscopy.

In Chapter 2, the intracellular localization and behavior of the TSWV glycoproteins were studied. In the absence of Gn, Gc was found to be retained in the ER, whereas Gn was able to, by itself, target to the Golgi complex. When co-expressed, Gn was able to rescue Gc from the ER, and co-translocate to the Golgi complex. Occasionally both glycoproteins were also observed at ER export sites. Surprisingly, Gc and Gn were able to induce the formation of (pseudo-) circular/pleomorphic membrane structures that co-localized with ER or Golgi markers, respectively.

In Chapter 3, the behavior of the glycoproteins was analyzed in the presence of the nucleocapsid protein N and FRET/FLIM was applied to the *in vivo* study of protein-protein interactions. Upon single expression, the N protein formed large cytoplasmic agglomerates due to homo-oligomerization as indicated by FRET/FLIM. N was also able to interact with both Gc and Gn at the ER and/or Golgi. Furthermore, a surprising concentration of Gc at specific areas of the ER was observed upon co-expression with N.

The translocation of N and dependence on cytoskeleton elements was analyzed in Chapter 4. The formation of large cytoplasmic agglomerations of N was found to be dependent on active actin filaments, but independent of microtubules. However, the interaction of N with the glycoproteins was not affected by any of the cytoskeleton inhibitors tested, suggesting that microtubules and actin filaments were not required for the transport of N to the ER and/or Golgi.

The specific change in the localization of the glycoprotein Gc within the ER by interaction with N was further investigated in Chapter 5 and it was shown that the two proteins co-localize at ER export sites. The interaction between N and the cytoplasmic tail of Gc was shown to be crucial for this localization since N was also able to induce the concentration at ER export sites of the ER-resident protein calnexin, upon exchange of its cytoplasmic tail by the one of Gc. Our results also suggested (some kind of) a connection between ER export sites and microtubules, since depolymerized α-tubulin was found to co-localize with the marker for these specific ER

domains.

The ER-retention of Gc upon single expression was further analyzed in Chapter 6. The characteristics of the transmembrane domain (TMD) of the glycoprotein were shown to be determinant for its ER-exit, since exchange by the TMD of Gn rendered its translocation to the Golgi complex. Furthermore, the TMD and CT of Gn were shown not to be sufficient for the interaction between the two glycoproteins, suggesting the importance of their luminal domain in this interaction. Using ER-to-Golgi transport inhibitors, viral glycoprotein transport to Golgi was demonstrated to occur via COPII vesicles and appeared to be sensitive to brefeldin A.

In Chapter 7 the major findings of this PhD research were discussed in a broader perspective and combined in a model for TSWV particle assembly in plant cells

SAMENVATTING

De centrale doelstelling van het in dit proefschrift beschreven onderzoek was het assemblageproces van het Tomatenbronsvlekkenvirus (Engels: Tomato spotted wilt virus; TSWV; genus *Tospovirus*, familie *Bunyaviridae*), een plant-infecterend membraanvirus, beter te begrijpen. Bij de aanvang van het onderzoek was reeds bekend dat dit proces een aantal opvallende fenomenen met zich meebrengt. Zo worden tijdens de infectie van een plantencel de virale ribonucleotideproteinen (RNPs; dwz het virale RNA genoom gecomplexeerd aan nucleocapside-eiwit) ingepakt door cisternen van het Golgi-apparaat waarbij als tussenproduct virusdeeltjes met een dubbele membraan worden gevormd. Vervolgens fuseren deze deeltjes met elkaar of met het endoplasmatisch reticulum (ER) waarbij deeltjes met een enkelvoudig membraan ontstaan die gezamenlijk ophopen in een grote membraan-omgeven vesikel en niet uitgescheiden worden. Omdat het TSWV zich ook vermenigvuldigt in tripsen (die het virus overdragen van plant naar plant), zal het virale assemblageproces compatibel moeten zijn met de membraanhoudende organellen en intracellulaire transportroutes binnen zowel planten- als insectencellen. Vast staat dat virale assemblage in het insect ten dele anders verloopt dan in de plant omdat er geen virusdeeltjes met dubbele membraan gevormd worden en de nieuwe deeltjes bovendien wel uitgescheiden dienen te worden.

Om meer inzicht te verkrijgen in de opeenvolgende stappen tijdens het virale assemblageproces en om op langere termijn de sleutelfactoren te identificeren die betrokken zijn bij de waargenomen verschillen tussen planten- en insectencel m.b.t. het assemblageproces, werd het gedrag van de drie structurele eiwitten van het virus nader onderzocht. Dit zijn het nucleocapside eiwit (N) en de beide glycoproteïnen Gc en Gn die zich in de virale envelop bevinden. Voor deze studies werd gebruikgemaakt van een *N. tobacco* protoplastensysteem waarin deze eiwitten efficiënt tot expressie kunnen worden gebracht door transfectie met specifieke genconstructen. Door middel van fusies van N, Gc en Gn met fluorescente eiwitten, konden de onderlinge interacties tussen de virale eiwitten in de levende cel onderzocht worden d.m.v. convocale microscopie. Door specifieke merkers toe te passen kon tevens hun intracellulaire positie ten opzichte van specifieke onderdelen van het endomembraan systeem en het cytoskelet geanalyseerd worden.

In hoofdstuk 2 is het intracellulaire gedrag van de beide glycoproteïnen van TSWV onderzocht. Tijdens eerder onderzoek met zoogdiercellen was al vastgesteld dat Gn en Gc elkaar complementeren tijdens het transport van het ER naar het Golgi systeem. In hoofdstuk 2 is nu aangetoond dat deze onderlinge samenwerking ook in de plantencel plaatsvindt: in afwezigheid van Gn wordt Gc vastgehouden in het ER, terwijl Gn wel zelfstandig naar het Golgi apparaat kan gaan. Wanneer beide glycoproteïnen simultaan tot expressie worden gebracht, wordt Gc geholpen door Gn bij het transport naar het Golgi apparaat. In sommige gevallen werden beide eiwitten gezien bij ER export sites (ERES). Tevens kon worden vastgesteld dat de Gn en Gc glycoproteinen de produtie van (bijna) cirkelvormige en pleomorphe membraanstructuren induceren, die co-lokaliseren met respectievelijk ER- en Golgi markers.

Om de situatie nog meer te doen gelijken op het natuurlijke infectieproces werden vervolgens de virale glycoproteïnen samen met het N eiwit tot expressie gebracht (hoofdstuk 3). Om *in vivo* de mogelijke interacties tussen deze drie virale eiwitten m.b.v. FRET/FLIM te analyseren, werd hierbij gebruikgemaakt van constructen voorzien van fluorofore groepen. Tijdens individuele expressie vormde het N eiwit agglomeraties in het cytoplasma door middel van homo-oligomerisering, zoals vastgesteld met FRET/FLIM. Indien het N eiwit tot expressie

werd gebracht samen met Gc en Gn, werden eiwit-eiwit interacties vastgesteld tussen zowel N en Gc als tussen N en Gn, bij het ER en/of het Golgi. Indien gelijktijdig tot expressie gebracht met het N eiwit, vormde Gc opvallende concentraties op specifieke punten binnen het ER.

De intracellulaire verplaatsing van het N eiwit en het eventuele belang van het cytoskelet hierbij is m.b.v. specifieke remmers geanalyseerd in hoofdstuk 4. Aldus bleek de vorming van de uit N eiwit bestaande agglomeraties in het cytoplasma afhankelijk te zijn van actine-filamenten, maar niet van microtubuli. De geteste remmers hadden echter geen enkele invloed op de interacties tussen de virale eiwitten. Dit wijst er op dat zowel actine als microtubuli niet betrokken zijn bij het transport van N eiwit naar ER en/of Golgi.

Het verschijnsel dat het Gc eiwit zich alleen in aanwezigheid van N concentreert op specifieke locaties binnen het ER is verder uitgediept in hoofdstuk 5. Daarbij werd vastgesteld dat deze locaties samenvallen met ERES. Door de cytoplasmatische staart van een ander ER eiwit, calnexine, te vervangen door de staart van Gc, kon vastgesteld worden dat dit domein cruciaal is voor binding met N eiwit en hun gezamenlijke ophoping bij ERES.

De retentie van het Gc eiwit in het ER bij afwezigheid van de andere virale eiwitten is nader onderzocht in Hoofdstuk 6. Door verwisseling van het transmembrane domein (TMD) van Gc met dat van Gn kon vastgesteld worden dat de mogelijkheid van Gc om al dan niet zelfstandig het ER te verlaten bepaald wordt door het TMD. Daarnaast werd vastgesteld dat voor Gn-Gc binding de TMD en cytoplasmatische staart van Gn niet voldoende zijn, dus dat ook de luminale delen van de beide glycoproteïnen bij hun interactie betrokken zijn. Door gebruik te maken van remmers van het ER-naar-Golgi transport werd aangetoond dat het transport van de glycoproteïnen plaatsvindt met behulp van het COPII mechanisme.

Tenslotte zijn in hoofdstuk 7 de belangrijkste bevindingen uit dit proefschrift in een breder perspectief geplaatst en ondergebracht in een model voor de assemblage van TSWV in de plantencel.

REFERENCES

REFERENCES

Adkins, S., Quadt, R., Choi, T.-J., Ahlquist, P. and German, T. (1995). "An RNA-dependent RNA polymerase activity associated with virions of Tomato spotted wilt virus, a plant- and insect-infecting bunyavirus." Virology 207(1): 308-311.

Alberts, B. (2002). Molecular biology of the cell. New York, N.Y., [etc.], Garland Science.

Alfadhli, A., Love, Z., Arvidson, B., Seeds, J., Willey, J. and Barklis, E. (2001). "Hantavirus nucleocapsid protein oligomerization." Journal of Virology 75(4): 2019-2023.

Anderson, G. W. and Smith, J. F. (1987). "Immunoelectron microscopy of Rift-Valley fever viral morphogenesis in primary rat hepatocytes." Virology 161(1): 91-100.

Andersson, A. M., Melin, L., Persson, R., Raschperger, E., Wikstrom, L. and Pettersson, R. F. (1997a). "Processing and membrane topology of the spike proteins G1 and G2 of Uukuniemi virus." Journal of Virology 71(1): 218-225.

Andersson, A. M., Melin, L., Bean, A. and Pettersson, R. F. (1997b). "A retention signal necessary and sufficient for Golgi localization maps to the cytoplasmic tail of a bunyaviridae (Uukuniemi virus) membrane glycoprotein." Journal of Virology 71(6): 4717-4727.

Andersson, I., Bladh, L., Mousavi-Jazi, M., Magnusson, K.-E., Lundkvist, A., Haller, O. and Mirazimi, A. (2004a). "Human Mxa protein inhibits the replication of Crimean-Congo hemorrhagic fever virus." Journal of Virology 78(8): 4323-4329.

Andersson, I., Simon, M., Lundkvist, A., Nilsson, M., Holmstrom, A., Elgh, F. and Mirazimi, A. (2004b). "Role of actin filaments in targeting of Crimean Congo hemorrhagic fever virus nucleocapsid protein to perinuclear regions of mammalian cells." Journal of Medical Virology 72(1): 83-93.

Aridor, M., Bannykh, S. I., Rowe, T. and Balch, W. E. (1999). "Cargo can modulate COPII vesicle formation from the endoplasmic reticulum." Journal of Biological Chemistry 274(7): 4389-4399.

Aridor, M., Fish, K. N., Bannykh, S., Weissman, J., Roberts, T. H., Lippincott-Schwartz, J. and Balch, W. E. (2001). "The Sar1 GTPase coordinates biosynthetic cargo selection with endoplasmic reticulum export site assembly." Journal of Cell Biology 152(1): 213-230.

Ashby, J., Boutant, E., Seemanpillai, M., Sambade, A., Ritzenthaler, C. and Heinlein, M. (2006). "Tobacco mosaic virus movement protein functions as a structural microtubule-associated protein." Journal of Virology 80(17): 8329-8344.

Bandla, M. D., Campbell, L. R., Ullman, D. E. and Sherwood, J. L. (1998). "Interaction of tomato spotted wilt tospovirus (TSWV) glycoproteins with a thrips midgut protein, a potential cellular receptor for TSWV." Phytopathology 88(2): 98-104.

Barco, A. and Carrasco, L. (1995). "Human virus protein, poliovirus protein 2bc, induces membrane proliferation and blocks the exocytic pathway in the yeast Saccharomyces-cerevisiae." EMBO Journal 14(14): 3349-3364.

Barlowe, C. and Schekman, R. (1993). "Sec12 encodes a guanine-nucleotide-exchange factor essential for transport vesicle budding from the ER." Nature 365(6444): 347-349.

Barlowe, C., Orci, L., Yeung, T., Hosobuchi, M., Hamamoto, S., Salama, N., Rexach, M. F., Ravazzola, M., Amherdt, M. and Schekman, R. (1994). "COPII: A membrane coat formed by Sec proteins that drive vesicle budding from the endoplasmic reticulum." Cell 77(6): 895-907.

Barlowe, C. (2002). "COPII-dependent transport from the endoplasmic reticulum." Current Opinion in Cell Biology 14(4): 417-422.

Boevink, P., Oparka, K., Cruz, S. S., Martin, B., Betteridge, A. and Hawes, C. (1998). "Stacks on tracks: The plant Golgi apparatus traffics on an actin/ER network." The Plant Journal 15(3): 441-447.

Booth, T. F., Gould, E. A. and Nuttall, P. A. (1991). "Structure and morphogenesis of Dugbe virus (bunyaviridae, nairovirus) studied by immunogold electron-microscopy of ultrathin cryosections." Virus Research 21(3): 199-212.

Borst, J. W., Hink, M., van Hoek, A. and Visser, A. J. W. G. (2003). "Multiphoton microspectroscopy in living plant cells." Proceeding of SPIE 4963: 231-238.

Boyko, V., Ferralli, J., Ashby, J., Schellenbaum, P. and Heinlein, M. (2000). "Function of microtubules in intercellular transport of plant virus RNA." Nature Cell Biololgy 2(11): 826-832.

Brandizzi, F., Frangne, N., Marc-Martin, S., Hawes, C., Neuhaus, J.-M. and Paris, N. (2002a). "The destination for single-pass membrane proteins is influenced markedly by the length of the hydrophobic domain." Plant Cell 14(5): 1077-1092.

Brandizzi, F., Snapp, E. L., Roberts, A. G., Lippincott-Schwartz, J. and Hawes, C. (2002b). "Membrane protein transport between the endoplasmic reticulum and the Golgi in tobacco leaves is energy dependent but cytoskeleton independent: Evidence from selective photobleaching." Plant Cell 14(6): 1293-1309.

Bucher, E., Sijen, T., de Haan, P., Goldbach, R. and Prins, M. (2003). "Negative-strand tospoviruses and tenuiviruses carry a gene for a suppressor of gene silencing at analogous genomic positions." Journal of Virology 77(2): 1329-1336.

Carette, J. E., Stuiver, M., Van Lent, J., Wellink, J. and Van Kammen, A. B. (2000). "Cowpea mosaic virus infection induces a massive proliferation of endoplasmic reticulum but not Golgi membranes and is dependent on de novo membrane synthesis." Journal of Virology 74(14): 6556-6563.

Carette, J. E., van Lent, J., MacFarlane, S. A., Wellink, J. and van Kammen, A. (2002). "Cowpea mosaic virus 32- and 60-kiloDalton replication proteins target and change the morphology of endoplasmic reticulum membranes." Journal of Virology 76(12): 6293-6301.

Chapman, E. J., Hilson, P. and German, T. L. (2003). "Association of the L protein and *in vitro Tomato spotted wilt virus* RNA-dependent RNA polymerase activity." Intervirology 46: 177-181.

Chapman, M. J., Dolan, M. F. and Margulis, L. (2000). "Centrioles and kinetosomes: Form, function, and evolution." Quarterly Review of Biology 75(4): 409-429.

Chen, S. Y., Matsuoka, Y. and Compans, R. W. (1991). "Assembly and polarized release of Punta toro virus and effects of brefeldin A." Journal of Virology 65(3): 1427-1439.

Crofts, A. J., Leborgne-Castel, N., Pesca, M., Vitale, A. and Denecke, J. (1998). "Bip and calreticulin form an abundant complex that is independent of endoplasmic reticulum stress." Plant Cell 10(5): 813-823.

Crofts, A. J. and Denecke, J. (1998). "Calreticulin and calnexin in plants." Trends in Plant Science 3(10): 396-399.

da Silva, L. L. P., Snapp, E. L., Denecke, J., Lippincott-Schwartz, J., Hawes, C. and Brandizzi, F. (2004). "Endoplasmic reticulum export sites and Golgi bodies behave as single mobile secretory units in plant cells." Plant Cell 16(7): 1753-1771.

da Silva, L. L. P., Taylor, J. P., Hadlington, J. L., Hanton, S. L., Snowden, C. J., Fox, S. J., Foresti, O., Brandizzi, F. and Denecke, J. (2005). "Receptor salvage from the prevacuolar compartment is essential for efficient vacuolar protein targeting." Plant Cell 17(1): 132-148.

da Silva, L. L. P., Foresti, O. and Denecke, J. (2006). "Targeting of the plant vacuolar sorting receptor BP80 is dependent on multiple sorting signals in the cytosolic tail." Plant Cell 18(6): 1477-1497.

de Haan, P., Wagemakers, L., Peters, D. and Goldbach, R. (1989). "Molecular-cloning and terminal sequence determination of the sRNA and mRNA of Tomato spotted wilt virus." Journal of General Virology 70: 3469-3473.

de Haan, P., Wagemakers, L., Peters, D. and Goldbach, R. (1990). "The s RNA segment of Tomato spotted wilt virus has an ambisense character." Journal of General Virology 71(5): 1001-1007.

de Haan, P., Kormelink, R., de Oliveira Resende, R., van Poelwijk, F., Peters, D. and Goldbach, R. (1991). "Tomato spotted wilt virus L RNA encodes a putative RNA polymerase." Journal of General Virology 72(9): 2207-2216.

Denecke, J., Goldman, M. H. S., Demolder, J., Seurinck, J. and Botterman, J. (1991). "The tobacco luminal binding-protein is encoded by a multigene family." Plant Cell 3(9): 1025-1035.

Denecke, J. and Vitale, A. (1995). "The use of plant protoplasts to study protein synthesis, quality control, protein modification and transport through the plant endomembrane system." Methods in Cell Biology 50: 335-348.

Ehrhardt, D. W. and Shaw, S. L. (2006). "Microtubule dynamics and organization in the plant cortical array." Annual Review of Plant Biology 57(1): 859-875.

Elliott, R. M. (1990). "Molecular biology of the *bunyaviridae*." Journal of General Virology 71: 501-522.

Elliott, R. M. (1996). The Bunyaviridae. New York, N. Y., Plenum Press.

Erhardt, M., Stoppin-Mellet, V., Campagne, S., Canaday, J., Mutterer, J., Fabian, T., Sauter, M., Muller, T., Peter, C., Lambert, A.-M. and Schmit, A.-C. (2002). "The plant Spc98p homologue colocalizes with {gamma}-tubulin at microtubule nucleation sites and is required for microtubule

nucleation." Journal of Cell Science 115(11): 2423-2431.

Foissner, I. and Wasteneys, G. O. (2007). "Wide-ranging effects of eight cytochalasins and latrunculin A and B on intracellular motility and actin filament reorganization in characean internodal cells." Plant Cell Physiology 48(4): 585-597.

Gadella, T. W. J. J. (1999). Fluorescence lifetime imaging microscopy (FLIM): Instrumentation and applications. Fluorescent and luminescent probes. Mason, W. T., Academic Press**:** 467-479.

Gadella, T. W. J. J., van der Krogt, G. N. M. and Bisseling, T. (1999). "GFP-based FRET microscopy in living plant cells." Trends in Plant Science 4(7): 287-291.

Gahmberg, N., Kuismanen, E., Keranen, S. and Pettersson, R. F. (1986). "Uukuniemi virus glycoproteins accumulate in and cause morphological-changes of the Golgi-complex in the absence of virus maturation." Journal of Virology 57(3): 899-906.

Gerrard, S. R. and Nichol, S. T. (2002). "Characterization of the Golgi retention motif of Rift Valley fever virus Gn glycoprotein." Journal of Virology 76(23): 12200-12210.

Goddette, D. W. and Frieden, C. (1986). "Actin polymerization - the mechanism of action of cytochalasin-d." Journal of Biological Chemistry 261(34): 5974-5980.

Goldbach, R. and Peters, D. (1996). Molecular and biological aspects of tospoviruses. The Bunyaviridae. Elliott, R. M. New York, N.Y., Plenum Press**:** 129-157.

Griffiths, G. and Rottier, P. (1992). "Cell biology of viruses that assemble along the biosynthetic pathway." Seminars in Cell Biology 3: 367-381.

Guha, S. and Bhattacharyya, B. (1997). "The colchicine-tubulin interaction: A review." Current Science 73(4): 351-358.

Hanton, S. L., Renna, L., Bortolotti, L. E., Chatre, L., Stefano, G. and Brandizzi, F. (2005). "Diacidic motifs influence the export of transmembrane proteins from the endoplasmic reticulum in plant cells." Plant Cell 17(11): 3081-3093.

Hanton, S. L., Matheson, L. A. and Brandizzi, F. (2006). "Seeking a way out: Export of proteins from the plant endoplasmic reticulum." Trends in Plant Science 11(7): 335-343.

Hanton, S. L., Chatre, L., Renna, L., Matheson, L. A. and Brandizzi, F. (2007). "De novo formation of plant endoplasmic reticulum export sites is membrane cargo induced and signal mediated." Plant Physiology 143(4): 1640-1650.

Haseloff, J., Siemering, K. R., Prasher, D. C. and Hodge, S. (1997). "Removal of a cryptic intron and subcellular localization of green fluorescent protein are required to mark transgenic arabidopsis plants brightly." PNAS 94(6): 2122-2127.

Heath, C. M., Windsor, M. and Wileman, T. (2001). "Aggresomes resemble sites specialized for virus assembly." Journal of Cell Biology 153(3): 449-456.

Hink, M. A., Bisseling, T. and Visser, A. J. W. G. (2002). "Imaging protein-protein interactions in living cells." Plant Molecular Biology 50(6): 871-883.

REFERENCES

Huang, L. Q., Franklin, A. E. and Hoffman, N. E. (1993). "Primary structure and characterization of an arabidopsis-thaliana calnexin-like protein." Journal of Biological Chemistry 268(9): 6560-6566.

Huang, M., Weissman, J. T., Beraud-Dufour, S., Luan, P., Wang, C., Chen, W., Aridor, M., Wilson, I. A. and Balch, W. E. (2001). "Crystal structure of Sar1-gdp at 1.7 a resolution and the role of the NH2 terminus in ER export." Journal of Cell Biology 155(6): 937-948.

Jantti, J., Hilden, P., Ronka, H., Makiranta, V., Keranen, S. and Kuismanen, E. (1997). "Immunocytochemical analysis of Uukuniemi virus budding compartments: Role of the intermediate compartment and the Golgi stack in virus maturation." Journal of Virology 71(2): 1162-1172.

Johnston, J. A., Ward, C. L. and Kopito, R. R. (1998). "Aggresomes: A cellular response to misfolded proteins." Journal of Cell Biology 143(7): 1883-1898.

Joshi, H. C. (1993). "Gamma-tubulin - the hub of cellular microtubule assemblies." Bioessays 15(10): 637-643.

Karimi, M., Inze, D. and Depicker, A. (2002). "Gateway(tm) vectors for agrobacterium-mediated plant transformation." Trends in Plant Science 7(5): 193-195.

Kaukinen, P., Koistinen, V., Vapalahti, O., Vaheri, A. and Plyusnin, A. (2001). "Interaction between molecules of hantavirus nucleocapsid protein." Journal of General Virology 82(8): 1845-1853.

Kikkert, M., van Poelwijk, F., Storms, M., Kassies, W., Bloksma, H., van Lent, J., Kormelink, R. and Goldbach, R. (1997). "A protoplast system for studying tomato spotted wilt virus infection." Journal of General Virology 78(7): 1755-1763.

Kikkert, M. (1999). Role of the envelope glycoproteins in the infection cycle of Tomato spotted wilt virus, Wageningen University. PhD Thesis.

Kikkert, M., van Lent, J., Storms, M., Bodegom, P., Kormelink, R. and Goldbach, R. (1999). "Tomato spotted wilt virus particle morphogenesis in plant cells." Journal of Virology 73(3): 2288-2297.

Kikkert, M., Verschoor, A., Kormelink, R., Rottier, P. and Goldbach, R. (2001). "Tomato spotted wilt virus glycoproteins exhibit trafficking and localization signals that are functional in mammalian cells." Journal of Virology 75(2): 1004-1012.

Kitajima, E., Avila de, A. C., Resende, R., Goldbach, R. W. and Peters, D. (1992a). "Comparative cytological and immunolgold labelling studies on different isolates of Tomato spotted wilt virus." Journal of Submicroscopic Cytology and Pathology 24: 1-14.

Kitajima, E. W., de O. Resende, R., de Avila, A. C., Goldbach, R. W. and Peters, D. (1992b). "Immuno-electron microscopical detection of Tomato spotted wilt virus and its nucleocapsids in crude plant extracts." Journal of Virological Methods 38(3): 313-322.

Kochs, G., Janzen, C., Hohenberg, H. and Haller, O. (2002). "Antivirally active Mxa protein sequesters la crosse virus nucleocapsid protein into perinuclear complexes." PNAS 99(5): 3153-3158.

Kolesnikova, L., Berghofer, B., Bamberg, S. and Becker, S. (2004). "Multivesicular bodies as a platform for formation of the marburg virus envelope." Journal of Virology 78(22): 12277-12287.

Kormelink, R., de Haan, P., Meurs, C., Peters, D. and Goldbach, R. (1992a). "The nucleotide sequence of the M RNA segment of Tomato spotted wilt virus, a bunyavirus with two ambisense RNA segments [published erratum appears in j gen virol 1993 apr;74(4):790]." Journal of General Virology 73(11): 2795-2804.

Kormelink, R., de Haan, P., Peters, D. and Goldbach, R. (1992b). "Viral RNA synthesis in tomato spotted wilt virus-infected Nicotiana rustica plants." Journal of General Virology 73(3): 687-693.

Kormelink, R., Storms, M., van Lent, J., Peters, D. and Goldbach, R. (1994). "Expression and subcellular location of the nsm protein of Tomato spotted wilt virus (TSWV)." Virology 200: 56-65.

Kuismanen, E., Hedman, K., Saraste, J. and Pettersson, R. F. (1982). "Uukuniemi virus maturation - accumulation of virus-particles and viral-antigens in the Golgi-complex." Molecular and Cellular Biology 2(11): 1444-1458.

Kuismanen, E., Bang, B., Hurme, M. and Pettersson, R. F. (1984). "Uukuniemi virus maturation - immunofluorescence microscopy with monoclonal glycoprotein-specific antibodies." Journal of Virology 51(1): 137-146.

Kumagai, F., Yoneda, A., Tomida, T., Sano, T., Nagata, T. and Hasezawa, S. (2001). "Fate of nascent microtubules organized at the M/G1 interface, as visualized by synchronized tobacco BY-2 cells stably expressing GFP-tubulin: Time-sequence observations of the reorganization of cortical microtubules in living plant cells." Plant Cell Physiology 42(7): 723-732.

Laporte, C., Vetter, G., Loudes, A. M., Robinson, D. G., Hillmer, S., Stussi-Garaud, C. and Ritzenthaler, C. (2003). "Involvement of the secretory pathway and the cytoskeleton in intracellular targeting and tubule assembly of Grapevine fanleaf virus movement protein in tobacco BY-2 cells." Plant Cell 15(9): 2058-2075.

Lappin, D. F., Nakitare, G. W., Palfreyman, J. W. and Elliott, R. M. (1994). "Localization of bunyamwera bunyavirus G1 glycoprotein to the Golgi requires association with G2 but not with NSm." Journal of General Virology 75(12): 3441-3451.

Latham, T. and Galarza, J. M. (2001). "Formation of wild-type and chimeric influenza virus-like particles following simultaneous expression of only four structural proteins." Journal of Virology 75(13): 6154-6165.

Leonard, V. H. J., Kohl, A., Osborne, J. C., McLees, A. and Elliott, R. M. (2005). "Homotypic interaction of bunyamwera virus nucleocapsid protein." Journal of Virology 79(20): 13166-13172.

Luders, J. and Stearns, T. (2007). "Microtubule-organizing centres: A re-evaluation." Nature Reviews Molecular Cell Biology 8(2): 161-167.

Lyons, M. J. and Heyduk, J. (1973). "Aspects of developmental morphology of California encephalitis-virus in cultured vertebrate and arthropod cells and in mouse brain." Virology 54(1): 37-52.

Maliga, P., Sz-Breznovits, A. and Marton, L. (1973). "Streptomycin-resistant plants from callus culture of haploid tobacco." Nature 244: 29-30.

Matheson, L. A., Hanton, S. L. and Brandizzi, F. (2006). "Traffic between the plant endoplasmic reticulum and Golgi apparatus: To the Golgi and beyond." Current Opinion in Plant Biology 9(6): 601-609.

Matsuoka, K., Schekman, R., Orci, L. and Heuser, J. E. (2001). "Surface structure of the COPII-coated vesicle." PNAS 98(24): 13705-13709.

Matsuoka, Y., Ihara, T., Bishop, D. H. L. and Compans, R. W. (1988). "Intracellular accumulation of punta toro virus glycoproteins expressed from cloned cDNA." Virology 167(1): 251-260.

Matzuoka, Y., Chen, S. Y., Holland, C. E. and Compans, R. W. (1996). "Molecular determinants of Golgi retention in the Punta toro G1 glycoprotein." Archives of Biochemistry and Biophysics 336: 184-189.

Milne, R. G. (1970). "An electron microscope study of Tomato spotted wilt virus in sections of infected cells and in negative stain preparations." Journal of General Virology 6: 267-&.

Mohamed, N. A., Randles, J. W. and Francki, R. I. B. (1973). "Protein composition of Tomato spotted wilt virus." Virology 56: 12-21.

Mohamed, N. A. (1981). "Isolation and characterization of subviral structures from Tomato spotted wilt virus." Journal of General Virology 53(2): 197-206.

Moreau, P., Brandizzi, F., Hanton, S., Chatre, L., Melser, S., Hawes, C. and Satiat-Jeunemaitre, B. (2007). "The plant ER-Golgi interface: A highly structured and dynamic membrane complex." J. Exp. Bot. 58(1): 49-64.

Morejohn, L. C. and Fosket, D. E. (1991). "The biochemistry of compounds with anti-microtubule activity in plant-cells." Pharmacology & Therapeutics 51(2): 217-230.

Murashige, R. and Skoog, F. (1962). "A revised medium for rapid growth and bioassays with tobacco tissue cultures." Physiology Plantarum 15: 473–497.

Murshid, A. and Presley, J. F. (2004). "ER-to-Golgi transport and cytoskeletal interactions in animal cells." Cellular and Molecular Life Sciences (CMLS) 61(2): 133-145.

Nagata, T., Inoue-Nagata, A. K., van Lent, J., Goldbach, R. and Peters, D. (2002). "Factors determining vector competence and specificity for transmission of Tomato spotted wilt virus." Journal of General Virology 83(3): 663-671.

Nebenfuhr, A., Gallagher, L. A., Dunahay, T. G., Frohlick, J. A., Mazurkiewicz, A. M., Meehl, J. B. and Staehelin, L. A. (1999). "Stop-and-go movements of plant Golgi stacks are mediated by the acto-myosin system." Plant Physiology 121(4): 1127-1141.

Nebenfuhr, A., Ritzenthaler, C. and Robinson, D. G. (2002). "Brefeldin A: Deciphering an enigmatic inhibitor of secretion." Plant Physiology 130(3): 1102-1108.

Ott, R. L. and Longnecker, M. (2001). An introduction to statistical methods and data analysis,

5th ed., Pacific Grove, CA: Duxbury.

Oufattole, M., Park, J. H., Poxleitner, M., Jiang, L. and Rogers, J. C. (2005). "Selective membrane protein internalization accompanies movement from the endoplasmic reticulum to the protein storage vacuole pathway in arabidopsis." Plant Cell 17(11): 3066-3080.

Peters, D. (1998). An updates list of plant species susceptible to tospoviruses. Recent progress in tospovirus and thrips research. Peters, D. and Goldbach, R. Wageningen, The Netherlands: 107-110.

Petterson, R. F. and Melin, L. (1996). Synthesis, assembly, and intracellular transport of *bunyaviridae* membrane proteins. The Bunyaviridae. Elliott, R. M. New York, N.Y., Plenum Press: 159-188.

Phillipson, B. A., Pimpl, P., daSilva, L. L. P., Crofts, A. J., Taylor, J. P., Movafeghi, A., Robinson, D. G. and Denecke, J. (2001). "Secretory bulk flow of soluble proteins is efficient and COPII dependent." Plant Cell 13(9): 2005-2020.

Pimpl, P. and Denecke, J. (2000). "ER retention of soluble proteins: Retrieval, retention, or both?" Plant Cell 12(9): 1517-1519.

Ramanathan, H. N., Chung, D.-H., Plane, S. J., Sztul, E., Chu, Y.-K., Guttieri, M. C., McDowell, M., Ali, G. and Jonsson, C. B. (2007). "Dynein-dependent transport of the Hantaan virus nucleocapsid protein to the ERGIC." Journal of Virology.: JVI.00418-00407.

Ravkov, E. V., Nichol, S. T. and Compans, R. W. (1997). "Polarized entry and release in epithelial cells of Black Creek canal virus, a new world hantavirus." Journal of Virology 71(2): 1147-1154.

Ravkov, E. V., Nichol, S. T., Peters, C. J. and Compans, R. W. (1998). "Role of actin microfilaments in Black Creek canal virus morphogenesis." Journal of Virology 72(4): 2865-2870.

Reichel, C., Mas, P. and Beachy, R. N. (1999). "The role of the ER and cytoskeleton in plant viral trafficking." Trends in Plant Science 4(11): 458-462.

Ritzenthaler, C., Nebenfuhr, A., Movafeghi, A., Stussi-Garaud, C., Behnia, L., Pimpl, P., Staehelin, L. A. and Robinson, D. G. (2002). "Reevaluation of the effects of brefeldin A on plant cells using tobacco bright yellow 2 cells expressing Golgi-targeted green fluorescent protein and copi antisera." Plant Cell 14(1): 237-261.

Rönnholm, R. (1992). "Localization to the Golgi complex of Uukuniemi virus glycoproteins G1 and G2 expressed from clones cDNAs." Journal of Virology 66: 4525-4531.

Rwambo, P. M., Shaw, M. K., Rurangirwa, F. R. and DeMartini, J. C. (1996). "Ultrastructural studies on the replication and morphogenesis of Nairobi sheep disease virus, a nairovirus." Archives of Virology 141(8): 1479-1492.

Saint-Jore, C. M., Evins, J., Batoko, H., Brandizzi, F., Moore, I. and Hawes, C. (2002). "Redistribution of membrane proteins between the Golgi apparatus and endoplasmic reticulum in plants is reversible and not dependent on cytoskeletal networks." The Plant Journal 29(5): 661-678.

Salanueva, I. J., Novoa, R. R., Cabezas, P., Lopez-Iglesias, C., Carrascosa, J. L., Elliott, R. M. and Risco, C. (2003). "Polymorphism and structural maturation of bunyamwera virus in Golgi and post-Golgi compartments." Journal of Virology 77(2): 1368-1381.

Sato, K. and Nakano, A. (2007). "Mechanisms of COPII vesicle formation and protein sorting." FEBS Letters 581(11): 2076-2082.

Seemanpillai, M., Elamawi, R., Ritzenthaler, C. and Heinlein, M. (2006). "Challenging the role of microtubules in tobacco mosaic virus movement by drug treatments is disputable." Journal of Virology 80(13): 6712-6715.

Shaw, K. L., Lindemann, D., Mulligan, M. J. and Goepfert, P. A. (2003). "Foamy virus envelope glycoprotein is sufficient for particle budding and release." Journal of Virology 77(4): 2338-2348.

Shi, X., Lappin, D. F. and Elliott, R. M. (2004). "Mapping the Golgi targeting and retention signal of bunyamwera virus glycoproteins." Journal of Virology 78(19): 10793-10802.

Shimmen, T. (2007). "The sliding theory of cytoplasmic streaming: Fifty years of progress." Journal of Plant Research 120(1): 31-43.

Smith, J. F. and Pifat, D. Y. (1982). "Morphogenesis of sandfly fever viruses (bunyaviridae family)." Virology 121(1): 61-81.

Snippe, M., Goldbach, R. and Kormelink, R. (2005a). Tomato spotted wilt virus particle assembly and the prospects of fluorescence microscopy to study protein-protein interactions involved. Advances in virus research, Academic Press. Volume 65**:** 63-120.

Snippe, M., Borst, J. W., Goldbach, R. and Kormelink, R. (2005b). "The use of fluorescence microscopy to visualise homotypic interactions of tomato spotted wilt virus nucleocapsid protein in living cells." Journal of Virological Methods 125(1): 15-22.

Snippe, M. (2006). Tomato spotted wilt virus particle assembly: Studying the role of the structural proteins *in vivo*, Wageningen University. PhD Thesis.

Snippe, M., Smeenk, L., Goldbach, R. and Kormelink, R. (2007a). "The cytoplasmic domain of tomato spotted wilt virus Gn glycoprotein is required for Golgi localisation and interaction with Gc." Virology 363(2): 272-279.

Snippe, M., Willem Borst, J., Goldbach, R. and Kormelink, R. (2007b). "Tomato spotted wilt virus Gc and n proteins interact in vivo." Virology 357(2): 115-123.

Soellick, T. R., Uhrig, J. F., Bucher, G. L., Kellmann, J. W. and Schreier, P. H. (2000). "The movement protein NSm of tomato spotted wilt tospovirus (TSWV): RNA binding, interaction with the TSWV n protein, and identification of interacting plant proteins." PNAS 97(5): 2373-2378.

Stefano, G., Renna, L., Chatre, L., Hanton, S. L., Moreau, P., Hawes, C. and Brandizzi, F. (2006). "In tobacco leaf epidermal cells, the integrity of protein export from the endoplasmic reticulum and of ER export sites depends on active copi machinery." The Plant Journal 46(1): 95-110.

Storms, M. M. H., Kormelink, R., Peters, D., Van Lent, J. W. M. and Goldbach, R. W. (1995).

"The nonstructural NSm protein of Tomato spotted wilt virus induces tubular structures in plant and insect cells." Virology 214(2): 485-493.

Takahashi, H., Saito, Y., Kitagawa, T., Morita, S., Masumura, T. and Tanaka, K. (2005). "A novel vesicle derived directly from endoplasmic reticulum is involved in the transport of vacuolar storage proteins in rice endosperm." Plant Cell Physiology 46(1): 245-249.

Takeda, A., Sugiyama, K., Nagano, H., Mori, M., Kaido, M., Mise, K., Tsuda, S. and Okuno, T. (2002). "Identification of a novel RNA silencing suppressor, NSs protein of Tomato spotted wilt virus." FEBS Letters 532(1-2): 75-79.

Tas, P. W. L., Boerjan, M. L. and Peters, D. (1977). "Structural proteins of Tomato spotted wilt virus." Journal Of General Virology 36(AUG): 267-279.

Tormakangas, K., Hadlington, J. L., Pimpl, P., Hillmer, S., Brandizzi, F., Teeri, T. H. and Denecke, J. (2001). "A vacuolar sorting domain may also influence the way in which proteins leave the endoplasmic reticulum." Plant Cell 13(9): 2021-2032.

Tsuda, S., Fujisawa, I., Ohnishi, J., Hosokawa, D. and Tomaru, K. (1996). "Localization of Tomato sotted wilt tospovirus in larvae and pupae of the insect vector *thrips setosus*." Phytopathology 86: 1199-1203.

Uhrig, J. F., Soellick, T. R., Minke, C. J., Philipp, C., Kellmann, J. W. and Schreier, P. H. (1999). "Homotypic interaction and multimerization of nucleocapsid protein of Tomato spotted wilt tospovirus: Identification and characterization of two interacting domains." PNAS 96(1): 55-60.

Ullman, D. E., Cho, J. J., Mau, R. F. L., Westcoc, D. M. and Custer, D. M. (1992). "A midgut barrier to Tomato spotted wilt virus acquisition by adult western flower thrips." Phytopathology 82: 1333-1342.

Ullman, D. E., German, T. L., Sherwood, J. L., Westcot, D. M. and Cantone, F. A. (1993). "Tospovirus replication in insect vector cells - immunocytochemical evidence that the nonstructural protein encoded by the s-rna of Tomato spotted wilt tospovirus is present in thrips vector cells." Phytopathology 83(4): 456-463.

van den Hurk, J., Tas, P. W. L. and Peters, D. (1977). "Ribonucleic-acid of Tomato spotted wilt virus." Journal of General Virology 36(JUL): 81-91.

van Knippenberg, I., Goldbach, R. and Kormelink, R. (2002). "Purified Tomato spotted wilt virus particles support both genome replication and transcription in vitro." Virology 303(2): 278-286.

van Poelwijk, F., Boye, K., Oosterling, R., Peters, D. and Goldbach, R. (1993). "Detection of the l protein of Tomato spotted wilt virus." Virology 197(1): 468-470.

Veijola, J. and Pettersson, R. F. (1999). "Transient association of calnexin and calreticulin with newly synthesized G1 and G2 glycoproteins of Uukuniemi virus (family bunyaviridae)." Journal of Virology 73(7): 6123-6127.

Verkleij, F. N., Devries, P. and Peters, D. (1982). "Evidence that Tomato spotted wilt virus-RNA is a positive strand." Journal of General Virology 58(FEB): 329-338.

Ward, T. H., Polishchuk, R. S., Caplan, S., Hirschberg, K. and Lippincott-Schwartz, J. (2001).

"Maintenance of Golgi structure and function depends on the integrity of ER export." Journal of Cell Biology 155(4): 557-570.

Ward, T. H. and Brandizzi, F. (2004). "Dynamics of proteins in Golgi membranes: Comparisons between mammalian and plant cells highlighted by photobleaching techniques." Cellular And Molecular Life Sciences 61(2): 172-185.

Watson, P., Forster, R., Palmer, K. J., Pepperkok, R. and Stephens, D. J. (2005). "Coupling of ER exit to microtubules through direct interaction of COPII with dynactin." Nature Cell Biology 7(1): 48-55.

Whitfield, A. E., Ullman, D. E. and German, T. L. (2004). "Expression and characterization of a soluble form of Tomato spotted wilt virus glycoprotein G(n)." Journal of Virology 78(23): 13197-13206.

Whitfield, A. E., Ullman, D. E. and German, T. L. (2005). "Tospovirus-thrips interactions." Annual Review of Phytopathology 43(1): 459-489.

Wijkamp, I., van Lent, J., Kormelink, R., Goldbach, R. and Peters, D. (1993). "Multiplication of Tomato spotted wilt virus in its insect vector, *frankliniella occidentalis*." Journal of General Virology 74: 341-349.

Wijkamp, I. (1995). Virus-vector relationships in the transmission of tospoviruses. Wageningen, the Netherlands, Wageningen University. PhD Thesis.

Wright, K. M., Wood, N. T., Roberts, A. G., Chapman, S., Boevink, P., MacKenzie, K. M. and Oparka, K. J. (2007). "Targeting of TMV movement protein to plasmodesmata requires the actin/ER network; evidence from FRAP." Traffic 8(1): 21-31.

Yang, Y.-d., Elamawi, R., Bubeck, J., Pepperkok, R., Ritzenthaler, C. and Robinson, D. G. (2005). "Dynamics of COPII vesicles and the Golgi apparatus in cultured Nicotiana tabacum BY-2 cells provides evidence for transient association of Golgi stacks with endoplasmic reticulum exit sites." Plant Cell 17(5): 1513-1531.

ACKNOWLEDGEMENTS

ABOUT THE AUTHOR

GRADUATE SCHOOL CERTIFICATE

ACKNOWLEDGEMENTS

These last few years have marked a very important and rewarding period of my life, both personally and professionally. I have many people to thank for that…

I would like to start by expressing my gratitude to my co-promotor and promotor. Richard, I almost can't find the words to thank you... All your support, interest and enthusiasm were contagious. Especially during the first one and half year of my research, when all the many attempts to express the glycoproteins seemed to fail, I never heard from you any word of disappointment. On the contrary, you always seemed to find the good side of every result and showed a lot of interest in my new ideas. I will never forget your reaction when I called you from Leeds, letting you know that we had finally been able to express the glycoproteins: after a loud "great", many other "greats" followed in a row and a lot of new interesting follow-up experiments immediately came to topic. We had the chance to try all these and many others of our ideas and the "greats" were always there for me whenever I was looking for support. Now it's my turn: it was GREAT to have you as my supervisor! Thank you! Rob, thank you so much for your supervision, interest, many fruitful discussions and very helpful advices. A very special "thank you" for all the effort you put on the final corrections of this thesis, greatly contributing for correlating the several subjects into the general context of virus assembly.

I would also like to thank Joan for his supervision and very nice discussions and advices, especially at the beginning of my research.

It was a pleasure to supervise Sjef, Rinat and Maartje. Thank you for the interest you always demonstrated, for your contributions to my research and for the many hours of very interesting discussions and fun. Maartje, a special "thank you" for your friendship, support and help with the graphical designing of the models.

One of the best memories I will take with me from my stay in Wageningen is the amazing atmosphere at Virology. There was always someone ready to help, to share, to give a word of support and, of course, to party. I will always remember the very nice PhD weekends, labtrips and all the other nice activities. To my "plant colleagues" Simone, Cristiano, Cristina, Marjolein, Hans, Dick Lohuis, Henriek, Etienne, Afshin, Marieke, Marcel, Dick Peters, Ingeborg, Esther, Jan, Hanke, Janneke, Marília, Claudine, Paul and Nina, thank you for all your help and for making the lab such a fun place to work at. To the colleagues from the baculovirus and whispovirus lab, Mark, Liljana, Monique, Els, Marcel, Gang, Jeroen, Hendrik, Angela and Just, thank you for all the gezelligheid. A special "thank you" to Jan, for teaching me how to work with the confocal microscope and his valuable advices on image processing. Mark, for you also a special "thank you" for your help with the statistical analyses. Also a special word of gratitude for Dick Lohuis, for all his help and advices. I would also like to thank Thea and Wout for all their help.

Besides many colleagues, I found many friends at Virology ... of the kind, I am sure, will last a life time... Si and Cris, I am really very grateful to have met you. Besides all the help in the lab, you made me laugh and have so much fun so many times, supported me with your advices and helped me waking up in the morning with our secret "chá mate meetings". And how great was it to be able to speak "science" in the lab in my own language? Thank you so much! Cristina, thank you for your friendship, for all our nice long talks and, of course, for being my paranimph. Marjolein, we traveled together throughout the "world of TSWV assembly" and your inputs, suggestions, help and friendship will never be forgotten. Etienne (and Danijela) thank you so

much for your friendship and for passing on to us the very nice apartment at the Schaepmanstraat. After many years of moving between places, we finally felt that we had a home in Wageningen.

Jan Willem, it was a pleasure to spend all those hours with you at the FLIM microscope. I learned a lot and for that and for your help I want to thank you.

Rikus, muito obrigada for allowing me to use your climate chamber.

I owe a very special word of gratitude to the group of Jurgen Denecke's lab in Leeds, expecially to Jurgen and Ombretta. With your help, we were able to express the viral glycoproteins, and the many discussions always ended up with very nice suggestions for experiments, many of which resulted in some of the most important findings described in this thesis. Thank you!

I would also like to thank the other members of our European Network on Biointeractions from Italy, UK, Switzerland, Sweden and Israel for the nice group meetings and discussions.

During these years in the Netherlands I have made many new friends, but the old ones were also always there for me... Together at the high school, separated at the university and rejoined in Wageningen starting our PhD researches almost at the same time, we ended up sharing a very similar path and defending our theses almost on the same day. Sónia, you have been a real friend and I want to thank you for always being there for me (and Hazel), and also for being my paranimph. You and Tiago have always made me feel closer to home and very lucky for having such friends just next door. Thank you for all the kilos of Portuguese products you brought me from Luxembourg and for all the nice dinners, movie nights, etc ... basically, for being there! Benji, for more than 6 years we have known each other (since my first day in Wageningen, when I came for my internship) and I feel very proud of having you as such a close friend. Thank you for all the relaxing weekends in Amsterdam, the talks, the laughs and for always being so close even when far away.

It is true when they say that childhood friendships can last forever. Janica, my "almost sister", and Maria, my long time confidant, thank you for always sending me your friendship from so far and for always freeing a lot of time to spend with me whenever I went back home.

My university years in Porto rewarded me with a great group of friends, who I can always count on. Regina, Ana, Carlos, João, Rita, Ritinha, Zezito, thank you for your friendship and for all the fun.

Een heel special dankwoord voor mijn Nederlandse familie. Klaasje, Tobias, Freek, Bram, Lieke en Opa, bedankt dat jullie me altijd het gevoel gegevenhebben erbij te horen. Tobias, ik zal je altijd missen...

Sjors, how can I thank you? For all your love, your friendship, your support… You have always been there for me in all possible ways. During my PhD research you always listened to me with interest, had a lot of patience at my most stressy moments and shared with me the joys. Your help was crucial! More than my boyfriend you are also my best friend. Thank you for being there!

I will end this long list of acknowlegements with the most important part, my family. Por todo o amor e os muitos mimos, um obrigada muito especial aos meus vôvôs e vóvós. Mamã e Papá, durante toda a minha vida o vosso apoio incondicional foi a peça chave no meu desenvolvimento. Apesar da distância, o vosso amor e carinho esteve sempre muito presente. Todo o estímulo, confiança e força que me transmitiram, ajudaram esta vossa filhota mimada a suportar a saudade. Obrigada, simplesmente, por serem vocês...
Este livro também é vosso...!

Daniela

ABOUT THE AUTHOR

Daniela Maria Oliveira Gandra Ribeiro was born on the 9th of October 1978 in Caldas de S. Jorge, Portugal. She studied Biochemistry, specialization in Applied Biochemistry, at the Science Faculty of the University of Porto, from which she graduated in 2001. During her studies, she was granted an Erasmus Program scholarship and spent seven months at the Industrial Microbiology Laboratory of Wageningen University where she conducted research involving the study of the effect of amino-terminal deletions on *Rhodotorula glutinis* epoxide hydrolase as well as of the isolation and characterization of an epoxide hydrolase-encoding gene from *Beauveria bassiana*. In 2002 she worked for six months under a young researcher fellowship at the Instituto de Tecnologia Química e Biológica of University of Lisbon. There, she researched the transcription factors codified by the Yap genes family in response to stress, in *Saccharomyces cerevisiae*. In November 2002 she started her PhD study at the Laboratory of Virology of Wageningen University, as part of a European Network on Bio-molecular Interactions in Plants, which resulted in the work presented in this thesis.

Education Statement of the Graduate School
Experimental Plant Sciences

The Graduate School
EXPERIMENTAL PLANT SCIENCES
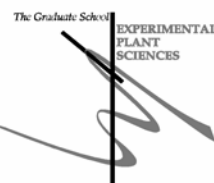
Issued to: Daniela Maria Oliveira Gandra Ribeiro
Date: 6 November 2007
Group: Laboratory of Virology, Wageningen University

1) Start-up phase	date
► **First presentation of your project**	
Intracellular membrane dynamics in virus-infected plant cells	Jun 23, 2003
► **Writing or rewriting a project proposal**	
► **Writing a review or book chapter**	
► **MSc courses**	
PCB-30306: Cell Biology and Advanced Imaging Technologies	May-Jul, 2003
► **Laboratory use of isotopes**	
Safe handling with radioactive materials and sources	Apr, 2004
Subtotal Start-up Phase	*9.0 credits**

2) Scientific Exposure	date
► **EPS PhD student days**	
PhD student day 2003 - Utrecht University	Mar 27, 2003
PhD student day 2004 - Vrije Universiteit Amsterdam	Jun 03, 2004
PhD student day 2005 - Radboud University Nijmegen	Jun 02, 2005
► **EPS theme symposia**	
Theme 2 "Interactions between plants and biotic agents", Leiden, The Netherlands	Jan 10, 2003
Theme 2 "Interactions between plants and biotic agents", Wageningen, The Netherlands	Dec 12, 2003
Theme 2 "Interactions between plants and biotic agents", Amsterdam, The Netherlands	Feb 02, 2007
► **NWO Lunteren days and other National Platforms**	
ALW Meeting Experimental Plant Sciences 2003, Lunteren, The Netherlands	Apr 07-08, 2003
Dutch Annual Virology Symposium 2003, Amsterdam, The Netherlands	Mar 7, 2003
ALW Meeting Experimental Plant Sciences 2004, Lunteren, The Netherlands	Apr 06-07, 2004
Dutch Annual Virology Symposium 2004, Amsterdam, The Netherlands	Mar 12, 2004
ALW Meeting Experimental Plant Sciences 2005, Lunteren, The Netherlands	Apr 04-05, 2005
Dutch Annual Virology Symposium 2005, Amsterdam, The Netherlands	Mar 4, 2005
ALW Meeting Experimental Plant Sciences 2006, Lunteren, The Netherlands	Apr 03-04, 2006
Dutch Annual Virology Symposium 2006, Amsterdam, The Netherlands	Mar 10, 2006
ALW Meeting Experimental Plant Sciences 2007, Amsterdam, The Netherlands	Apr 02-03, 2007
Dutch Annual Virology Symposium 2007, Amsterdam, The Netherlands	Mar 9, 2007
► **Seminars (series), workshops and symposia**	
Current Themes in Ecology: Global Ecology, Wageningen, The Netherlands	Apr 17, 2003
Molecular Advances in Vaccinology, Utrecht, The Netherlands	Oct 28, 2005
Current Themes in Ecology: Influenza Ecology and Pandemics, Wageningen, The Netherlands	Apr 19, 2006
Organisation of the Plant Secretory Pathway – the Golgi/ER interface, Wageningen, The Netherlands	Apr 27, 2006
Viruses – exploring natures's own nanoparticles, Wageningen, The Netherlands	May 12, 2006
European Flying Seminar:Small RNA, chromosome organization and gene expression, Wageningen, The Netherlands	Oct 23, 2006
► **Seminar plus**	
► **International symposia and congresses**	
6th European Plant Endomembrane Meeting, Glasgow, U.K.	Aug 21-23, 2003
7th European Plant Endomembrane Meeting, Neuchatel, Switzerland	Sep 08-10, 2004
Fourth Joint Meeting of Dutch and German Plants Virologists, Wageningen, The Netherlands	Mar 10-11, 2005
Focus on Microscopy 2005, Jena, Germany	Mar 20-23, 2005
International Congress of Virology, San Francisco, USA	Jul 23-28 2005
8th Informal European Plant Endomembrane Meeting, Paris, France	Aug 31- Sep 01, 2005
13th International Conference on Negative Strand Viruses, Salamanca, Spain	Jun 17-22, 2006
Imaging Membrane Dynamics Meeting, London, UK	Sep 14-17, 2006
► **Presentations**	
7th European Plant Endomembrane Meeting, Neuchatel, Switzerland (ORAL)	Sep 08-10, 2004
Mid-term meeting of the EU network on Biointeractions, Leeds, UK (ORAL)	Nov 19, 2004
International Congress of Virology, San Francisco, USA (ORAL)	Jul 23-28 2005
8th Informal European Plant Endomembrane Meeting, Paris, France (ORAL)	Aug 31- Sep 01, 2005
ALW Meeting Experimental Plant Sciences 2006, Lunteren, The Netherlands (ORAL)	Apr 03-04, 2006
13th International Conference on Negative Strand Viruses, Salamanca, Spain (POSTER)	Jun 17-22, 2006
Imaging Membrane Dynamics Meeting, London, UK (POSTER)	Sep 14-17, 2006
EPS Theme 2 Symposium "Interactions between plants and biotic agents", Amsterdam, The Netherlands, (ORAL)	Feb 02, 2007
► **IAB interview**	Jun 03, 2005
► **Excursions**	
Subtotal Scientific Exposure	*23.3 credits**

3) In-Depth Studies	date
► **EPS courses or other PhD courses**	
GFP and LUC: applications of light reporters in biology, Wageningen, The Netherlands	Apr 11-12, 2005
► **Journal club**	
Member of the literature discussion group, Laboratory of Virology	2002-2007
► **Individual research training**	
Protoplasts preparation and electroporation and pulse-chase analysis, Leeds, UK	Jan 24-28, 2003
Subtotal In-Depth Studies	*5.1 credits**

4) Personal development	date
► **Skill training courses**	
Techniques for Writing and Presenting a Scientific Paper	Nov 22-25, 2004
Guide to digital scientific artwork	Dec 14-15, 2004
Career Perspectives	Apr-May 2006
► **Organisation of PhD students day, course or conference**	
► **Membership of Board, Committee or PhD council**	
► **Membership of Board, Committee or PhD council**	
Subtotal Personal Development	*3.6 credits**

TOTAL NUMBER OF CREDIT POINTS*	**41.0**

Herewith the Graduate School declares that the PhD candidate has complied with the educational requirements set by the
Educational Committee of EPS which comprises of a minimum total of 30 credits

* A credit represents a normative study load of 28 hours of study